The Interfacial Integrity Of Dental Restorations: Exploring The Effect Of Oral Biofilms, Mechanical Challenges, And Antimicrobial Treatments

A DISSERTATION
SUBMITTED TO THE FACULTY
OF UNIVERSITY OF MINNESOTA
BY

Carola Carrera Vidal

IN PARTIAL FULFILLMENT OF THE REQUIREMENTS
FOR THE DEGREE OF
DOCTOR OF PHILOSOPHY

Thesis adviser: Dr. Joel Rudney

May 2016

Acknowledgments

Doing a PhD is not a solitary path; many people around me participated in different ways in attaining this goal, including family, friends and colleagues.

My deepest gratitude is for my advisers, Dr. Joel Rudney, Dr. Alex Fox and Dr. Conrado Aparicio. Each of them contributed to my growth as a researcher. Thanks to Dr. Rudney for all his support and guidance while conducting my dissertation project. Thanks to Dr. Fok for encouraging me to be meticulous and pursue things beyond I thought I would do. Thanks to Dr. Aparicio for giving his great advise and offering me many opportunities to expand my potential. I also would like to thank the members of my committee for all their guidance during the last stage of my PhD.

I am very grateful of meeting such wonderful group of people at the MDRCBB. Special thanks to Bonita Vanheel, Young Heo, Yuping Li, Caixia Lan, Ian Huxford, Maria Pintado and Ralph Delong. I also want to thank Ruoqiong Chen for all her training and Mike Weston for being a great support during my research.

Thanks to my friends Rafi Huntley and Claudia Fernandez. They made my life in Minnesota a very pleasant experience. To my friends and colleagues in Chile, who believed in me and encouraged me to pursue my goals. Special thanks to Rodrigo Giacaman for all his support and advise during this journey.

I also would like to acknowledge the government of Chile (Becas Chile program) and the Doctoral Dissertation Fellowship for funding my studies and research.

Last but not the least, I would like to express my most profound gratitude to my dear family in Chile and my future husband Aaron Broege. They have walked by me during this experience showing their unconditional love and support. Thanks for your guidance and encouragement, especially during the difficult times.

Table of Contents

List of Tables

List of Figures

Part I - Interfacial Integrity of Dental Composite Restorations

Chapter 1. Introduction

1.1 Performance Of Dental Restorations

The conventional treatment for cavitated caries lesions is dental restorations. One of the most recent reports informed that around 166 million restorations were placed in the United States in 2005 (1). However, clinical studies suggest that about 50% of dental restorations are replacements (2, 3). Dental practice research findings revealed that when dentist are confronted with the decision of replace or repair, 75% chooses replacement (4). Thus, is not surprising that restoration replacement accounts for about 70% of all operative work (5) and place a big economical burden to the healthcare system in the United States.

Among the restorative materials used for direct dental restorations, dental amalgams and resin composites are the common choice. Albeit dental amalgams have been used successfully for over 150 years, their use is declining due to their non-esthetic appearance and their association with environmental pollution and health effects due to mercury release (6). On the other hand, dental composites are becoming a preferred option (7, 8) mostly because their improved handling properties and patient's demands for tooth colored restorations. In addition, resin composites offer adhesion to the tooth structure, minimizing the amount of tooth removal and encouraging the practice of minimal invasive dentistry. Also, because of their good mechanical properties their indications are now extended to a large variety of clinical situations including load-bearing restorations in the posterior region of the mouth. Nevertheless, despite their numerous advantages and versatility, dental composites are not immune to failure. Indeed, several clinical studies have found that dental composites display higher failure rates (9-11) and shorter longevity (12) compared to dental amalgams. The often-cited reasons for failure are secondary caries and restoration fracture (9-13).

1.1.1 Clinical Evidence

The two most recent randomized clinical trials comparing dental amalgams and dental composites for posterior restorations were conducted in children of age ranging

between 6 to12 years old. In the study conducted by Soncini et al. (11) higher number of replacements were reported for composites (21.9%) compared to amalgams restorations (15.9%) over a 5 year follow up. Also, the need for replacement increased significantly with the number of restorations placed in each individual and the size of the restoration for both materials. Most replacements were caused by new caries or secondary caries. In the case of composite restorations 52% was replaced due to secondary caries. The Casa Pia study conducted by Bernardo et al. (9) found that the mean annual failure rates ranged from 0.16% to 2.83 % for amalgam restorations and from 0.94% to 9.43 % for composite restorations depending on the location, size and number of surfaces. It was noted that larger composites or composites with 4 or more restored surfaces displayed the lowest survival rate (50%) after 7 years of monitoring. The more frequent cause for failure was secondary caries and restoration fracture for both materials. From the failures due to secondary caries, 77.9 % were in the composite group, while only 22.1% were observed in the amalgam group. The overall risk of developing secondary caries was 3.5 times higher in the composite group. After 7 year the overall survival rate was 94.4% for amalgams and 85.5% for composites.

Using a retrospective design Opdam et al. (14) studied the survival of class-II amalgams and composite restorations relative to patients' caries risk, defined as low or high. Interestingly, after 12 years of service, the restorations placed in the high-risk caries group showed significantly lower survival rates (60%) compared with those placed in the low-risk group (80%). According to their findings, composites restorations tended to perform similarly to amalgams in the combined and low risk group; however, in the high caries risk population, composites performed worse, with a higher incidence of secondary caries. These outcomes were further supported by a recent meta-analysis of twelve longitudinal studies on the longevity of posterior dental composites restorations (15). The authors found that for posterior teeth the risk of restoration failure was higher in high caries risk populations compared to low risk. Also, during the first year of service, posterior composite restorations failed more frequently due to endodontic reasons, however following the first year, secondary caries incidence increased and became the major reason of failure after 4 years of service (15). In addition, larger restorations failed

more frequently (14-16), which might be not surprising considering that dental composites were originally recommended for small restorations. However, the material is in increasing use for large restorations in the posterior region.

A major drawback of restoration replacements of composite restorations is the sacrifice of sound dental tissue during the elimination procedure of the failed restoration. It has been shown that removal of composite restorations increases significantly the cavity volume in comparison with removal of amalgams (17). Millar et al. showed an increment of 37% in the cavity size due to elimination of direct composites (18). Also, greater loss of dental tissue during replacement occurs with deeper original preparations (19). The removal procedure can be very detrimental for dental patients facing several replacements, as additional sound tooth-structure will be lost with each re-treatment. Over the lifetime of a patient, repeated replacements will conduct to more tooth removal and more complex restorative procedures that ultimately could end in tooth loss. This condition generates a biological and economical impact for dental patients and the health care system.

1.2. Review On Secondary Caries

1.2.1 Definition And Histopathology

The term secondary caries or recurrent caries is used in dentistry to describe a caries lesion at the margin of an existing dental restoration (20) (Fig. 1.1). Secondary caries can affect dentition regardless the restorative procedure or material.

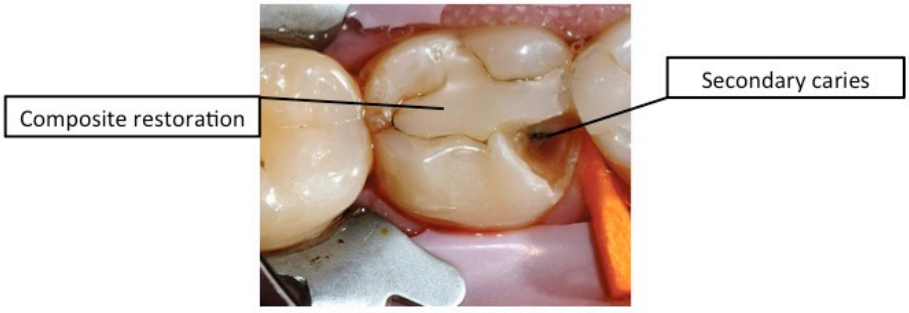

Figure 1.1 Clinical visualization of secondary caries next to a class-II composite restoration, fracture of the mesio-buccal cusp is also observed.

During the early 70's secondary caries was first described in specimens restored with dental amalgams. It was defined as a combination of an outer lesion and a wall lesion with the outer lesion considered essentially as a new caries process in the dental structure next to the restoration (21). The outer lesion was the consequence of dental plaque accumulation that progressed following the direction of the enamel rods generating the same histological stages as primary caries, i.e. surface lesion, body of the lesion, dark zone and translucence zone (22). The wall lesion appeared as a narrow demineralized enamel or dentin band at the tooth-restoration interface. This lesion was thought to develop independently of the outer lesion as consequence of microleakage at the dental restoration interface (23, 24) (Fig. 1.2). In extensive lesions, however, the outer lesion can extend to the tooth-restoration interface making difficult to distinguish the two parts separately. Once the demineralization process has reached the dental enamel junction (DEJ), it extends to dentin as in primary caries (Fig. 1.2).

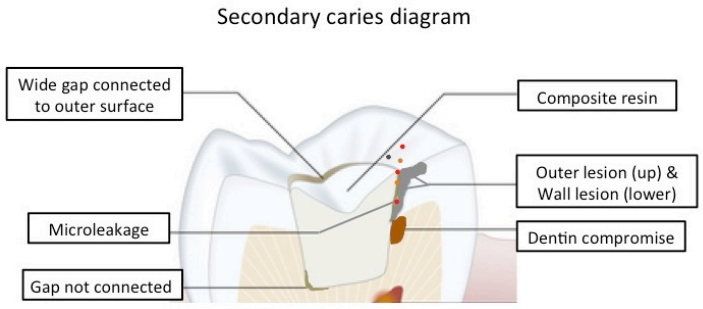

Figure 1.2 Secondary caries next to a composite restoration. Microleakage of different molecules occurs in the presence of a gap connected with the outer surface. A wall lesion is created along the adhesive interface, while an outer lesion is present next to the restoration. When the enamel demineralization reaches the DEJ the process spreads as in primary caries. A gap not connected with the outer margin is also displayed. Modified from (25).

Initial studies of secondary caries around dental composites found that the amount of wall lesions was significantly less compared to dental amalgams (26-28). Since then, some researches have refuted the idea of a wall lesion as a separated entity, explaining that it corresponds to the extension of the outer lesion towards the interface (20, 29). *In-vitro* and clinical data supports the idea of the outer lesion as a critical step for the development of a secondary lesion (30, 31). Although, other investigations sustain that wall lesions can exist independent of the outer lesion when an interfacial gap is present (32, 33). Unfortunately, up to date there is no agreement on this matter and the topic remains unclear.

1.2.2 Incidence Of Secondary Caries

The cumulative incidence of secondary caries for composite fillings was recently reported by Nedeljkovic et al. The analyses included 247 clinical trials on dental composites and dental adhesives from 2000 to 2014. (34). Findings revealed that caries incidence varied considerably among the studies, ranging from 0% to 44% (4, 9, 11, 34). The source of this large variation came from differences in the type of materials, operators and procedures used. One important observation was that very frequently the trials conducted in academic settings reported lower or 0% of secondary caries incidence compared to practice-based reports. As a reason for that difference they suggested that in academic-based studies the operators are more trained and calibrated compared to general practitioners. Plus, in the majority of the studies in the academic setting a low caries risk population was chosen, which might have influenced the results.

Overall, the incidence of secondary caries was higher for posterior restorations followed by anterior and cervical restorations. Also, the incidence significantly increased with increasing periods of observation, except for cervical restorations, which remained constant. The lower caries incidence displayed by cervical lesion must be taken with caution as many of the studies included non-caries cervical lesions. For anterior and posterior restorations the highest median incidence of secondary caries was recorded in long-term studies (> 5 years). Posterior restorations showed an incidence of 1.7%, from

which class-II restorations displayed significantly higher caries incidence compared to class-I (34). In addition, to compare composites and amalgams restorations, a subset of studies with a follow up period between 1 and 7 years was analyzed separately. For these set of studies, the incidence of secondary caries ranged between 0% and 4.9% for dental amalgams and between 0% and 12.7% for dental composites (34).

Lastly, in one of the studies reporting a secondary caries incidence of 6.5%, most of the cases occurred in the high caries risk population (63%). This suggests that dental composites might perform worse under cariogenic challenge, which has been pointed out by others (14).

1.2.3 Location Of Secondary Caries

The available information on location of secondary caries comes from early studies that used questionnaires and diagrams meant to gather specific locations from dental practitioners. The data collected indicated that 80% to 90% of the clinically diagnosed secondary caries was detected at the gingival margin of class II and class V restorations, irrespective of the restorative material used (Fig. 1.3). Occlusal caries next to Class I or II restorations was rarely seen, but when diagnosed, it was found to be slightly higher in composite compared to amalgams restorations (30, 35, 36).

Contemporary clinical studies on the longevity of dental composite usually fail to report specific locations of secondary caries, making difficult to confirm these results. However, it is clinically possible that secondary caries develops more frequently at the gingival margin as several factors may influence this trend including, i) The gingival margin accumulates more dental plaque because is more difficult to clean. This occurs especially in class II restoration where the gingival margin is located interproximally, ii) Gingival margins in proximal boxes are complex to restore. There is less visibility, making difficult to properly adapt the restorative material. Also gingival margin are prone to contamination by the gingival fluid, iii) The curing light is usually positioned far from the material, especially in deep class II, which can affect polymerization, iv) Bonding is likely to be less effective as enamel is usually lost in preparations involving a

gingival floor (36). All these factors could make this location more susceptible to develop secondary caries over time.

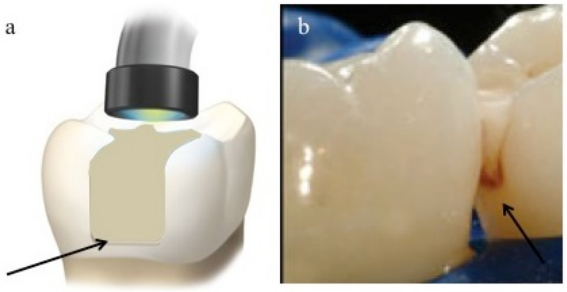

Figure 1.3. Gingival margin are the most commonly affected by secondary caries. (a) Shows an inadequate adaptation of the composite resin to the floor of the proximal box, which will be later infiltrated by oral fluids and bacteria. Modified from (37). (b) Secondary caries detected at the gingival margin of a composite restoration (38).

1.2.4 Etiology And Microbiology Of Secondary Caries

Secondary caries as primary caries is the result of an imbalance between demineralization and remineralization processes that naturally occur in the tooth. This imbalance is due to an ecological shift of the commensal microflora favoring the selection for aciduric and acidogenic microbial species. The ecological shift responds to external challenges, such as frequent sucrose consumption or decrease in salivary flow, that ultimately result in reduced pH levels. This environmental acidification constitutes the main driving force for the phenotypic and genotypic changes in the microbial community during the development of a caries lesion (39, 40). The selected microorganisms adapt to this new environment providing a more cariogenic phenotype (41).

Very little is known about the specific microbiota composition involved in secondary caries. Some caries associated species such as *mutans streptococci*, *Actinomyces naeslundii genospecies 2*, and *lactobacilli* were reported to be commonly present in secondary caries sites around composite restorations (42). In the early 2000's Splieth et al. (43) isolated up to 83 bacterial species under composites and amalgams diagnosed with secondary caries. The results showed that microbial diversity was much greater under composites than amalgams. Indeed, seventy species were isolated from the composite restored teeth, including mostly anaerobic gram-negative rods, whereas for amalgams only 13 were detected of which facultative anaerobic gram-positive rods were predominant. Despite the great difference in bacterial number the authors reported a similar ratio between aerobic and anaerobic species for composites and amalgams, with anaerobic species being predominant. The number of bacteria was also positively correlated to the caries activity (43). A similar study was conducted by Mo et al. (44), the findings showed that the most predominant bacteria isolated included: *Prevotella*, *Veillonella*, *Lactobacillus*, *Streptococcus mutans*, *Neisseria*, and *Actinomyces*; followed by *Peptostreptococcus*, *Fusobacterium*, and *Porphyromonas gingivalis*; and occasionally *Capnocytophaga*. However, no differences were found between amalgams and composites restorations.

Overall, the current knowledge about the microbiology of secondary caries is very limited and maybe biased as the available information comes from microbial culturing techniques, which neglect all the uncultivable bacteria. In the recent decade 16sRNA techniques have started to unveil the large diversity of microorganisms present in the dental plaque. Some recent findings in primary caries have shown that not only *Streptococcus mutans* and *Lactobacillus* -classical caries associated pathogens- are involved in the development of caries, but also other aciduric and acidogenic species including yeasts (40, 45). Current efforts are being done to elucidate the microbiota associated with dental caries. However, knowing only about its composition does not provide information about the phenotype of the caries associated-microbiota. It might be better to understand the function rather than the composition since the microbial

community may involve a high number of diverse bacteria but working together as one organism (46).

1.3 Factors Contributing To Failure Of Dental Composites

1.3.1 Polymerization Shrinkage And Shrinkage Stress

Up to date, the majority of dental composites are composed by dimethacrylate-based polymeric matrix, reinforcing fillers (radiopaque glass or silica), silane coupling agent to bind the filler to the organic matrix, and initiator/activator chemicals that modulate the polymerization reaction (47). The process involves reaction of the monomers with the neighboring molecules to form a large 3D polymer matrix. During polymerization, the monomers come close together reducing the intermolecular space. This dimensional change is known as polymerization shrinkage (48). One of the major consequence of polymerization shrinkage is the generation of contraction stresses within the material that cannot be relaxed by displacements in the structure or deformations on the free surfaces (49). As the matrix becomes polymerized the movements of the constituent molecules become restricted. The internal stresses can be transferred to the bonded surfaces leading to failure or debonding when the amount of stress surpasses the bond strength of the interface (50-52). The spaces between the delaminated parts are usually known as interfacial gaps (Fig. 1.2). These gaps might be or not connected to the outer surface. If the interfacial gap is connected to the outer environment is likely to lead to microleakage of oral fluids, bacterial acids or other oral metabolites into the interface affecting its integrity.

The development of enhanced bonding systems with increased bond strength and dental composite materials with reduced shrinkage polymerization are current goals of adhesive dentistry to overcome the consequences of shrinkage stress.

1.3.2 Gap Formation And Microleakage

As mentioned above, the formation of interfacial gaps and consequent microleakage are undesirable clinical situations. There is current controversy about the relevance of microleakage and gaps for the development of secondary caries. Initial research indicated that microleakage was necessary for the formation of wall lesions. It was suggested that this kind of lesions could form independently of the outer lesion because the penetration of hydrogen ions from the outer environment could be sufficient to promote demineralization at the interface (21, 23, 24). However, several studies have challenged this idea because so far any of the restorative materials is able completely eliminate microleakage around dental restorations (53, 54). New perspectives are emphasizing the relevance of biofilm formation in driving the caries process. Kidd et al. suggested that microleakage alone might not lead to active demineralization beneath a restoration (22). Only when bacterial invasion and biofilm accumulation takes place at the tooth-restoration interface wall lesions may develop. Here is when the size of the formed gap becomes relevant. It is logical to think that larger gaps might allow bacterial passage and accumulation of biofilm at the interface.

Several studies have been conducted in the presence of a cariogenic biofilm to determine the correlation between the gap size and the establishment and progression of secondary caries (22, 32, 33, 55-57). Totiam et al. (57) found that the gap size did not affect the demineralization depth of the outer lesion for both enamel and dentin when two gaps sizes where compared (50µm and 500µm), however, when a larger array of gap widths were tested (0 to 1000 µm) an increase in lesion depth was observed with wider gaps. For wall lesions, an increase on gap width significantly increased the wall lesion area in dentin. Similar results were reported by Dierke et al. (32), in which a significant increase in wall lesion area was detected in enamel between the 50µm and 250µm gaps. For dentin, differences were found between gaps of 50µm and 100µm. In addition, Cenci et al. (55) showed that mineral loss was higher with increasing gap sizes when composite was the restorative material but not for other materials such as glass-ionomers. Recent data investigating a possible a minimum threshold for gap size and caries development in dentin did not find any relationship between gap size and wall lesion development, also

there was no clear trend for increasing lesion progression with wider gaps. Interestingly, demineralization was seen with small gaps of 50μm (58).

A main drawback in research investigating the role of gap in caries formation is the experimental model. In these systems blocks of composites are situated next to a block of dentin or enamel. In many studies no adhesives procedures are used or the adhesive is left intentionally on the dentin side, which is unrealistic. Clinically, gaps can be formed at different locations depending where the failure takes place. A recent study evaluating the role of the adhesive location versus the development of secondary caries found that when the adhesive is left on the dentin side no caries progression is found at the wall next to the composite. On the other hand, when the gap was designed with the adhesive on the composite side, lesion depth and mineral loss was significantly higher than the no gap group and the group where adhesive was left in the dentin side (59). These results demonstrate how the experimental design of gaps may affect the results.

Until now the main conclusion that can be drawn from these studies is that the concomitant presence of cariogenic biofilm and gap at the interface may lead to caries lesion, however, there is no clarity if there is a minimum threshold after which further demineralization is enhanced. It is important to mention that current models to study interfacial gaps may be not representative of the natural progression of secondary caries.

1.3.3 Plaque Accumulation

An aspect that initially was thought to contribute to failure of dental composites was their capability to accumulate more plaque on their surface compared to other restorative materials (60, 61). More recently, Padovani et al. (62) and Auchill et al. (63) showed *in-situ* that resin composites actually form biofilms of similar thickness as amalgams and other restorative materials. The main difference though was related to the viability of the biofilm. In this respect, biofilms collected from composites surfaces were considerable more viable compared to the ones collected from amalgams and glass-ionomers. The reduced viability found in amalgams and glass-ionomers is thought to respond to

antimicrobial properties of the metallic ions present in amalgams and the fluoride content in the case of glass-ionomers.

Research has been conducted to determine whether the composite formulation might influence bacteria attachment as the chemistry of dental composites varies considerably among the commercial products. Studies have shown that bacteria attachment is very similar among different types of composites(64-66), except for silorane-based materials, which tend to accumulate less biofilm (64, 66). It was suggested that the reduced bacterial attachment was in response to their higher hydrophobicity compared to BisGMA-based composites, although no further explanation was provided.

Roughness has been proposed as an important factor that can modulate the adherence of oral bacteria to dental materials. Mei et al. reported an increment in streptococcal adhesion forces to resin composites with increased surface roughness (67). Also, more biofilm accumulated over dental composites with higher values of surface roughness (68). A recent review article proposed that roughness values above 0.2μm would facilitate biofilm formation on restorative dental materials (69). Nevertheless, the final roughness value in a dental restoration is difficult to control since the extent of roughness will depend on the material's composition (70) as well as the polishing method used after the material has polymerized (71, 72). Currently, there is no suggested finishing protocol to decrease biofilm attachment over the surface of dental composites.

Even though it seems reasonable that smoother surfaces should lead to less attachment and accumulation of biofilm the final effect of surface roughness on bacterial attachment might vary with the size and shape of bacterial cells and other environmental considerations. Thus, it is thought that there is no universally optimum roughness that can block adhesion of all oral microorganisms (73). Another relevant aspect is that in the oral cavity, the tooth and also the restorative material are coated with a thin film formed mostly by proteins, called acquired or salivary pellicle. This pellicle can influence the underlying surface roughness increasing the microbial attachment regardless the polishing treatment (74). Moreover, other environmental factors can affect the surface. It is known that in the presence of fermentable carbohydrates, such as sucrose or starch, cariogenic biofilms produce extracellular matrix mostly composed by exopolysaccharides

(EPS) (75, 76). Studies using *S. mutans* have shown that glucosyltransferases, which mainly produce EPS, can be adsorb to the tooth surfaces or other oral microorganisms generating more sites for production of EPS and microbial attachment (77). Therefore, in the presence of sources of carbohydrates EPS production can provide specific binding sites for bacterial attachment modifying the original surface (75).

1.3.4 Lack Of Antimicrobial Activity

Weather or not dental composites restorations accumulate more biofilm or a different biofilm composition compared to other materials, they definitely do not prevent biofilm formation. Several studies have been conducted to assess if composites display some degree of antimicrobial activity always reporting negative results (78-81). This is very different from findings reported on amalgams restorations, in which different degrees of antimicrobial activity are found depending on the chemical composition of the amalgam (82, 83). Evidently, this is a relevant aspect, as so far, secondary caries would not develop in the absence of biofilm.

1.3.5 Decreased Ability To Seal In The Long Term

Contemporary dental composites restorations rely on dental adhesives to achieve adhesion to the tooth structure. Despite the major advances in the bonding capabilities of dental adhesives, the bonded interface is still is the weakest component of the composite restorative system (84).

In general, the adhesive procedure involves the removal of mineral phase from enamel or dentin by etching, followed by priming and infiltration of adhesive resins into the microporosities generated by etching. Although evidence has shown an initial effective bonding and sealing capability, adhesive systems cannot prevent future failure of the interface (56). Furthermore, their stability and ability to maintain a sealed margin decreases dramatically over time (85, 86). More specific details will be discussed below.

1.4 Review On Bonding To The Tooth Structure

Current adhesives can provide adhesion to dental hard tissues through two main approaches: etch-and-rinse and self-etching. Both strategies can achieve similar micro-mechanical bonding results but using different mechanisms.

1.4.1 Etch And Rinse Adhesion Mechanism To Enamel And Dentin

The etch-and-rinse approach consists in three main steps. In the first step conditioning of the tooth substrate is achieved by applying 30-40wt% phosphoric acid etchant for a certain amount of time followed by water rinsing to stop the etching reaction. The purpose of this procedure is to remove a certain amount of mineral content to create irregularities that are used for retention. After etching, the second step involves the use of hydrophilic monomers to prime the substrate for the next step, which is the subsequent application of the adhesive resin. The adhesive resin is formulated with hydrophobic resin monomers that are similar to those in composite restorative materials. When all these steps are done separately the technique is known as a three-step procedure. However, the simplification of this technique led to a two-step approach in which the primer and the adhesive resin are combined into a single bottle (87).

In enamel, the process of conditioning with phosphoric acid removes a few micrometers of the superficial layer and selectively dissolves prismatic and interprismatic enamel. This leaves behind a surface with increased roughness and surface area. After priming, the adhesive resin infiltrates the etched enamel pits by capillary action. The infiltration by the resin monomers leads to the formation of two kinds of resin tags after polymerization, macro and micro-tags. Macro-tags are formed surrounding the enamel prisms, and micro-tags are formed within small etch-pits at the core of the enamel prims. The latter are thought to generate most of the micro-mechanical interlocking (88).

The mechanism of adhesion to dentin is quite different and it is mostly influenced by the chemical composition and structural organization of dentin. Unlike enamel dentin contains 50% of mineral content, followed by 30% of organic components (mostly type I collagen) and around 30% water. In addition, the presence of dentinal tubules (remnants

of the migration tracks of odontoblasts during dentinogenesis) provides great heterogeneity to the tissue as the number and diameter of the tubules vary according to the location within the tooth. Also, the dentin that forms the wall of the tubules has a different composition with high mineral content and scarce presence of collagen. The water content also varies regionally being in greater quantity next to the pulp and decreasing towards the DEJ. On top of these structural regional differences within the tissue, the process of cavity preparation and/or caries removal leaves a 1-2μm thick layer of cutting debris covering the surface and also plugging the entrance of the dentinal tubules, denominated smear layer (89). All these characteristics make dentin a challenging substrate for adhesion.

In dentin, the etching procedure with 37wt% phosphoric acid, results in removal of the smear layer plus it generates demineralization 3 to 5μm deep. This superficial demineralization of dentin leaves exposed a collagen scaffold that is almost depleted from minerals. This collagen mesh is able to create a micro-retentive network after resin infiltration and polymerization (90), commonly known as hybrid layer (91). Simultaneously with hybridization, the unplugged dentinal tubules are filled with the adhesive resin, forming resin tags upon polymerization. This provides additional micro-mechanical retention (88).

Effective bonding to dentin highly depends on the degree of resin infiltration and hybridization. In order to achieve good infiltration the exposed collagen should be fully expanded to facilitate the penetration of the resin monomers. After the etch-and-rinse step, the remaining water supports the collagen mesh keeping it expanded. If the water is fully removed by post-conditioning air-drying the collagen scaffold will collapse, severely compromising infiltration (88).

Re-expansion of the collagen mesh is therefore crucial, otherwise it will form a compact mesh that is impenetrable to resin (92). There are different techniques to treat dentin after conditioning to prevent collagen collapse, however, these procedures are dependent on the kind of solvent used to carry the functional monomers. When the solvent is water a dry technique is recommended since the water will re-expand the collagen mesh. On the other hand if the solvent is acetone for example, keeping the

dentin moist is required (wet bonding), as the acetone will chance and displace the water from the collagen mesh. The spaces will then be filled with the infiltrating monomer (93). Ideally, the solvent in combination with hydrophilic monomers will keep it the collagen expanded during adhesive infiltration. In general, the wet bonding approach has been recommended to avoid the problems generated by the collapse of collagen. Nevertheless, in the clinical setting is very difficult to know whether or not the proper moisture for the bonding technique was reached as there is no objective way to determine it. In addition, the moisture in dentin is not uniform so it is very easy to over-dry and over-wet in the same preparation.

Excess of water or overwetting can also become a problem when there is not complete displacement by the solvent. Actually, in the presence of excess water the polymerization of the adhesive resin inside the hybrid layer can be compromised or the water may occupy the space needed for the adhesive resin (92). Incomplete infiltration leaving exposed collagen at the bottom of the hybrid layer has been frequently reported for etch-and-rinse systems (Fig. 1.4). This exposed collagen is the responsible for the so-called nanoleakage described by Sano et al. (94), in which leakage was found in specimens with no gaps. This revealed that the hybrid layer contained open interconnected paths that could allow water movement, which becomes problematic over time (see bellow section 1.5.1).

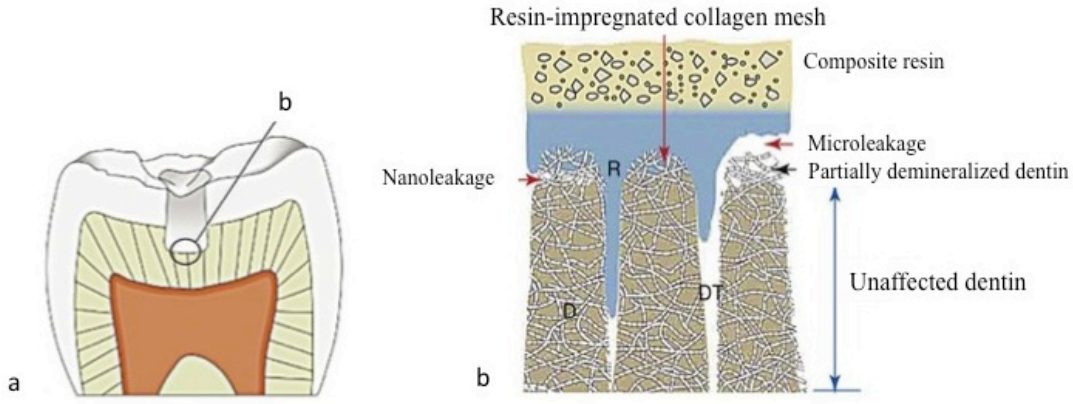

Figure 1.4 (a) Schematic representation of the bonded tooth. (b) Histological representation of the adhesive and hybrid layer formed during the adhesive procedure with an etch-and-rinse system. The adhesive resin is shown in blue penetrating the demineralized collagen matrix and unplugged dentinal tubules. Zones of incomplete infiltration are denominated zones with nano-leakage (95). The presence of larger gaps will lead to microleakage and bacterial invasion.

1.4.2 Self-Etch Adhesion Mechanism To Enamel And Dentin

Self-etch adhesives were initially created to diminish and optimize the time needed to do the bonding procedure. They were developed by increasing the amount of acidic monomers in HEMA/water-based adhesives. They do not involve a separate etch-and-rinse procedure. In this case the incorporated acidic monomers simultaneously condition and prime enamel and dentin. According to the amount of clinical steps they can be divided in self-etch two steps or one step. In the first one, conditioning and priming is performed first, followed by application of the adhesive resin. The second one is called all-in-one adhesive, here all the three components are combined into one single application (96). Also according to their acidity they can be further classified in ultra-mild ($pH \geq 2.5$), mild ($pH \approx 2$), intermediate ($pH \approx 1.5$) and strong ($pH \leq 1$).

In enamel, self-etch adhesives generally do not generate the same porosity pattern as the etching with phosphoric acid. Morphological analysis of enamel treated with different self-etch agents revealed etching patterns ranging from absent to moderate (97). In these systems the enamel's etching pattern varies according to the level of aggressiveness of the self-etching adhesives (98). Strong self-etch systems perform better than higher pH bonding systems creating a resin-infiltrated enamel layer of ~3 μm whereas mild bonding systems create a layer of approximately 1.5 μm (99). However, the thickness is still below compared to what is reached with etch-and-rinse systems (~7μm).

Ultrastructural analysis of several self-etch systems showed that the primary route for the acidic monomers is in between the enamel crystals and along the interprismatic spaces. Light-curing of these monomers and copolymerization with the overlying

adhesive resin forms the continuous bond with the enamel (99). Nonetheless, the shallower etching pattern on enamel and subsequent reduced micro-mechanical retention might endanger bonding. Thus, bonding of self-etch systems to enamel still remains critical.

In dentin, the bonding mechanism depends on the acidity of the adhesive system. Alike etch-and-rinse the adhesion obtained with mild self-etch adhesives adhesion is based in hybridization, although the demineralization of dentin is more superficial, generating a shallower hybrid layer. An important difference here, at least for mild adhesives, is that the collagen matrix still conserves some hydroxyapatite crystals bound to the collagen fibrils. This residual hydroxyapatite can act as a moiety for chemical bonding with the adhesive resin. It has been studied that some of the functional monomers included in self-etching adhesive formulations might have additional chemical interaction that could contribute to chemical bonding and therefore the overall adhesion potential (100). Yoshida et al. found that the common monomer 10-methacryloxydecyl dihydrogen phosphate (10-MDP) readily adhered to hydroxyapatite establishing a bond that remained stable after hydrolytic challenge. Lower binding capability was found for 4-methacryloxyethyl trimellitic acid (4-MET) and for 2-methacryloxyethyl phenyl hydrogen phosphate (phenyl-P), for which the binding was not hydrolytically stable. It was suggested that carboxylic and phosphate groups contained in these functional monomers can function as proton donors, binding ionically with the calcium present in hydroxyapatite (100). Although this suggests an additional chemical interaction contributing to the overall bonding, the interaction of self-etch adhesives with hydroxyapatite it is highly dependent of the type of functional monomer and also on the rest of the formulation in the adhesive system, therefore, it is considered a secondary mechanism of adhesion.

In the case of strong self-etch adhesives the mechanism resemble the interfacial interlocking of an etch-and-rinse adhesive producing resin tags and a 3-5μm thick hybrid layer. In this case, the hybrid layer is also depleted of minerals (88). Intermediate self-etch adhesives exhibit a more gradual transition from the hybrid layer to the unaffected

dentin with a demineralized top layer and a partially demineralized base (88), providing better interlocking than mild adhesives because of their higher acidity (96).

For self-etch adhesives in general the level of moisture present in dentin is not an inconvenient as the acidic monomers are very hydrophilic. Collagen collapse and incomplete infiltration are avoided because demineralization and infiltration occurs concomitantly. Consequently, the degree of infiltration of the exposed collagen is expected to be the same as the degree of demineralization.

1.5 Degradation Of The Dentin-Adhesive Interface

Even though there have been several advances in dental adhesion, there is no doubt that the clinical performance is still questionable as dentin remains a challenging substrate. Sound dentin is an intrinsically hydrated tissue composed on average by 50% mineral phase, 30% of organic components and 20% of water. Demineralized dentin is even more challenging, as the ratio between organic matrix an water is drastically changed. The composition of dentin after conditioning switches to 30% organic and 70% water (87). The utilization of wet bonding to prevent collagen collapse and the incorporation of acidic and hydrophilic monomers to improve initial bonding to the intrinsically wet dentin, have failed to provide long term durability of the bond.

1.5.1 Hydrolytic Degradation: Effects Of Water

One of the major challenges in dental bonding is the presence of water, either the intrinsic water coming from dentin or the one contained in the adhesive formulation. Water leads to the most important mechanisms for degradation, which is hydrolysis of the adhesive resin and leaching of its components. Hydrolysis is the process by which ester bonds or other functional groups present in the adhesive resin polymer are broken by water attack. It been demonstrated that the mechanical properties of adhesives resins are affected in a time dependent manner by the degree of water sorption. This uptake of water induces plasticization and decrease in the elastic modulus (101, 102). In

methacrylate-based polymers and their variants, the presence of several functional bonds/groups such as esters, urethanes, hydroxyls and amides among others, makes them susceptible to water mediated degradation (103). It being shown that highly hydrophilic resins display the highest degree of water sorption, solubility and water diffusion (104, 105). Unfortunately, because of the high concentration of acidic monomers, self-etch adhesives are extremely hydrophilic, which makes them even more prone to hydrolysis.

1.5.2 Hydrolytic Degradation: Sources Of Water

Incomplete infiltration of the resin in etch-and-rinse is one of the reasons for exposure to dentin water. This incomplete infiltration responds to a gradient in monomer concentration through out the hybrid layer. For instance, with a two-step adhesive the percentage of resin decreases to 50% when it reaches the half of the demineralized dentin, dropping to 20% at the bottom of the demineralized dentin (106). This incomplete infiltration leaves exposed collagen, which is susceptible to hydrolysis and enzymatic degradation.

Also, the simplification of the bonding technique led to the use of more hydrophilic monomers and the combination of the hydrophilic and hydrophobic monomers into one single application. With this kind combination a hydrophobic layer impermeable to water or fluids is not longer achieved during hybridization. Indeed, it has been shown that both etch-and-rise and self-etch adhesive behave as permeable membranes after polymerization, allowing water movement along and through the interface (107-110). Initially, this was seen to occur with etch-and-rinse adhesives because of incomplete infiltration of the resin monomers, however, several studies of self-etch hybrid layers have found passage of water even in the absence of incomplete resin infiltration. This was discovered through nanoleakage studies using silver as a tracer on specimens free of gaps. Two modes of nanoleakage were described (108-110). The first one consisted in several silver deposits surrounding the unstained collagen fibers. These deposits formed a horizontal or oblique complex, with additional streaks of silver nitrate extending perpendicularly from the hybrid layer into the adhesive layer, forming dendritic shapes.

This particular mode of nanoleakage was denominated reticular nanoleakage. In the second mode or spotted mode, silver spotting was observed distributed randomly within the adhesive and the hybrid layer. These findings also suggested that nanoleakage was not necessarily caused by the differences between demineralization and resin infiltration, as water channels were also found in the surface of the hybrid layer (111). Later studies have evaluated the permeability of the hybrid layer *in vivo*, formation of dentinal fluid droplets was found over the surface of the adhesive layers after the adhesive polymerization (107).

All these results revealed permeable sites in the adhesive and hybrid layer that allowed water movements. These forms of nanoleakage were later identified as water tree channels and suggested as a potential mechanism for degradation of the adhesive resin (108).

Besides the water already present in dentin, a large amount of water is usually added to the formulation of adhesives to induce the dissociation of the acidic methacrylate monomers into their ionized form in order to penetrate and modify the smear layer and dentin. Unfortunately, with some formulations the water is difficult to evaporate completely, especially in HEMA-water based systems. It is known that the presence of HEMA lowers the vapor pressure of water making it even more difficult to remove (112). Thus, if residual water is still present, the hydrophobic monomers resist diffusing into the collagen mesh, which leads to physical separation of the hydrophilic and hydrophobic phases. In HEMA containing systems, the excess of water and consequent phase separation results in a weak porous web dominated by a HEMA-rich matrix with islands of hydrophobic monomers instead of a robust hybrid layer (113, 114). Moreover, excess of water also affects the degree of conversion interfering with the polymerization process (115) and increasing permeability of the adhesive (116).

Also, dental restorations and the interface are exposed to a wide variety of fluids with the potential of inducing degradation during lifetime. It has been shown that external water/fluids can infiltrate the hybrid layer through unpolymerized sites or regions with poor cross-linking. The final effect is also plasticization of the adhesive resin and further degradation of the bond (86, 117).

1.5.3 Enzymatic Degradation Of The Resin

In addition to hydrolytic degradation, the oral cavity imposes several other biological challenges to the integrity of dental restorations, among them salivary enzymes seem to play a role in the degradation of the dentin-resin bond. The first evidence came from studies reporting on surface degradation of composites after exposure to human saliva (118, 119). According to the chemistry of dental composites, it was speculated that human salivary esterases had the potential to break down ester bonds present in the polymer backbone. Degradation models were created using either cholesterol esterase (CE) or pseudocholinesterase (PCE). Since then several studies demonstrated that BisGMA/TEGDMA based composites can be degraded by these enzymes. High performance liquid chromatography in combination with mass spectroscopy has been used to detect biodegradation byproducts after incubation of dental composites with esterases at different time points. The exposure to esterases yielded to the following degradation products: Methacrylic acid (MA), bishydroxypropoxyphenyl-propane (BisHPPP), triethylene glycol methacrylate (TEGMA) and triethynele glycol (120-122). Similar results were obtained when purified enzymes were replaced by human saliva derived esterases at concentrations found in the oral cavity (121, 123). More recently, the effect of esterase activity on the interfacial integrity of specimens prepared with a three-step etch-and-rinse adhesive has been tested. Adhesive-dentin specimens were subjected to human derived esterases (HDE) up to 180 days. The results showed that fracture toughness was significantly reduced in the specimens incubated with HDE compared to baseline values and control samples exposed to phosphate buffer for the same period of time. Also, significantly higher levels of BisHPPP were found in the group exposed to the enzymes (124). Lately, Kermanshahi et at. (125) reported increased bacterial microleakage in dentin-resin specimens after 30 and 90 days of exposure to CE and PCE, evidencing that the presence of esterase activity could accelerate the degradation of the interface

So far, the effect of esterases or human saliva esterase activity has been the most investigated biological aspect for resin degradation. Their presence in the oral cavity is almost ubiquitous as they can be produced by several sources, such as salivary glands, or

secreted during inflammatory responses, among others (126). This highlights the importance of biological factors in the degradation of the interface. New research has suggested a possible role of oral bacteria in the degradation of dental resins and the adhesive interface (127), but the knowledge is still very scarce.

1.5.4 Degradation Of The Exposed Collagen Matrix

It been shown that incomplete infiltration is a usual drawback generated from a mismatch between the depth in demineralization an resin infiltration, which is characteristic in etch-and-rinse systems, although it has been recently described in self-etch systems as well (128). Besides the consequences described above related to resin degradation, this incomplete infiltration leaves exposed naked collagen fibrils. These fibrils are susceptible to hydrolytically degradation by the surrounding water. Aging studies have shown that degradation of the adhesive layer by resin elution further exposes collagen fibers, leaving behind a disorganized collagen network, which dissolves completely over time (86, 129). Initially, this was thought to be consequence of water-mediated degradation, but more recently, it was found that endogenous proteases present in dentin were partially responsible for the breakdown of the exposed collagen. This was demonstrated when exposed collagen matrix was completely degraded after storage in artificial saliva but not in the group incubated with enzymes inhibitors (130). It was hypothesized that host-derived matrix metallo proteinases (MMPs) were the responsible for the degradation of dentin hybrid layers. Since then, several studies have shown a correlation between the presence of active forms of endogenous proteases in dentin matrices and premature degradation of hybrid layers (131-133). MMPs are calcium- and zinc-dependent endopeptidases involved in dentin remodeling during development (134) , which can become active when exposed to an acidic environment (135). Dentin treatment with both etch-and-rinse and self-etch adhesive systems can activate the precursor forms of these proteases ultimately leading to collagen degradation (132, 136).

The use of proteases inhibitors during the bonding procedure has shown to preserve the hybrid layer and improve the durability of the bonds (137), further supporting the role of MMPs in hybrid layer degradation.

1.5.5 Mechanical Degradation Of The Adhesive Interface

Although many studies have been conducted on the mechanical degradation of composites (138-142) much less in known about the mechanical degradation of the interface and its overall contribution to the interfacial failure. Mechanical degradation refers to the breakdown of the polymer chains by mechanical means. Dental composites restorations are continuously exposed to forces since they have to withstand mastication and other para-functional habits such as bruxism. The study of fatigue, that is, mechanical degradation under subcritical loads, is becoming more relevant. Fatigue involves the weakening of the material when it is subjected to cycles of loading and unloading. Under this condition, failure occurs due the growth of small defects that lead to structural damage (139). Contrary to static loading, cyclic loading of specimens resembles the mechanical challenges present in the oral cavity. Usually the numbers of cycles to failure can be used to predict the fatigue resistance of a certain material.

For interfacial integrity studies, a mixed mode can be used by challenging the substrate to a number of loading cycles and then testing for fracture toughness or bond strength.

Only few studies have been conducted to study the interfacial integrity of adhesive interfaces. Using different fatigue configurations, i.e. tensile, bending and compression (143-145), researches have showed that cyclic loading leads to mechanical degradation of the interface. For instance, dentin-adhesive interfaces made with each of four different adhesives (1 etch-and-rinse, 1 self-etch two steps and 2 all in one self-etch) were exposed to increasing amounts of loading cycles, followed by microtensile bond strength test. All adhesives displayed a decrease in bond strength with increasing amount of cycles, the interface made with the etch-and-rinse adhesive tend to perform better than the all-in-one adhesives (144). Another study using four-point bending showed that resin-dentin beams

failed with lower number of cycles when the load applied increased from 55% to 99% of the bending strength. All specimens failed at the interface, demonstrating that the interface is less resistance to fatigue than composite or dentin. Plus, the bending strength of the bonded beams was around 50% of the solid dentin and composite beams (145). Similar findings were reported by Frankenberger et al. but using cyclic push-out strength test (146).

Failure will depend on the natural flaws present at the interface, which can be generated during the bonding procedure, and increased or enlarged during the mechanical challenges. Although relevant information is obtained from fatigue behavior studies, most of them fail in taking into consideration other factors that are recognized challenges of the oral cavity. Thus, little is known about the relative contribution to interfacial failure.

1.6 Common In-Vitro Methods To Study Interfacial Integrity: Bond Strength

Adhesive dentistry revolutionized the practice of operative and preventive dentistry by providing bonding to the hard tissues of the tooth. Dental bonding relies on the formation of a micro-mechanical interlocking between the dental material and the tooth tissues by the application of an adhesive resin. Different methods can be used to study the bond and the interfacial integrity over time. Bond strength methods are the most popular and commonly used. Many new materials and adhesives are tested with these methods before being marketed.

During the past decades, several strength tests have been applied to assess the bond strength of the interface created during the bonding procedure. The values of bond strength obtained with the test are utilized to make a prognosis on the clinical performance of an adhesive system and/or dental material. All tests are based on the amount of load required to disrupt the bonded interface between the dental restoration and the tooth structure with failure occurring in or near the adhesive/adherent interface (147).

Tensile (TBS), shear (SBS), microtensile (μTBS) and microshear (μSBS) test are among the most popular bond strength tests in dentistry, with tensile and shear performed

almost exclusively until the mid-nineties (148). The difference between the tensile/shear and microtensile/shear test is the size of the bonded area used for the test, ranging between 7 to 28mm^2 for TBS and SBS compared to areas less than 2mm^2 for μTBS and μSBS (148-151). For this reason the first two methods were categorized as macro tests (Fig. 1.5), whereas the second ones were classified as micro bond strength tests. In all of them the value of stress at failure is reported as the load at failure divided by the cross-sectional area of the bonded section. This outcome is denominated the nominal bond strength.

1.6.1 Macro Tests

Much of the information published on bond strength came from macro bond strength methods. These tests were gradually displaced because they presented several shortcomings that made them less reliable. Disadvantages such as a high percentage of cohesive failures in the substrate, low bond strength values, non-uniform stress distribution and large coefficient of variation in the results were reported frequently. For both tensile and shear, a large number of cohesive failures were commonly described in dentin, which was associated with the large bonded areas (152, 153). Because of this, the measured bond strength values reported many times corresponded to the intrinsic strength of the substrate rather than the interfacial strength, generating misleading results (152). Furthermore, non-uniform stress distribution was found at the interface when tensile and shear methods were studied using finite element analyses (154). For the tensile test the stress distribution showed to be somehow uniform in the bulk of the composite, however the amount of stress rapidly increased towards the edges of the specimen, where it concentrated at its maximum. Analysis of SBS showed also a non-uniform stress distribution at the interface, plus other types of stresses were identified. It was found that tensile stresses were predominant rather than shear at the loading point. It was also demonstrated that incrementing the loading distance from the surface of dentin created increasing interfacial tensile/compressive stresses, which were provoked by an increase

in the bending moment. Therefore, the definition of the loading point influenced the results (154).

In addition, it was shown that bond strength values were highly dependent on the geometry of the specimens, the nature of the load application, and the presence or absence of adhesive flash at the interface (154, 155). Moreover, FEA also showed that the greater the mismatch in the elastic modulus between the components, the higher the stress concentration at the interface, which ultimately leads to lower bond strengths values. When composites with increasing elastic modulus were tested, a negative correlation with bond strength values was observed, (148, 154), being more marked in shear rather than tensile test (148).

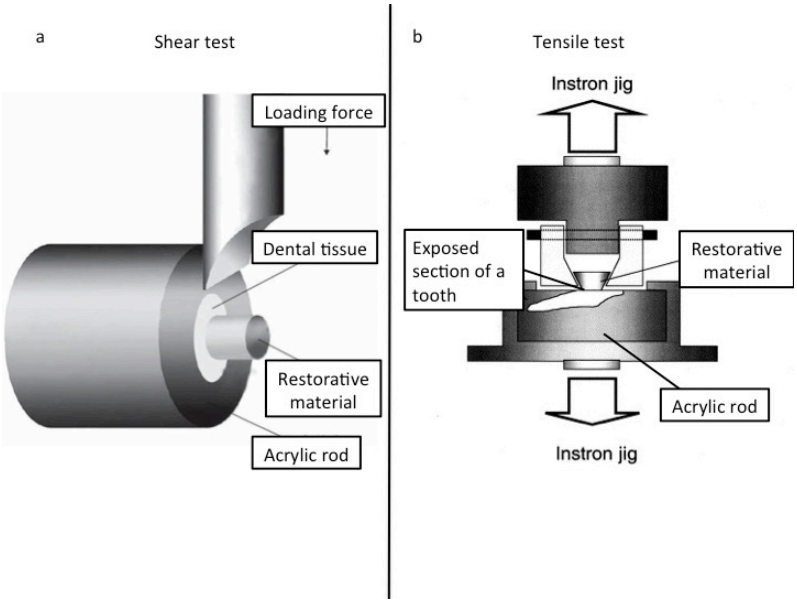

Figure 1.5 (a) Shear bond strength set up. Load is applied with a chisel-shaped loading jig. Modified from (156). (b) Sample set up for a tensile bond strength test. The whole tooth is embedded in acrylic resin exposing the region of interest. Modified from (157).

1.6.2 Micro tests

The reduction in the bonded area proposed by Sano et al. (150) led to higher bond strength values and less percentage of cohesive failure for the μTBS. This was explained by the volume dependency of strength early described by Griffith (158). Bond strength values at failure are not only dependent on the fracture strength but also dependent on the presence of flaws in the tested specimen. The volume dependency means that when the specimen is smaller it will be less likely to contain big flaws that conduct to failure. On the other hand the larger specimens the greater the probability of encountering large flaws that will lead to failure and therefore lower bond strength values.

1.6.3 Microtensile Test

The μTBS test was developed to minimize the disadvantages of the tensile test providing new benefits at the same time. The most relevant advantages include a decrease in the amount of cohesive failures, regional assessment of bonding to the tooth tissues, a more uniform distribution of the tensile load relative to tensile test, accelerated aging due to short diffusion distance and relatively easier fracture mode evaluation (159). However, the modification of the test was not free of flaws. Several inconveniences were derived from the specimen preparation, specimen configuration and fixation procedure.

a) Specimen preparation

The process of specimen preparation involves a reduction in the cross-sectional area below 1mm^2. Many different shapes for the specimen have been reported including; hourglass, slab, stick, and dumbbell shapes, all with different cross-sections (Fig. 1.6). All these shapes intended to reach a more uniform stress distribution at the interface. To prepare these specimens, however, several trimming steps must be followed (Fig. 1.6). The technique then becomes very laborious and sensitive. The machining process induces mechanical stress and wear, leading to cracks in the dental substrates. This has been associated to the high percentage of pre-test failure, where basically the specimen breaks

or debonds before the test or fails under low loads. This in particular affects enamel, when samples are evaluated under the microscope more microcracks are observed in enamel than in dentin, probably because of its high elastic modulus and brittleness (160). To reduce the occurrence of pre-test failures some laboratories suggested the use of a notch-less stick or non-trimming technique (161).

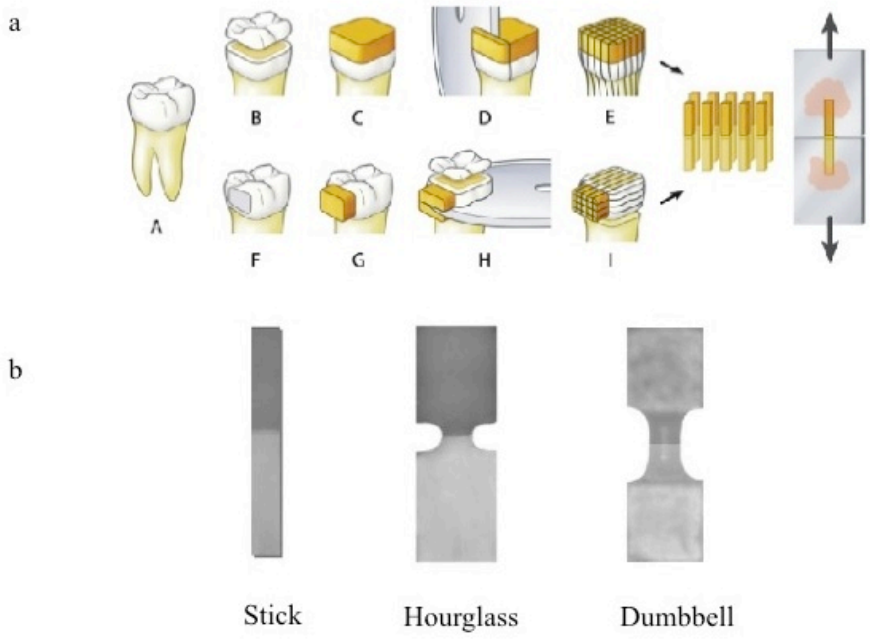

Figure 1.6 (a) Upper sequence shows the trimming steps to obtain dentin μTBS specimens (B to E), whereas the lower one displays the steps for enamel specimens (F to I) (162). (b) Different specimens shape, Hourglass and Dumbbell require further machining steps (163).

b) Specimen configuration

It been shown that the type of configuration will affect the stress distribution. FEA showed that maximum stresses for the dumbbell shape sample occur at the curved notches of the dentin and composite, whereas for hourglass shape the maximum stresses concentrated at the edges of the adhesive, and tend to extend into the nearby composite and dentin. The stick shape specimen displayed a maximum stress concentration in the middle of the adhesive zone. Overall, the dumbbell geometry induce relatively high

stresses spread in the middle region of the dumbbell, whereas the in the hourglass shape the high stresses were more concentrated in the adhesive zone. The stick shape showed less localized high stresses. When the adhesive zone at the interface was further analyzed it was found that dumbbell and stick behave similarly, with more uniform stress along the adhesive. The hourglass shape showed stress concentration at the edges, which make this region likely to initiate failure (164). A cylindrical section in the dumbbell design resulted in less stress concentration at the edges compared with the squared configuration (163).

Currently, there is a still lack of agreement regarding the configuration of the specimens, making comparison among different groups and research centers very challenging as the configuration influences the stress distribution and therefore the results. Whatever the shape selected one of the most important aspects is that the bonded surface must be completely normal to the load applied, which in many cases might be difficult since the specimens might not be adequately trimmed or the fixation mechanism does not provide such precision. When this requirement is not met a uniform stress distribution at the interface is compromised (159).

c) Specimen fixation

To carry out a μTBS test a special device is needed to fix the specimens. Different types have been developed to counteract initial shortcomings seen in μTBS tests. In general, they can be divided in active and passive devices. Active apparatus fix the specimen by mechanical or adhesive means, whereas the passive device will secure the specimen by a complementary shape interlock, without inducing major pre-stresses or bending as it occurs with the active devices. A common active method is the use of a cyanoacrylate glue to immobilize the sample to a loading jig, as shown in figure 1.7b and c. The problem with gluing the sample is that several parameters are not easily controlled, for example, specimen dehydration can happen if fixing the specimen takes too long, also excess of glue can cover part of the adhesive interface, setting of the glue might induce unknown stresses to the specimens, removal of intact specimen for further analyses can

become very challenging, inadequate alignment may easily occur, strength of the glue might be lower than the interface fracturing first or detaching before the test, and removal of the glue from the jig might be difficult for consequent test. In addition, in order to fix the specimen a minimum amount of area is needed, which can be challenging with such small specimen (159). To improve alignment of the specimen a metallic device formed by two identical aluminum parts and a central groove parallel to the load applied was proposed. This device, named Geraldeli's jig (165), allowed self-alignment of specimens before testing avoiding bending and increasing the number of glued surfaces. Soon after a device consisting of two equal aluminum parts, a central self-aligning notch and lateral shoulders for passive gripping was developed, denominated Dircks device (166). Some FEA studies have been conducted to determine the influence of specimen geometry, fixation device and fixation method. Soares et al. (163) studied the stress distribution under tensile load in hourglass, dumbbell and stick configuration specimens relative to attachment conditions. Specimens fixation was simulated to have the only the posterior wall bonded, or posterior, superior and lateral surfaces or all surfaces bonded. When the shapes were analyzed independently of the attachment the stick shape generated the most uniform stress distribution in agreement with similar reports. However, when attachment was factored in, the stress distribution was highly dependent on the fixation method, irrespective the configuration of the specimen. Increasing the number of bonded surfaces to the device improved the stress distribution. Nonetheless, non-uniform stresses were generated. Tensile stresses were concentrated at the posterior surface while compressive stresses at the front of the specimen. It was found that shear stress was created in the specimen under tensile loading. Another FEA study revealed that the larger the distance from the anterior surface of the specimen to the posterior attachment the higher the stress concentration at the posterior wall (167). Raposo et al. (168) compared the stress distribution of a dumbbell configuration using a Dircks device (passive fixation) with a stick shape bonded to a notched Geraldeli Jig. The dumbbell shape generated a much more uniform stress distribution all over the specimen compared to the bonded stick, which displayed high stress concentration at the posterior bonded wall starting at the edges of the bonded area and spreading into the adhesive layer. Some degree of stress

concentration was seen at the posterior surface of the dumbbell shape that it is in contact with the internal face of the device but the higher stress concentration was found at shoulders for contact with the device, but those did not spread to middle center of the specimen. These studies clearly demonstrated that stress distribution is highly dependent on the configuration of the specimen, but most importantly that this dependency is defined by the attachment method.

Considering all the factors previously discussed it seems evident the level of discrepancy currently found in the literature regarding performance of dental adhesive and dental composites. There are still many inconvenient aspects with the current methods to assess bond strength. Many efforts are conducted to solve for this issues and to gain a better understanding of the methods itself. A recent review of bond strength reporting on several bonding agents revealed that the coefficient of variation remains large even with the introduced modification to the micro-tensile test for example. Plus there has been a major awareness of how intensive and laborious the technique became without major benefits in the results. Lack of standardization has been the largest problem given the different kind of specimen configuration and preparation, devices, fixation, storage time, cross-speed rate and experimental conditions such as temperature and humidity, all of them showing some degree of influence in the final results (159).

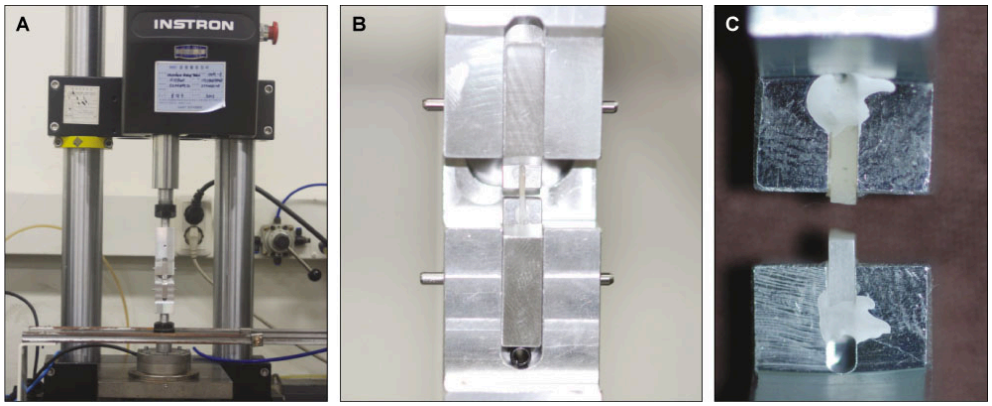

Figure 1.7 (a) Experimental set up for a μTBS test using Intron machine. (b) Close up from a). c) Stick specimen bonded to the loading jig with cyanoacrylate glue (169).

1.6.4 Micro-Shear Test

Sooner after the μTBS test was proposed, a reduction in bonded area was also introduced for the shear test (149). For this test, tooth slices are obtained from either enamel or dentin with a thickness of ~1mm but much larger in diameter and glued to an aluminum platform. Then several small cylinders (~0.7 mm in diameter and ~0.4 mm in height) made out of restorative materials are then bonded to the slices (Fig. 1.8). Shear strength is calculated from the equation $\tau=F/(\pi R^2)$ where τ was the interfacial shear strength, F is the load at failure and R is the radius of the resin cylinder. Alike μTBS the modification to shear test allowed regional mapping of dentin or enamel by testing small areas as well as depth profiling. Also, multiple specimens could be obtained from a single tooth. These advantages were presented without the inconvenience of intensive tooth sectioning and machining work as in the μTBS test, therefore, less worrisome about possible introduction of stress, cracks or larger flaws zones during preparation procedure. Initial FEA data showed that the combination of tensile and shear stress was still present. The authors suggested that by controlling the loading conditions and the length of the specimen, predominant shear stress could be obtained (149). However a more recent FEA conducted by Placido et al. (170) comparing the stress distribution between shear and μSBS revealed that even with the smallest load application distances, defined as 0.05 mm for μSBS and 0.25 mm for shear, a non-uniform shear stress distribution was detected. This effect was more pronounced in the μSBS test. Moreover, zones with the highest stress concentration showed a predominant tensile stress over the shear stress, while only in zones with low stress concentration shear stress was predominant. This indicates that failure might occur due to tensile rather than shear stress.

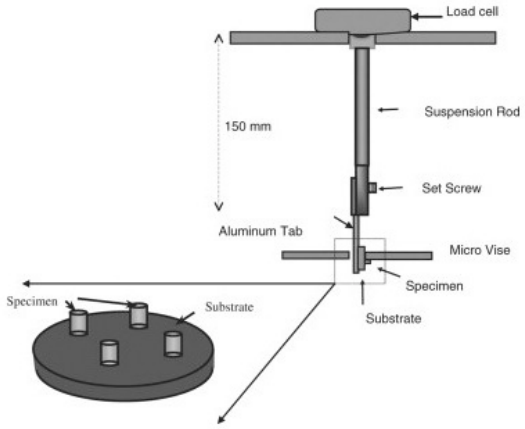

Figure 1.8 Original μSBS experimental set up proposed by McDonough et al (149).

1.7 Common In-Vitro Methods To Study Interfacial Integrity: Microleakage

Microleakage of dental restorations refers to the penetration of oral fluids, molecules, ions or bacteria along the restorative material and the tooth interface (24, 171). This microleakage is the consequence of a lack of total adaptation of the material to the cavity walls produced by non-adhesive material or poor adhesion, mostly due to polymerization shrinkage. Lack of adaptation was very likely with the first dental composites. Early reports suggested that the clinically undetectable microleakage was the responsible for the formation of the wall lesions around amalgams, similar findings were reported for dental composite but the formation of wall lesion was less pronounced (26-28).

In general, *in-vitro* microleakage studies are conducted to test how much a material would leak after that it is in contact with dental tissues. These tests can be designed under several different conditions and are meant to predict the clinical behavior of a particular material.

Unfortunately, multiple reviews in microleakage have questioned the validity of this method to predict clinical performance of dental composites and other restorative materials (172-174). Much of the uncertainty comes from lack of standardization between the studies. Usually many investigations reporting on the same material are not comparable because several of the experimental parameters are not the same or are not

included in the description of the study. It is been shown that differences in the type of curing light, layering technique, and composite structure or physical characteristics lead to different microleakage results (175, 176). Therefore drawing conclusions from only one study is not reliable.

The technique is usually very simple and inexpensive. It is performed by doing a dental restoration on an extracted tooth, followed by protective varnish coating of every surface except for the tooth-restoration margin. The tooth or teeth are then immersed in a specific dye, usually methylene blue, rhodamine or silver nitrate, although other dyes have been used as well. The specimens are stored with the dye between 2 and 24 hours, after storage they are removed from the solution and sectioned into two halves or more. The specimens' sections are scrutinized by optical means for visualization of the dye penetration into the interface (Fig. 1.9a) (85).

One of the major criticisms of *in-vitro* microleakage studies comes from the destructive nature of the test, as mentioned before usually two or more sections are evaluated, which are intimately related. The evaluated zone then depends on how many sections were obtained and also where the specimens were cut, which is usually done randomly. These sections might be not representative of the microleakage around the whole restorative material as it is only a two dimensional evaluation on some specific zones of the restoration.

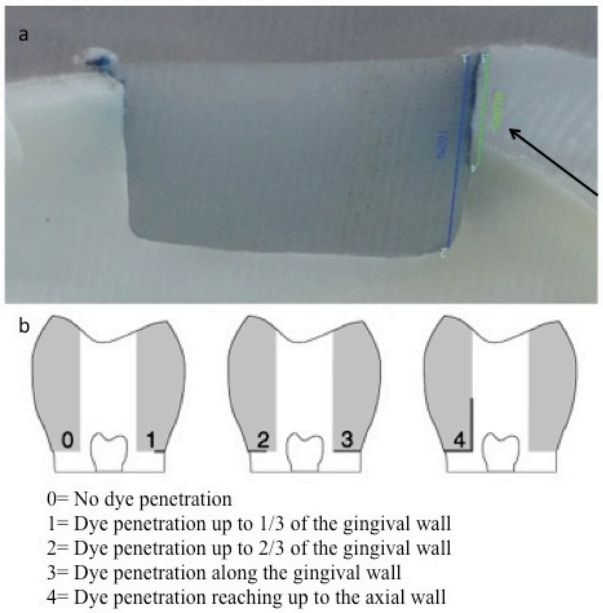

Figure 1.9 (a) Example of dye penetration in one tooth section, in this case the level of penetration is calculated as the percentage of the length of the wall (177). (b) Example of a non-parametric scale for semi-quantification (178).

Another main shortcoming is the qualitative character of the method. After sectioning, the penetration of the dye along the interface is confirmed or not by visual inspection using a microscope. The results are then reported as positive or negative for penetration. In an attempt to add some level of quantification some rating scales of the penetration have been suggested (Fig. 1.9b). The problem is that different rating scales are commonly reported. Currently, there is no correlation among the different scales, besides the fact that in general a higher number in the scale indicates greater penetration into the interface (173), therefore comparing results or establishing a microleakage rating among the materials for further clinical correlation becomes almost impossible.

More recent efforts are done to improve the microleakage technique by applying non-destructive 3D methods and a quantitative analysis (173, 179) (see chapter 2). A main conclusion from these studies is that microleakage is greatly non-uniform therefore what is seen in one section of the tooth does not correlate with other sections. This highlights the need for improving current techniques.

All mentioned above might partially explain why there has been no correlation between the amount of microleakage and the clinical performance of dental composite restorations.

1.8 Problem Statement

In summary, considering all the reviewed topics above it is clear that the performance of dental composite restorations depends greatly on the integrity of the bonded interface. The breakdown of the interface might lead to higher incidence of secondary caries. To achieve bond to the tooth structure dental composites system rely on the use of dental adhesives. A complex joint is then formed by the modified tooth substrate (hybrid layer or bonded layer), the adhesive system and the composite material. Each of the components of the interface is susceptible to failure by many different factors. Polymerization shrinkage stress generated by dental composites during curing induces microspaces at the bonded interface that can be later colonized by oral biofilm leading to secondary caries. In addition, mechanical challenge coming from mastication or other parafunctional habits can further expand any initial flaw contained in the bonded area. Biochemical degradation may also take place when the interface is exposed to water, oral fluids or chemicals coming from food sources. So far many studies have focused in the role of saliva and water in the breakdown of the interface, but much less is know about the degradation potential of the oral biofilm.

Moreover, common techniques to study the interfacial integrity such as bond strength tests including the macro and micro variants of tensile and shear test, and microleakage present several limitations that might conduct to misleading conclusions.

In the first part (chapter 2 and 3) two innovative techniques to study the interfacial integrity of dental composite restorations are proposed. The next section is focused on the study of the role of a multispecies biofilm on the degradation of the interface of model composite restoration (chapter 4). The last section presents a model to study the combined effect of mechanical loading and microbial challenge on the integrity of the interface (chapter 5).

1.9 Aims

Aim 1. To develop a method for quantifying leakage in composite resin restorations after curing, using non-destructive X-ray micro-computed tomography (micro-CT), silver nitrate staining and image segmentation. (Chapter 2)

- Sub-aim 1. To obtain a three-dimensional rendering of leakage behavior around a dental composite restoration using micro-CT.
- Sub-aim 2. To quantity leakage around class-I composite restorations using micro-CT and image segmentation.
- Sub-aim 3. To compare leakage around dental restorations performed with a low-shrinkage composite system and a high shrinkage composite system.

Aim 2. To develop a variant of the disk in diametral compression or Brazilian Disk Test to measure dentin-composite interfacial bond strength. (Chapter 3)

- Sub-aim 1. To develop a suitable specimen to measure dentin bond strength using disk in diametral compression test.
- Sub-aim 2. To assess dentin bond strength of several adhesive/composite systems using a variant of the disk in diametral compression.
- Sub-aim 3. To evaluate the interfacial failure in a disk under diametral compression using Acoustic Emission and Digital Image correlation.
- Sub-aim 4. To compare bond strength values and failure mode among different combinations of adhesive and composite systems.

Aim 3. To test the hypothesis that multiespecies oral biofilms play a role in the degradation of the dental composite interface in a dentin disk model. (Chapter 4)

- Sub-aim 1. To study the effect of a multispecies oral biofilm on the interfacial integrity of dental composite model restorations.
- Sub-aim 2. To evaluate the effect of the presence of sucrose in the oral biofilm-interface interaction.
- Sub-aim 3. To study the influence of the composite formulation on the interaction between a multispecies biofilm and interfacial integrity.

Aim 4. To test the hypothesis that the combined effect of mechanical loading and oral biofilm further reduces the fracture strength of restored teeth in a human tooth model. (Chapter 5)

- Sub-aim 1. To study the combined effect of a multispecies biofilm and mechanical loading on the interfacial integrity of dental restorations.
- Sub-aim 2. To evaluate the role of sucrose on the combined effect of mechanical and microbial challenge on the adhesive interface.

Chapter 2. The Use of Micro-CT with Image Segmentation to Quantify Leakage in Dental Restorations

This chapter consists of the manuscript published in Dental Materials. I am the primary author of this paper. I participated in the design of the experiments and conducted the experimental trials. I worked in collaboration with a researcher from the college of science and engineering to develop a method for image segmentation.

Summary

Objective: To develop a method for quantifying leakage in composite resin restorations after curing, using non-destructive X-ray micro-computed tomography (micro-CT) and image segmentation.

Methods: Class-I cavity preparations were made in 20 human third molars, which were divided into 2 groups. Group I was restored with Z100 and Group II with Filtek LS. Micro-CT scans were taken for both groups before and after they were submerged in silver nitrate solution ($AgNO_3$ 50%) to reveal any interfacial gap and leakage at the tooth restoration interface. Image segmentation was carried out by first performing image correlation to align the before- and after-treatment images and then by image subtraction to isolate the silver nitrate penetrant for precise volume calculation. Two-tailed Student's t-test was used to analyze the results, with the level of significance set at $p<0.05$.

Results: All samples from Group I showed silver nitrate penetration with a mean volume of 1.3 ± 0.7 mm^3. In Group II, only 2 out of the 10 restorations displayed infiltration along the interface, giving a mean volume of 0.3 ± 0.3 mm^3. The difference between the two groups was statistically significant ($p < 0.05$). The infiltration showed non-uniform patterns within the interface.

Significance: We have developed a method to quantify the volume of leakage using non-destructive micro-CT, silver nitrate infiltration and image segmentation. Our results confirmed that substantial leakage could occur in composite restorations that have imperfections in the adhesive layer or interfacial debonding through polymerization shrinkage. For the restorative systems investigated in this study, this occurred mostly at the interface between the adhesive system and the tooth structure.

2.1 Introduction

One of the major functions of a dental restoration is to cover the exposed dental tissues following caries removal. A tight seal around the margin will provide protection against pulpal damage and recurrent tooth decay (85). Despite the many advances in adhesive technologies, it remains a challenge to adequately seal the restoration margins and prevent leakage for a sufficiently long period of time. Therefore, new adhesive systems and composite materials are still being developed which require assessment (54).

Several techniques have been used to assess interfacial gap formation and microleakage, but the results vary considerably (53). The majority of them involve the use of dyes as tracers: a dental restoration is immersed in a specific dye solution for a period of time, after which the specimen is sectioned for visual examination of dye penetration around the restorative material (85). One of the main drawbacks of this method is that it only provides a qualitative assessment, namely, confirmation of the presence or absence of the dye in the particular section studied. A variant of this approach incorporates a non-parametric scale, providing a semi-quantitative score according to the degree of dye penetration. However, the score definitions and the scale used vary among the studies, making the results from them not comparable. This qualitative or semi-quantitative evaluation makes the test itself not very reliable or discriminative. In addition, evaluation can only be carried out in the plane through which the sample is sectioned, which can be misleading because dye infiltration does not occur uniformly throughout the interface (see later). Therefore, it is necessary to develop techniques to accurately quantify interfacial leakage.

X-ray micro-computed tomography (micro-CT) has been used recently to study composite shrinkage, gap formation and microleakage (180-184). It allows 3D reconstruction of the entire dental restoration and its surrounding tissues. The different components are identified based on the differences in their ability to attenuate the X-ray, with the differences being converted into a range of greyscale values. Micro-CT has the advantage of being non-destructive, i.e., the specimens do not need to be destroyed, allowing them to be reused for temporal assessment, for example.

In order to use micro-CT to study interfacial integrity in composite restorations, a radiopaque dye is often necessary (181, 182). This is because the low density of most dental adhesives makes it difficult to distinguish them from any gaps that may form at the tooth-restoration interface. Previous studies exploring marginal infiltration of glass-ionomer sealant (181) and Class-II composite restorations (182) showed that marginal leakage along the interface could be traced when micro-CT is used in combination with a radiopaque dye. However, in both of these studies only a cross-sectional analysis was performed, with a non-parametric scale being applied to assess infiltration. The assessments were therefore only semi-quantitative, as explained above.

3D analysis of polymerization shrinkage of a dental composite and the resulting gap formation has been performed using micro-CT to predict microleakage (183, 184). In (183), composites placed in plastic holders with different volumes were studied. To evaluate shrinkage, the volume of the composite before and after curing was calculated after 3D reconstruction. Also, direct measurement of the gap between the composite and the holder was performed to predict leakage. Gap formation and, hence, the predicted microleakage was shown to be non-uniform around the interface, being highly dependent on the C-factor, i.e. the ratio between the bonded and unbonded surfaces, and the composite volume (183). A later study reported similar results when composite restorations were placed in human molars (184). These studies showed that 3D quantitative assessment of microleakage could be obtained with micro-CT, which overcame one of the main disadvantages of conventional techniques for microleakage analysis. However, in both of these studies an adhesive was not used in order to simplify the system, possibly because the radiolucency of the adhesive would make it difficult to differentiate it from a gap in the micro-CT images. Needless to say, clinically, the adhesive plays an important role in the formation of interfacial gaps and must therefore be included when microleakage and gap formation are being studied. Additionally, in the latter study (184) the dental restoration was placed only in the dentin portion of the cavity, leaving bonding to the enamel surface out of the investigation. The reason for this omission was the difficulty to separate the grey values of enamel and those of the restoration in the CT images.

In order to properly assess leakage, it is important to replicate the clinical situation as closely as possible in any in vitro study by involving all the components in a restored tooth. To overcome the limitations associated with the techniques mentioned above, the aim of this study is to propose an improved and more comprehensive method using micro-CT to quantify interfacial leakage in dental restorations.

Recently, interfacial debonding of composites restorations that occurred during polymerization was monitored in situ using the Acoustic Emission (AE) technique (185). AE events were recorded in real time from human molars with Class-I cavities restored with either Z100™ (Z100) or Filtek™ LS (LS) (both from 3M ESPE, St. Paul, MN, USA) during curing. The number of AE events recorded from the specimens restored using Z100 was much higher than that found in the specimens restored with LS. The results were confirmed by micro-CT imaging which showed clear interfacial debonding in the former but not the latter. These AE results will be compared directly with the volumetric calculation of the dye penetrant obtained in this study.

2.2 Materials And Methods

Sample preparation

Twenty human third molars were selected for this study. The use of human molars was approved by the University of Minnesota Institutional Review Board. The teeth were cleaned by removing the soft tissues and hard deposits attached to the surface and then kept in 0.1% thymol solution. Class-I cavity preparations, approximately 2-mm high, 2-mm wide and 4-mm long, were made on the occlusal surface of each tooth. The teeth were divided randomly into two groups of 10. Group I was restored with Z100 (Table 2.1), which was considered for the purpose of this paper as a high-shrinkage composite. Group II was filled with LS (Table 2.1), a low-shrinkage composite by comparison. For Group I, total etching of the tooth cavity was performed with 37% Scotchbond™ Etchant for 20 s, followed by rinsing with the triple syringe for 40 s. Adper™ Single Bond II (3M ESPE, St. Paul, MN, USA) was then used as the bonding system. For Group II, Filtek™

LS System Adhesive (3M ESPE, St. Paul, MN, USA), a self-etch primer and bonding system, was used. The manufacturer's guidelines were followed closely when applying the bonding systems. After placing the bonding system, the corresponding composite, either Z100 or LS (both A2 shade), was placed incrementally into the cavity. Each layer of composite, which was no more than 2-mm thick, was cured for 40 s, utilizing an Elipar™ S10 LED curing light (3M ESPE, St. Paul, MN, USA) with an irradiance of 1200 mW/cm^2. Thereafter, each restoration was polished by using a polishing cup.

Table 2.1 Compositions of composites and adhesives used for Class-I restorations (obtained from manufacturer's data sheets (3M ESPE))

Product	Composition	Batch number
Z100™ Restorative	Silane treated ceramic, triethylene glycol dimethacrylate (TEGDMA), bisphenol a diglycidyl ether dimethacrylate (BISGMA), 2-benzotriazolyl-4-methylphenol.	N362970
Filtek™ LS Low Shrink Posterior Restorative	Silane treated quartz, 3,4 epoxycyclohexylcyclopolymethylsiloxane, bis-3,4 epoxycyclohexylethyl-phenyl-methylsilane, yttrium trifluoride, mixture of other by-products mixture of epoxy-mono-silanole by-products, mixture of epoxyfunctional di- and oligo-siloxane by-products, mixture of alpha-substituted by-products borate(1-), tetrakis(pentafluorophenyl)-(4-(methylethyl)phenyl)(4-methylphenyl)iodonium.	N296926

Adper Single Bond Plus	Ethyl alcohol, silane treated silica (nanofiller), bisphenol a diglycidyl ether dimethacrylate (BISGMA), 2-hydroxyethyl methacrylate(HEMA), glycerol 1,3-dimethacrylate, copolymer of acrylic and itaconic acids, water, diurethane dimethacrylate (UDMA) diphenyliodonium hexafluorophosphate, ethyl 4-dimethyl aminobenzoate (EDMAB).	N509492
Filtek™ LS System Adhesive Self-Etch Primer and Bond	Primer: Bisphenol a diglycidyl ether dimethacrylate (BISGMA), 2-hydroxyethyl methacrylate (HEMA), Phosphoric acid-methacryloxy-hexylesters mixture, ethanol, water, silane treated silica, 1,6-hexanediol dimethacrylate, (dimethylamino)ethyl methacrylate, Copolymer of acrylic and itaconic acid, Phosphine oxide, Dl-camphorquinone, Ethyl 4-dimethyl aminobenzoate, Methyl alcohol	N348567
	Bond: Substituted dimethacrylate, silane treated silica, triethylene glycol dimethacrylate (TEGDMA), phosphoric acid methacryloxy- hexylesters mixture, Dl-camphorquinone, 1,6-hexanediol dimethacrylate.	N391675

Each sample was then positioned in a plastic holder and fixed with acrylic resin with the purpose of avoiding sample movement during the experiment (Fig. 2.1). The holder was specially machined to generate an interlock with the supporting base attached to the stage inside the micro-CT chamber so that the sample could be placed in the same position and orientation for scanning before and after treatment with silver nitrate. The crown was covered with nail polish, leaving a gap of ~1 mm around the tooth-restoration interface. This allowed the silver nitrate to penetrate the interfacial gaps that might form and prevented it from entering the interface through other defects on the crown surfaces.

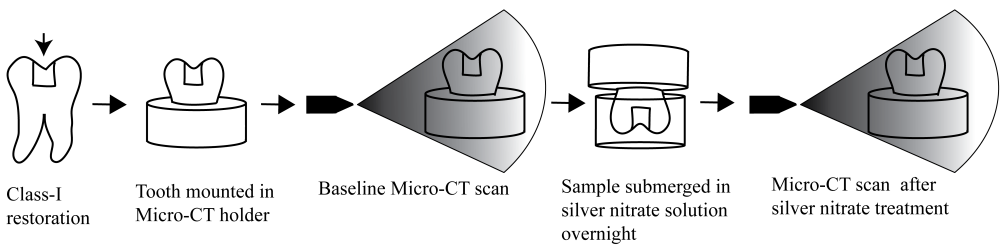

Figure 2.1 Experimental set up and workflow for the leakage study: A Class-I restoration was placed on the occlusal surface of a third molar. The restored tooth was then fixed within a holder with acrylic resin for micro-CT scanning. A baseline scan was first obtained before the restored tooth was submerged in $AgNO_3$. After that, a second micro-CT scan was taken using the same position and operational parameters as for the baseline.

Scanning and $AgNO_3$ Treatment

Scanning of the specimens was performed using a Micro-CT machine (XT H 225, Nikon Metrology Inc., Brighton, MI, USA); see Fig. 2.1. The scanning parameters used were 90 kV, 90 μA, 708 ms of exposure, 720 projections and 4 frames per projection. The position of each specimen within the micro-CT machine for the baseline scan was stored in a file that could be loaded in a subsequent scan to return it back to the same position (Fig. 2.1). The total scanning time was approximately 30 minutes for each specimen. A small piece of wet cotton was used to cover the specimen to prevent it from drying and cracking during scanning.

To reveal any interfacial defects or debonding between the restoration and the tooth structure after curing, the specimens were submerged in a radiopaque silver nitrate solution ($AgNO_3$, 50% w/w) (182) overnight (Fig 2.1). The pH of the $AgNO_3$ solution was measured as ~3.3.

Both groups were subjected to a second scan after submersion in the $AgNO_3$ solution (Fig. 2.1). The same scanning parameters as those for the baseline scans were used to ensure consistency in the greyscale values. The baseline sample position was then loaded to ensure that each specimen was rescanned in the same position within the micro-CT machine to minimize misalignment of the two image sets.

Image processing

3D reconstructions were done using the software CT Pro 3D (Nikon metrology, Inc., Brighton, MI, USA). The same volume of interest (VOI) was used for both the baseline and post-treatment scans to give the same spatial resolution. Initial visualization and 3D rendering was performed using VGStudio MAX 2.1 (Volume Graphics GmbH, Heidelberg, Germany). All the reconstructed images were scrutinized, slice-by-slice, for silver nitrate penetration, as indicated by a bright line formed by the radiopaque dye along the interface. For comparison, a series of bucco-lingual cross-sectional images were retrieved from both the baseline and the post-treatment scans for each of the samples.

It was not possible to completely isolate the voxels corresponding to the penetrant in the post-treatment images (Fig. 2.2a) by simply selecting the narrow range of grey values for this material because some of the components of the restoration also had similar grey values. This can be seen in Fig. 2.2b in which the silver nitrate and the dense components in the restoration are highlighted by the same false color. To overcome this issue, an image correlation function was used to align the images taken before and after dye penetration as- shifting of images in space was likely the result of play in the fixture and/or the moving table of the micro-CT system (186). The image alignment was followed by image subtraction to remove the composite restoration and dental tissues from the images, leaving behind the silver nitrate only (Fig. 2.2c). Thus, the grey values of the baseline images were subtracted from those of the post-treatment images. The image processing was carried out using MATLAB and the Image Processing Toolbox (Mathwork®) (187). The image subtraction procedure resulted in new image stacks, which could then be rendered to reveal the thin layer of silver nitrate in 3D space (Fig. 2.2d). The final subtracted images were exported as bmp extension files for further analysis.

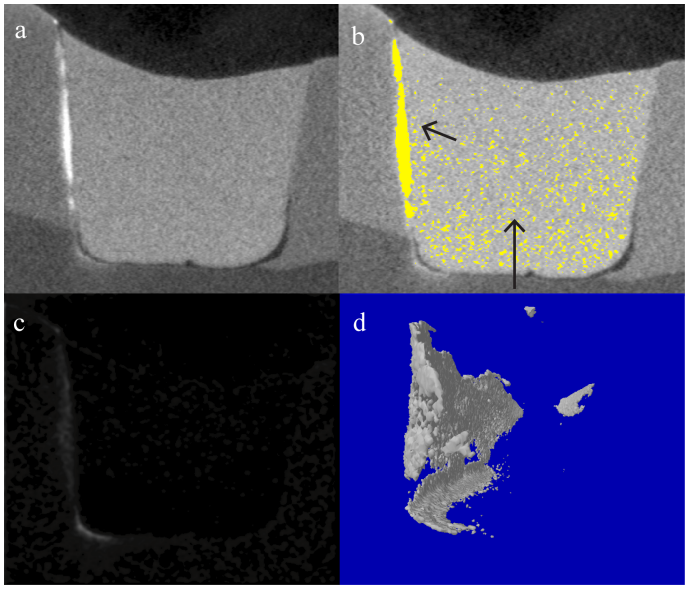

Figure 2.2 (a) Image from a Group-I sample of the penetrant along the tooth-restoration interface. (b) A false color plot illustrating the difficulty to isolate the silver nitrate penetrant which shares the same grey values with the dense components in the restoration. (c) Image of the penetrant isolated after image subtraction. (d) 3D rendering of the silver nitrate penetrant using the subtracted image stack.

In theory, only the voxels corresponding to the silver nitrate penetrant would have non-zero grey values after image subtraction. However, the presence of noise resulted in regions with non-zero grey values that were not occupied by silver nitrate. To better quantify the silver nitrate penetration, the resulting subtracted images were further processed using SkyScan CT-analyzer Version 1.1 (Bruker microCT, Kontich, Belgium). First, a region of interest was defined to remove most of the background information. A threshold grey value was then selected to remove the remaining background and to reduce the noise for the subsequent image binarization step. The threshold value was chosen such that the amount of silver nitrate identified at the tooth-restoration interface was not altered significantly while removing the remaining background and noise elsewhere, as shown in Figs. 2.3a-b. The resulting binary images were visually compared with the post-treatment images to further confirm that the threshold value selected was

appropriate. 3D rendering of the silver nitrate penetration was then performed, followed by calculation of its volume and the mean value for each group of specimens.

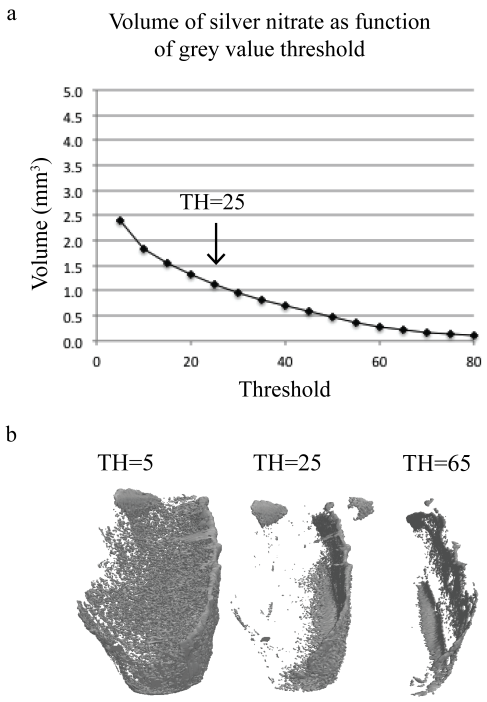

Figure 2.3 (a) Threshold grey value used to isolate volume of silver nitrate infiltration (indicated by the arrow) (b) An example of 3D rendering of the silver nitrate with different threshold (TH) grey values.

Scanning electron microscopy (SEM)

To further confirm the presence of silver nitrate, SEM was performed using a tabletop environmental scanning electron microscope (TM-3000, Hitachi, High-Technologies Corporation, Tokyo, Japan). This equipment allowed uncoated samples to be scanned. The crown was separated from the root and several cross-sections were obtained from it using an Isomet^{TM} diamond saw (Buehler, Lake Bluff, IL, USA). The SEM settings were: X50 magnification, COMPO mode and an operating voltage of 15 kV. The COMPO mode gives not only topographical details but also contrast to the image due to different

average atomic number composition within the sample. The higher the atomic number the brighter the image. Electron dispersive spectroscopy (EDS) was also performed to confirm the presence of silver nitrate.

2.3 Statistical Analysis

A two-tailed Student's t-test (Microsoft® Excel® 2011, version 14.2.4) was carried out to determine if there was a statistically significant difference in the mean volume of silver nitrate penetration between the two groups. The level of statistical significance was set at $p < 0.05$.

2.4 Results

At initial examination, all samples from Group I showed silver nitrate penetration to some degree (Fig. 2.4). Whereas in Group II, only 2 out of the 10 restorations displayed infiltration along the interface, and preliminary inspection showed that the amount of penetration was lower than that found in Group I (Fig. 2.5).

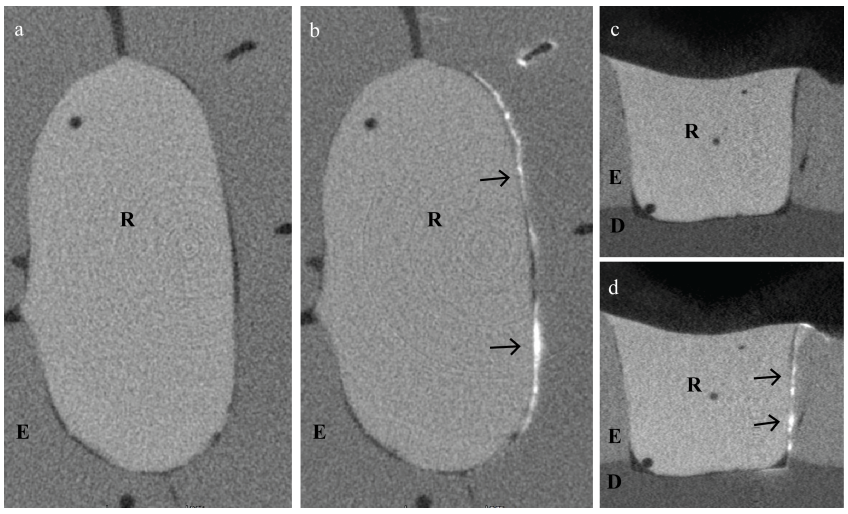

Figure 2.4 (a) and (c) are cross-sections from the top view and front view, respectively, of a sample from Group I before treatment with silver nitrate. (b) and

(d) show the same cross-sections after treatment with silver nitrate. The arrows indicate where traces of silver nitrate were found. R= restoration, E=enamel, D=dentin.

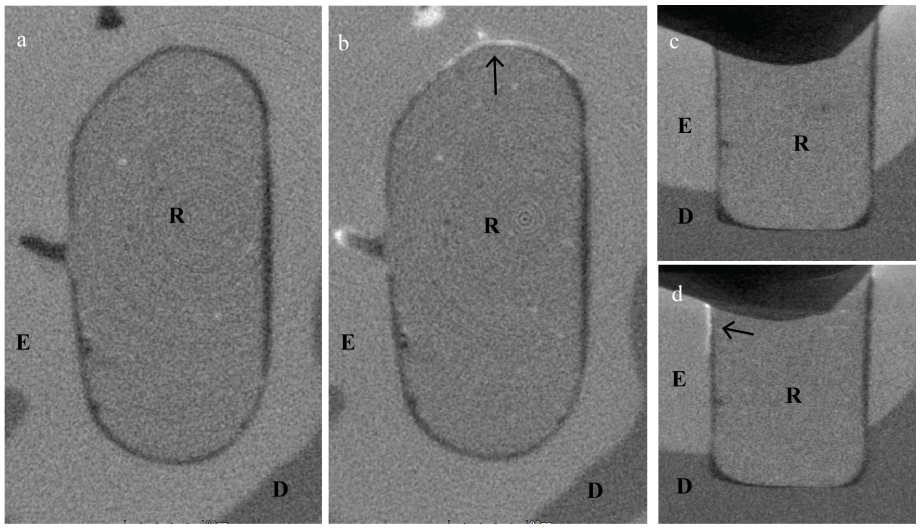

Figure 2.5. (a) and (c) are cross-sections from the top view and front view, respectively, of a sample from Group II before treatment with silver nitrate. (b) and (d) show the same cross-sections after treatment with silver nitrate. In this case, while traces of silver nitrate were found, as indicated by the arrows, the quantity was less than that in the Group-I sample (Fig. 2.4). R= restoration, E=enamel, D=dentin.

It can be seen that the silver nitrate penetration was non-uniform around the tooth-restoration interface, and tended to be on one side of the interface only. With regard to its exact position, it was found that the penetration mainly occurred between the adhesive system and the dental tissue for both materials. Figures 2.6a and 2.6b show SEM images of the sample selected from Group I, which confirmed that silver nitrate penetration had taken place between the adhesive (dark grey) and the tooth tissues (light grey). The same trace of silver nitrate can be seen in the micro-CT image of approximately the same section of the same sample in Fig. 2.6c, albeit at a lower resolution.

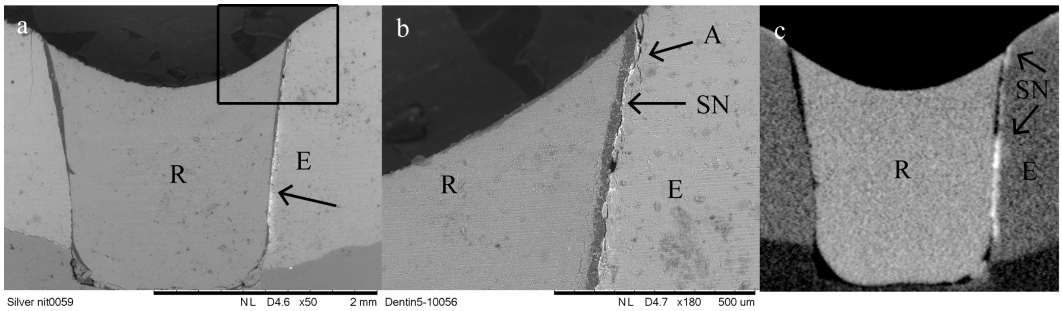

Figure 2.6. (a) Silver nitrate penetration (shown in white and indicated by the arrow) under SEM examination. (b) A magnified view of (a), showing that the infiltration and hence debonding took place between the enamel and the adhesive. (c) A micro-CT image of the cross-section examined by SEM that shows the same infiltration of the penetrant. A= adhesive system, R= restoration, E= enamel, D= dentin and SN= silver nitrate.

Calculation of the volume of silver nitrate penetration (Table 2.2) showed that the specimens prepared with the high-shrinkage composite (Group I) displayed a higher amount of silver nitrate infiltration when compared to those made with the low-shrinkage composite (Group II). The mean values for Group I and Group II were 1.3 ± 0.7 and 0.3 ± 0.3 mm^3, respectively (Fig. 2.7a). The difference between the two groups was statistically significant ($p < 0.05$). Similar results can be seen in the number of AE events recorded (Fig. 2.7b) for specimens prepared with the same two composites (185).

Table 2.2 Volume of silver nitrate penetration (mm^3) along the interface in Class-I preparations restored with either a high- or low-shrinkage composite

Sample No.	Group I[a]	Group II[b]
1	1.4	0.0[d]
2	2.0	0.0[d]
3	1.4	0.0[d]
4	1.9	0.1
5	0.6	0.4
6	2.6	0.0[d]
7	0.7	0.0[d]
8	1.0	0.0[d]
9	0.9	0.0[d]
10	0.7	0.0[d]
Mean	1.3 (0.7)[c]	0.3 (0.3)[c]

[a] Group I = Class-I preparations restored with Z100 (high-shrinkage composite)
[b] Group II= Class-I preparations restored with LS (low-shrinkage composite)
[c] Standard deviation
[d] Where silver nitrate was not found visually the volume of microleakage was assumed to be 0.0 mm^3

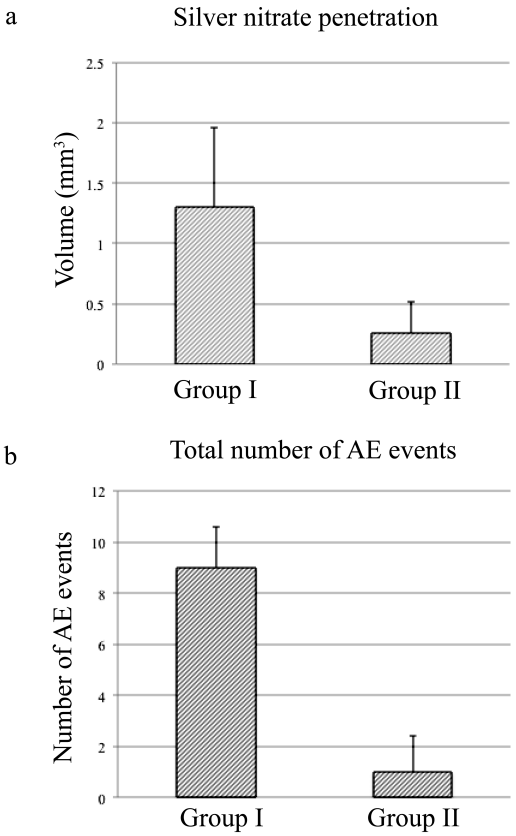

Figure 2.7 (a) Mean values of silver nitrate penetration along the tooth-restoration interface for Groups I and II. (b) Mean number of AE events recorded for Groups I and II. Taken from Li et al. (185). Group I are samples restored with Z100, while Group II are samples restored with LS.

2.5 Discussion

Given that failure of composite restorations due to secondary caries is still a major concern in operative dentistry (9, 188), issues such as polymerization shrinkage of composites, interfacial gap formation and leakage continue to be important research topics. We have presented here a technique, using radiopaque dye penetration, Micro-CT and image segmentation, to quantify leakage at the tooth-restoration interface. This approach has the advantage of being non-destructive, quantitative and 3D in its analysis. Specifically, it allows the spatial distribution of the interfacial leakage along the cavity

walls and floor to be visualized in 3D, which cannot be obtained easily using traditional techniques that require sectioning of the specimen. These features make this method much more comprehensive and quantitative. In contrast, traditional methods for microleakage studies can only provide limited, or even unrepresentative, information, unless multiple sections of the sample are analyzed.

The use of a radiopaque dye to highlight the defective or debonded areas is still necessary with the new technique if the low radiopacity of the adhesive systems, as was the case in this study, renders them indistinguishable from the background or the defects are too small for micro-CT to resolve.

As mentioned previously, micro-CT has been used to obtain 3D mapping of the polymerization shrinkage to predict microleakage (183). In that study, gap formation was calculated as the distance between the delaminated composite and the wall of a polymethyl-methacrylate mold that simulated the tooth cavity. Gaps greater than 16μm were considered to be "leaking". However, an adhesive was not used in that study. As a result, the interfacial gap formed was likely to be unrealistically large due to the lack of bonding, even though some of it could have been overcome by the shrinkage stress had an adhesive been used. A later study (184) reported that shrinkage mainly occurred at the top surface and gradually diminished with depth. However, leakage was predicted only qualitatively from the shrinkage profiles. Again, no bonding system was used in this later study. Therefore, the predicted leakage was probably overestimated.

The proposed technique, specifically the precise alignment and subsequent subtraction of images taken before and after submersion in silver nitrate, can overcome the aforementioned shortcomings, allowing the study of gap formation and leakage to be undertaken in a more realistic scenario, with all the components of a restored tooth being involved in the study.

Using image correlation and image subtraction, the volume of the silver nitrate penetration along the tooth-restoration interface could be calculated without interference from the restoration and the dental tissues. The remaining background and noise were separated from the images by setting to black the pixels with a grey value below a certain

threshold during the binarization. The threshold selection was guided by observation of the original post-treatment images before image subtraction.

The results presented herein showed a significantly greater amount of dye penetration in the samples restored with Z100, a high-shrinkage composite, when compared to those restored with LS, a low-shrinkage restorative material (Fig. 2.7a). These data are in agreement with a previous study that used AE to quantify debonding at the tooth-restoration interface during curing of the restorations (185). In that study, samples restored with Z100 displayed a much higher number of AE events during curing than those restored with the low-shrinkage composite LS (Fig. 2.7b). The current results showed that, for both groups, the infiltration mainly occurred between the bonding agent and the tooth structure. The adhesive-tooth interface therefore seemed to be the weakest part of the restorative system.

Our results also agree with those from Krifka et al. (189) in which Class-V restorations made with Filtek LS showed the lowest dye penetration before and after thermal and mechanical challenge, when compared to a group of methacrylate-based composite resins with varying viscosities. Bagis et al. (190) also found no microleakage in Class-II MOD restorations prepared with Filtek LS in comparison with restorations of nano-hybrid methacrylate based composites, made with either oblique or vertical layering techniques. However, in their study, only one cross-section per specimen was used and only the gingival aspect was assessed. Contrary to all the above results, a recent microleakage study that evaluated bucco-lingual sections of Class-V restorations in primary canines after thermo-cycling reported that LS performed better than methacrylate composite only when the adhesive system was used with acid etching. LS had the highest microleakage scores when used as indicated by the manufacturer (191).

Despite the use of incremental filling, significant leakage still occurred in the Z100 samples. It may be the case that the shrinkage stress, albeit reduced, was still high enough to cause gap formation. However, as shown by Sano et al. (94), the hybrid layer in this restorative system may contain imperfections. Their work demonstrated penetration of silver nitrate into the hybrid layer even in the absence of micro-sized interfacial gaps. The observed leakage was thought to occur through nano-sized paths and porosities within the

hybrid layer or within demineralized submicron spaces that failed to be completely sealed by the adhesive. The much lower dye penetration shown in the LS group might be explained by its low polymerization shrinkage, but LS uses a two-step self-etching adhesive that is different from the total etch and rinse used for Z100. Self-etch adhesives reduce the risk of incomplete resin infiltration by being able to infiltrate the exposed collagen with adhesive up to the same depth of demineralization (96). For this reason, some two-step self-etch adhesives have shown less nanoleakage when compared with a total etch adhesive (192, 193). It should also be noted that the penetration of the silver nitrate into the interfacial gap might not be complete. Also, when the silver nitrate reached the dentin, it could penetrate into the tubules. Therefore, the volume of leakage does not necessarily equal to that of the interfacial imperfections or gaps formed, although they are expected to be highly correlated.

2.6 Conclusions

We have developed a more comprehensive method to study interfacial leakage. Using silver nitrate infiltration and image subtraction, we were able to use micro-CT to quantify leakage in 3D, overcoming previous limitations with this technique. Our results confirmed that leakage occurred mostly at the interface between the adhesive system and the tooth structure. The same technique can be used to analyze leakage in other restorations types, for example sealants and dental implants.

2.7 Acknowledgement

We would like to acknowledge the Minnesota Supercomputer Institute (MSI), University of Minnesota, for the provision of Matlab software used for image alignment and subtraction; Dr. Robert Jones for his assistance in this study; and the National Institute of Health, USA, for their financial support through Grant 1 R01 DE021366.

Chapter 3. Dentin-Composite Bond Strength Measurement Using The Brazilian Disk Test

This chapter consists of the manuscript submitted for publication to Dental Materials. I am the first author of this paper. I participated in the design of the experiments and conducted the experimental trials. I worked in collaboration with members of the MDRCBB to develop a method for bond strength measurements

Summary

Objectives: This study presents a variant of the Brazilian disk test (BDT) for assessing the bond strength between composite resins and dentin.

Methods: Dentin-composite disks (ϕ 5 mm × 2 mm) were prepared using either Z100 or Z250 (3M ESPE) in combination with one of three adhesives, Adper Easy Bond (EB), Adper Scotchbond Multi-Purpose (MP) and Adper Single Bond (SB), and tested under diametral compression. Acoustic emission (AE) and digital image correlation (DIC) were used to monitor debonding of the composite from the dentin ring. A finite element (FE) model was created to calculate the bond strengths using the failure loads. Fracture modes were examined by scanning electron microscopy (SEM).

Results: Most specimens fractured along the dentin-resin composite interface. DIC and AE confirmed interfacial debonding immediately before fracture of the dentin ring. Results showed that the mean bond strength with EB (14.9±1.9 MPa) was significantly higher than with MP (13.2±2.4 MPa) or SB (12.9±3.0 MPa) ($p<0.05$); no significant difference was found between MP and SB ($p>0.05$). Z100 (14.5±2.3 MPa) showed higher bond strength than Z250 (12.7±2.5 MPa) ($p<0.05$). Majority of specimens (91.3%) showed an adhesive failure mode. EB failed mostly at the dentin-adhesive interface, whereas MP at the composite-adhesive interface; specimens with SB failed at the composite-adhesive interface and cohesively in the adhesive.

Conclusions: The BDT variant showed to be a suitable alternative for measuring the bond strength between dentin and composite, with zero premature failure, reduced variability in the measurements, and consistent failure at the dentin-composite interface.

Clinical significance:

The new test could help to predict the clinical performance of adhesive systems more effectively and consistently by reducing the coefficient of variation in the measured bond strength.

3.1 Introduction

An often cited reason for the failure of composite restorations is the breakdown of the tooth-composite interface (173), whereas mechanical forces resulting from composite polymerization shrinkage and/or mastication are the main reasons for this breakdown (139, 194). The marginal gaps thus formed around the restoration would allow bacterial invasion and biofilm accumulation, leading to secondary caries (55).

Bond strength testing is therefore routinely used to assess the interfacial strength between the tooth and restoration. Different bond strength tests have been developed over the years, with the shear (SBS) and tensile bond strength (TBS) tests being the most popular. However, there are certain drawbacks associated with these tests (148, 154, 159). For example, difficulties with machining, handling, aligning and fixing the matchstick specimens are some of the problems encountered in the TBS test (148, 159). Also, when the bond strength is comparable or higher than the fracture strength of the substrates, a high percentage of cohesive fracture in the substrates may result with the TBS test (152). Similarly, in the SBS test, cohesive failure often occurs within the dental or composite substrate (148, 153, 195). Obviously, for a bond strength test to be valid, failure must initiate from the interface (196). In addition to the above problems, analyses have shown that the stress distribution at the tooth-restoration interface of some of the specimens is highly non-uniform and greatly depends on the material property mismatch, specimen geometry and attachment conditions (155, 197-199). In the SBS test specimen, for example, the dominant stress state is that of tension rather than shear (154, 170, 198).

As an alternative bond strength test, we recently proposed a variant of the Brazilian disk test (BDT), or disk in diametral compression, to assess the interfacial debonding of endodontic posts from root dentin (200). The BDT has been used widely for testing the tensile strength and fracture toughness of brittle materials. It has also been used to test the interfacial fracture toughness of various dissimilar materials (201, 202). During the test, tensile stresses are introduced in the horizontal direction, i.e. transverse to the applied vertical compressive load. The force required to cause failure is used to estimate the tensile strength (203). In the previous work (200), the disk specimen consisted of a

slice of root dentin with a section of a circular post cemented in the enlarged concentric root canal. The dentin itself was surrounded by a layer of resin composite to form a disk of 10-mm diameter and 2-mm thick. Using the acoustic emission (AE) and digital image correlation (DIC) techniques, we confirmed that fracture of the disk under diametral compression was initiated by debonding at the post-dentin interface. Compared with some of the other bond tests for endodontic posts, the modified Brazilian disk test had the advantages of simpler specimen preparation and reduced variations in the results. In this paper, we introduce another modification of the BDT specimen that is more suitable for assessing the bond strength of direct composite restorations. Our goal is to determine whether the new test specimen would retain the advantages seen in its previous form for endodontic post testing. Again, DIC and AE were used to validate the test.

3.2 Materials and Methods

Sample preparation

The root portions from approximately 30 bovine incisors were removed and cut into two halves. The cut was made perpendicularly to the long root axis, with each half having an approximate length of 6-7 mm. From these, the halves that had a root canal larger than the intended diameter were rejected. Next, the canal of each selected root segment was enlarged with a 1.9-mm diameter fiber post drill (3M ESPE, Dental products, St. Paul, MN, USA) to obtain a circular hole of ~2-mm diameter. Afterwards, the root segments were trimmed down using a lathe to remove the cementum and the external layer of dentin to produce hollow dentin cylinders of 5-mm outer diameter and 2-mm inner diameter (Fig. 3.1).

The machined dentin cylinders were randomly assigned to three bonding systems: Total-etch Adper™ Single Bond Plus (SB), Self-etch Adper™ Easy Bond Adhesive (EB) and total-etch Adper™ Scotchbond™ Multi-Purpose Adhesive (MP); see Table 3.1. Each bonding system was applied to the inner surface of the hollow dentin cylinders with a microbrush and subsequently cured according to the manufacturer's instructions. After

this, the canal of each cylinder was restored with either Filtek™ Z250 Universal Restorative or Z100™ Restorative; see also Table 3.1. The composites were applied incrementally to minimize shrinkage stress, with each layer being less than 2-mm thick. The first increment was placed in the middle section of the cylinder and the subsequent increments placed at its ends. The first increment was cured from both ends for 20 s each. The end increments were cured from the respective ends of the cylinder for 40s. Light curing was done with an Elipar Trilight (3M ESPE, Dental Products, St. Paul, MN, USA) curing light operated at 800 mW/cm^2.

The filled dentin cylinders were cut using an Isomet^{TM} (Buehler, Lake Bluff, IL, USA) diamond saw into 2-mm thick dentin-resin composite disks; see Fig 3.1 and inset in Fig. 3.2. Around 2 to 3 disk specimens could be obtained from each root segment. The disks were examined for defects under a microscope (Olympus MVX10, Olympus America Inc.) with a magnification of 3.2X. Defective samples with pores on the surface, air bubbles that could be clearly seen in the composite, irregularities or cracks were removed from the study. A total of 15 to 17 disks were used for each group and they were stored in 0.1% thymol solution at 4°C overnight before testing.

Table 3.1 Compositions of composites and bonding systems used in this study.

Z100™ Restorative	Silane treated ceramic, triethylene glycol dimethacrylate (TEGDMA), bisphenol a diglycidyl ether dimethacrylate (BISGMA), 2-benzotriazolyl-4-methylphenol*.	N362970
Filtek™ Z250 Universal Restorative	Silane treated ceramic, bisphenol a polyethylene glycol diether dimethacrylate (BISEMA6), diurethane dimethacrylate (UDMA), bisphenol a diglycidyl ether dimethacrylate (BISGMA), triethylene glycol dimethacrylate (TEGMA), benzotriazol, ethyl 4-dimethyl aminobenzoate (EDMAB)*.	N326080

Adper Single Bond Plus	Ethyl alcohol, silane treated silica (nanofiller), bisphenol a diglycidyl ether dimethacrylate (BISGMA), 2-hydroxyethyl methacrylate(HEMA), glycerol 1,3-dimethacrylate, copolymer of acrylic and itaconic acids, water, diurethane dimethacrylate (UDMA) diphenyliodonium hexafluorophosphate, ethyl 4-dimethyl aminobenzoate (EDMAB) *.	N509492
Adper™ Easy Bond Self-Etch Adhesive	Bisphenol a diglycidyl ether dimethacrylate (BISGMA), 2-hydroxyethyl methacrylate, ethanol, water, phosphoric acid-6-methacryloxy-hexylesters, silane treated silica, 1,6-hexanediol dimethacrylate, copolymer of acrylic and itaconic acid, (dimethylamino)ethyl methacrylate camphorquinone, 2,4,6-trimethylbenzoyldiphenylphosphine oxide*.	N497589
Adper™ Scotchbond™ Multi-Purpose Adhesive	Primer: Water, 2-hydroxyethyl methacrylate (HEMA), copolymer of acrylic and itaconic acids Bond: Bisphenol a diglycidyl ether dimethacrylate (BISGMA), 2-hydroxyethyl methacrylate (hema), triphenylantimony*.	N491015 N494505

***Obtained from manufacturer's data sheets (3M ESPE).**

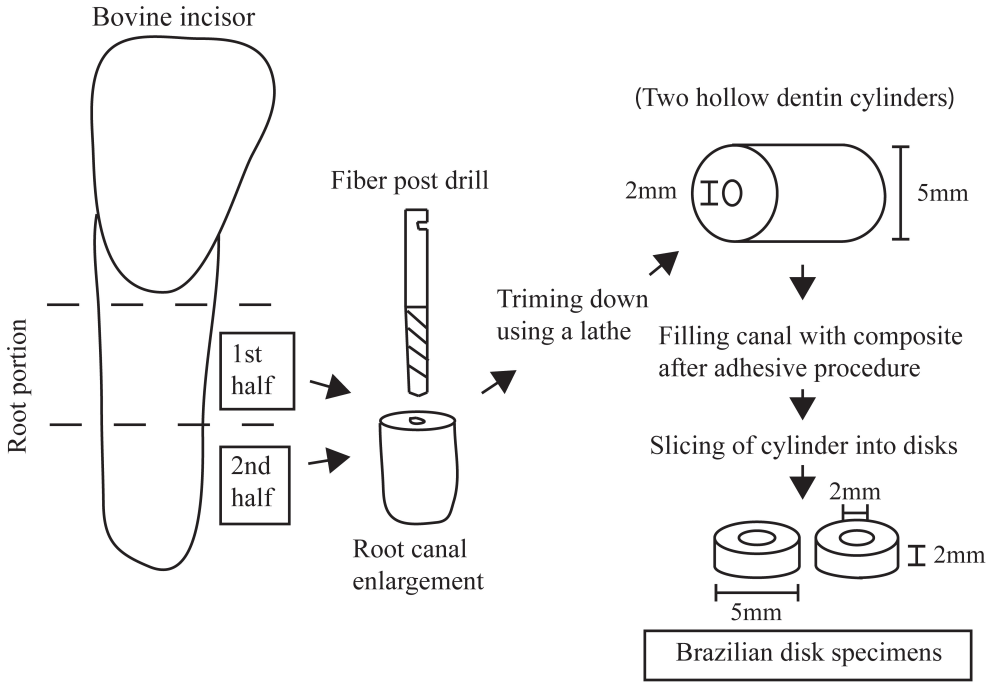

Figure 3.1 Schematic representation of the technical steps to obtain the modified Brazilian disk.

Diametral compression

The diametral compression test was carried out using a Universal Test Machine (858 Mini Bionix, MTS, USA), with the specimen located between two steel components with flat surfaces (Fig. 3.2). A loading rate of 0.5 mm/min was applied to fracture the samples. The load and displacement time histories were recorded during the loading process.

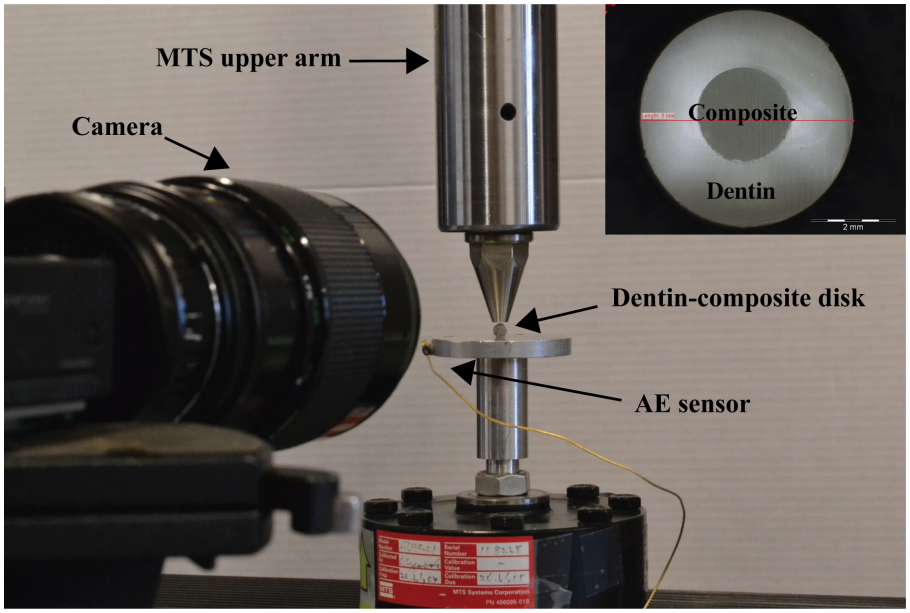

Figure 3.2 Experimental setup for diametral compression, digital image correlation and acoustic emission measurement. Inset: Modified Brazilian disk for assessing interfacial debonding between root dentin and direct composite restoration.

Acoustic Emission (AE) measurement

An AE system (Physical Acoustics Corporation, NJ, USA) was used to monitor microcracking of the specimens during loading. The AE sensor was attached to the lower support plate (Fig. 3.2). Signals detected by the sensor were passed through a preamplifier of 10-dB gain with a band pass of 100 kHz-2MHz and a threshold set at 35 dB. The AE results were used together with the load time histories and DIC data (see below) to identify the point at which interfacial debonding first occurred.

Digital Image Correlation (DIC)

Surface deformation of the disks was measured by using DIC to identify interfacial debonding. This technique utilized a non-contact optical method for tracking movements of surface features. The system consisted of a high-speed CCD camera (Point Grey

Grasshopper GRAS-20S4C-C) and propriety software (DaVis 7.2, LaVision-GmbH, Goettingen, Germany) for displacement and strain calculation (Fig. 3.2b). To allow deformations to be determined, the disk surface facing the CCD camera was first sprayed with a white fixation paint (Krylon products group, Cleveland, OH, USA) followed by a thin layer of charcoal particles (Sigma Aldrich, St. Louis, MO, USA). These created irregular speckles on the surface for local displacement tracking. A reference image was taken before the specimen was loaded. During loading, further images were taken at 10-20 frames per second (fps) for comparison with the reference image. The proprietary software was then used to calculate the full-field strain maps, and interfacial debonding could be identified from the strain concentration developed.

Finite Element (FE) simulation

There is no simple analytical solution for the stress distribution within the dentin-composite disk. The FE method was therefore used to calculate the interfacial bond strength based on the load that caused debonding. Due to symmetry, a 2-D model representing a quadrant of the disc specimen (Fig. 3.3a) was constructed using Hypermesh 11.0 (HyperWorks, Altair Engineering, Troy, MI, USA). Appropriate boundary conditions were assigned to the vertical and horizontal planes of symmetry of the quadrant model (Fig. 3.3a). A point load was applied downward at the topmost node of the model to simulate diametral compression. To capture the stress distribution at the dentin-composite interface accurately, the regions around the interface were meshed more finely than other regions. This numerical model was then exported to ABAQUS (version 6.10-EF1; Dassault Systèmes Simulia, Waltham, MA, USA) to solve for the stresses. The model was meshed with the plane-stress elements CPS4I and CPS3 (204). All materials were assumed to be isotropic, homogeneous and behave linear elastically. The material properties for each component are listed in Table 3.2. Figure 3.3b shows the radial stress distribution within the disk and the node at the interface (indicated by the arrow) where debonding was assumed to initiate.

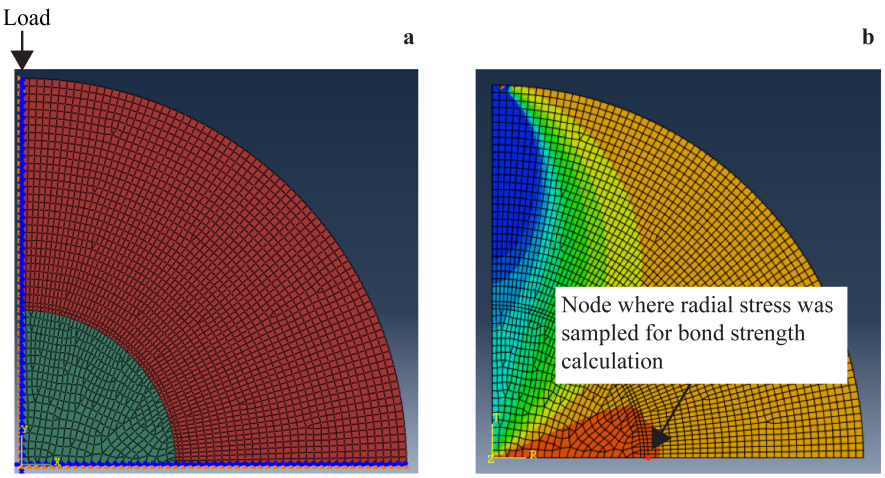

Figure 3.3 (a) 2-D quadrant FE model for the dentin-composite disk specimen. Load was applied at the topmost node, indicated by the arrow. (b) Radial stress distribution within the disk specimen. The arrow indicates the node where stress was sampled for bond strength calculation.

Table 3.2 Material Properties for the Finite Element Models

Material	Elastic modulus (GPa)	Poisson's ratio	Reference
Z100	8.5	0.3	(205)
Z250	12	0.3	(206, 207)
Dentin	18.6	0.31	(208)

Scanning electron microscopy (SEM)

To evaluate the mode of interfacial debonding, SEM images of the fracture surfaces of the specimens were obtained using an environmental scanning electron microscope (TM-3000, Hitachi, High-Technologies Corporation, Tokyo, Japan) with the following settings: X50 magnification, compo mode and 15 kV.

3.3 Statistical Analysis

A two-way analysis of variance (ANOVA) was used to explore the effect of the composite and adhesive systems on the bond strength and the interaction between them. To determine whether a significant difference in bond strength existed among the different combinations of composites and adhesives, a one-way Anova was carried out using Tukey's HSD test as the *post hoc* test. Fisher's exact test was used to analyze the failure modes and their association with the composite and adhesive systems used. SAS® 9.3 Software (SAS Institute Inc., Cary, NC, USA) was used to perform the statistical analysis.

3.4 Results

Figs. 3.4a and 3.4b show a disk specimen before and after fracture when subjected to diametral compression. Fig. 3.4c shows a different specimen after fracture with the paint removed from the surface. Most of the specimens (n=84) fractured along part of the dentin-composite interface, with the fracture path extending into the dentin roughly along the vertical diameter, as indicated by the arrows in Fig. 3.4c. Eight specimens (8.7%) had fracture involving the composite. From the DIC results (Fig. 3.4d), which showed the emergence and evolution of strain concentrations on the disk surface, it was observed that in most of the specimens debonding at the interface took place before the fracture extended into the outer dentin ring (Figs. 3.4d).

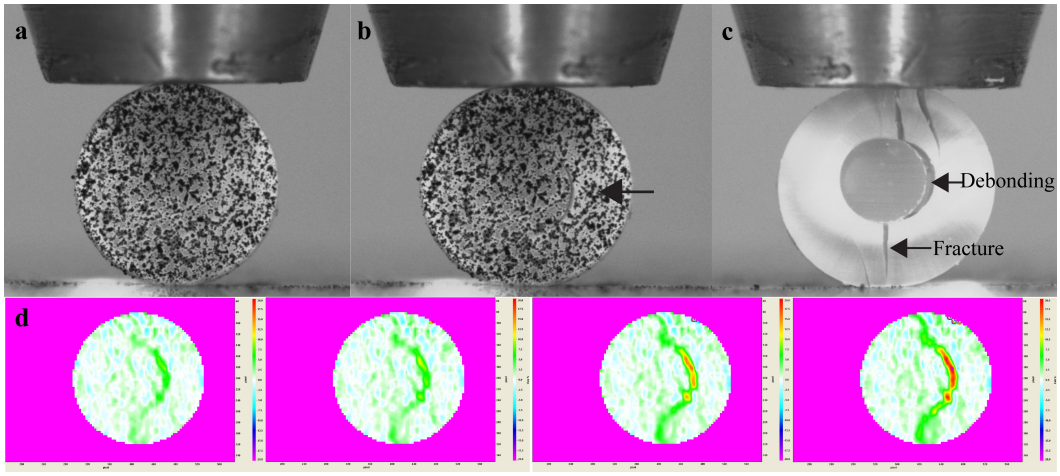

Figure 3.4 A dentin-composite disk subjected to diametral compression. (a) Disk specimen before loading - its surface had been sprayed with white paint and black powder to create speckles for DIC analysis. (b) The same specimen after fracture, with debonding between the restorative material and the dentin ring as indicated by the arrow. (c) A different specimen with painting removed to reveal the fracture pattern. (d) DIC results showing the emergence and spread of strain concentrations during diametral compression.

Most of the samples exhibited an approximately linear load-displacement behavior until the first peak was reached (Fig. 3.5a). The first partial drop in load coincided with the appearance of the strain concentrations at the dentin-composite interface in the DIC images (Fig. 3.4d) as well as the first major AE signal. Thus, the first load peak was taken to be the load that caused interfacial debonding. The climbing to the second peak and the subsequent complete drop in load showed, respectively, the loading and final separation of the two halves of the debonded disk. It can be seen that both the interfacial and bulk fractures were preceded by the occurrence of AE events (Fig. 3.5a).

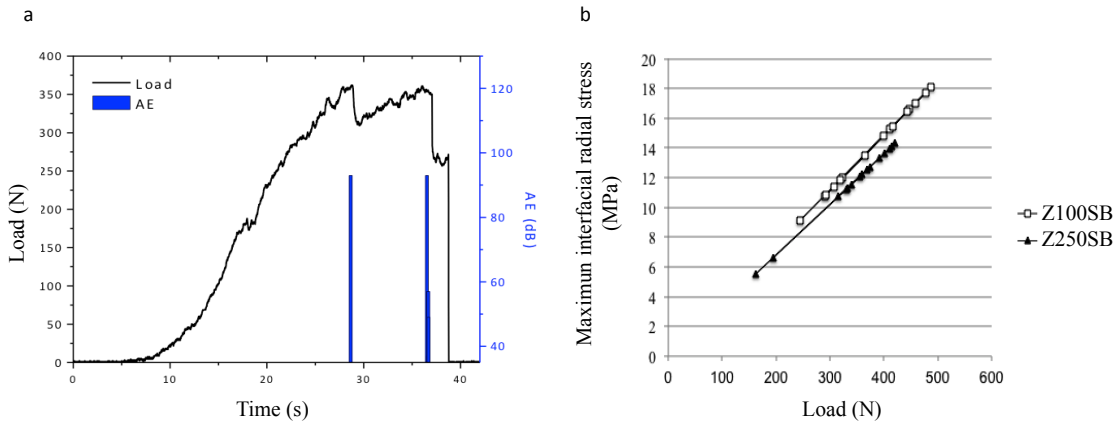

Figure 3.5 (a) A typical time history of the load and AE events for the dentin-composite disk specimen. (b) The maximum interfacial radial stress as a function of load (□ Z100, ▲Z250).

Fig. 3.5b shows the FE-predicted maximum interfacial radial stress (the one responsible for debonding) as a function of load for the two material systems. The results for bond strength, as derived from using the first peak load (Fig. 3.5a), are summarized in Table 3.3. From the table, it can be noted that the mean bond strength values for the different bonding systems had the following ranking: EB > MP > SB, irrespective of whether Z100 or Z250 was used. With Z250, the bond strength with EB was significantly greater than those with MP and SB ($p<0.05$); but no significant differences were detected between SB and MP. Despite showing the same trend, no significant differences were detected amongst the adhesives when Z100 was used.

Two-way ANOVA analysis confirmed that there was no interaction between the bonding system and the composite ($p>0.05$). However, the individual effects of the composite and the adhesive system on the bond strength were statistically significant ($p<0.05$ for both). When the results for all three adhesives were pooled together, Z100 gave significantly higher bond strength than Z250 ($p<0.05$).

Table 3.3 Mean, ± standard deviation and coefficient of variation (CV) for dentin bond strength (DBS) of each combination of adhesive and composite.

	Z100 DBS (MPa)	CV (%)	Z250 DBS (MPa)	CV (%)
EB	15.4 (2.1)^{Aa}	13.6	14.3 (1.4)^{Aa}	9.8
MP	14.1 (1.7)^{Aa}	12.1	12.2 (2.5)^{ABa}	20.5
SB	14.0 (2.8)^{Aa}	20	11.7 (2.5)^{Ba}	21.4

Same upper/lower case letter in a column/row indicates no statistically significant differences at p=0.05 level.

Representative SEM images of the predominant failure mode for each composite/adhesive combination are shown in Fig. 3.6. The different interfacial failure modes identified from the SEM images of the fracture surfaces were classified and presented in Table 3.4. The mode of failure was considered as adhesive when it involved the dentin-adhesive interface, the composite-adhesive interface or only the adhesive itself. A cohesive failure was defined as a failure involving only the dentin or the composite. A mixed-mode failure was defined as a combination of adhesive and cohesive failures.

Adhesive failure was found to be predominant, accounting for 80 to 100% of all failures (Table 3.4). In addition, as displayed in Fig. 3.6, each composite/adhesive combination seemed to present a distinct adhesive failure mode. To explore the association between the composite/adhesive system and the actual mode of adhesive failure, the latter was subdivided according to the exact position of failure, i.e., composite-adhesive interface, adhesive-dentin interface, or within the adhesive layer itself. The results are summarized in Fig. 3.7, which shows that the mode of adhesive failure was largely determined by the bonding system; the composite did not have much effect. Fig. 3.6b shows that EB, when combined with either Z100 or Z250, exhibited an

adhesive failure involving the adhesive-dentin interface, as one half of the fracture surface showed the adhesive layer (dark) and the other half showed the dentin surface. In the case of MP, fracture mostly involved the composite-adhesive interface regardless of the composite used. SB showed a mixed mode of adhesive failure: in about half of the specimens, the adhesive layer itself failed cohesively (Fig. 3.6e and f); the rest failed at the composite-adhesive interface. Fisher's exact test confirmed the association between the type of adhesive and the failure mode ($p<0.0001$).

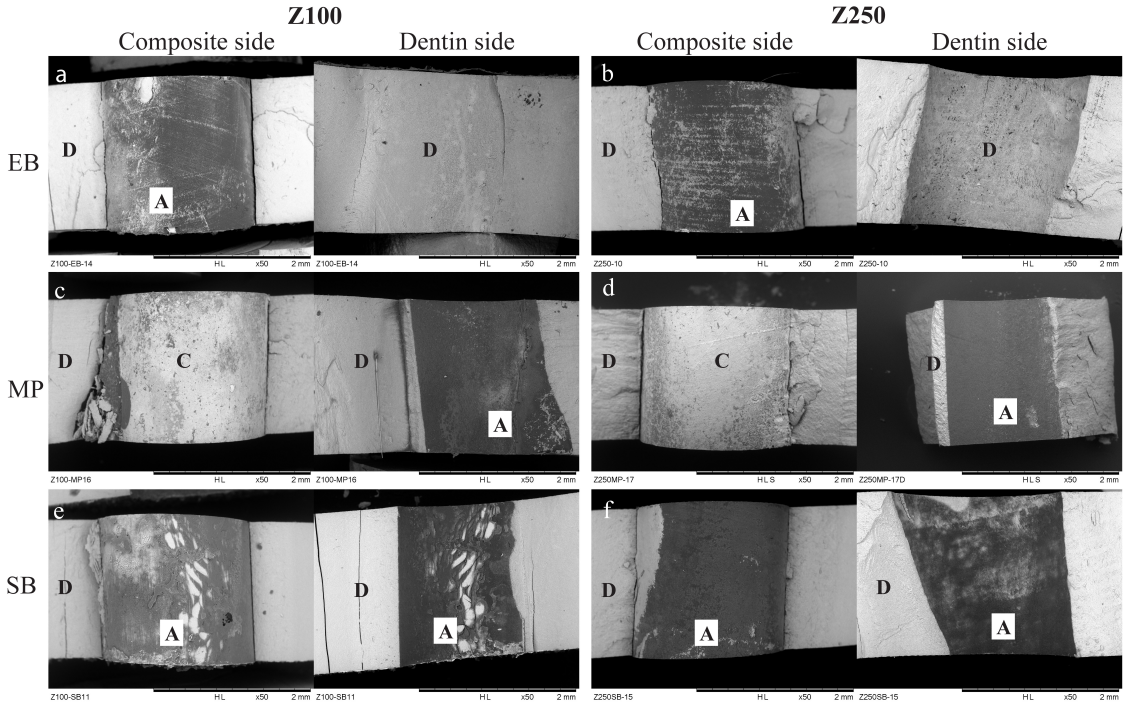

Figure 3.6 SEM images of fracture surfaces of specimens from the diametral compression test. A= adhesive, C= composite and D=dentin.

Table 3.4 Frequency and percentage of failure mode by composite/adhesive combination

	Failure Type		
Combination of composite/adhesive	Adhesive n° (%)	Mixed n° (%)	Cohesive n° (%)
Z100/EB (n=15)	13 (86.7)	1 (6.7)	1 (6.7)
Z100/MP (n=16)	16 (100.0)	0 (0.0)	0 (0.0)
Z100/SB (n=15)	12 (80.0)	0 (0.0)	3 (20.0)
Z250/EB (n=15)	12 (80.0)	2 (13.3)	1 (6.7)
Z250/MP (n=16)	16 (100.0)	0 (0.0)	0 (0.0)
Z250/SB (n=15)	15 (100.0)	0 (0.0)	0 (0.0)
Total	84 (91.3)	3 (3.2)	5 (5.4)

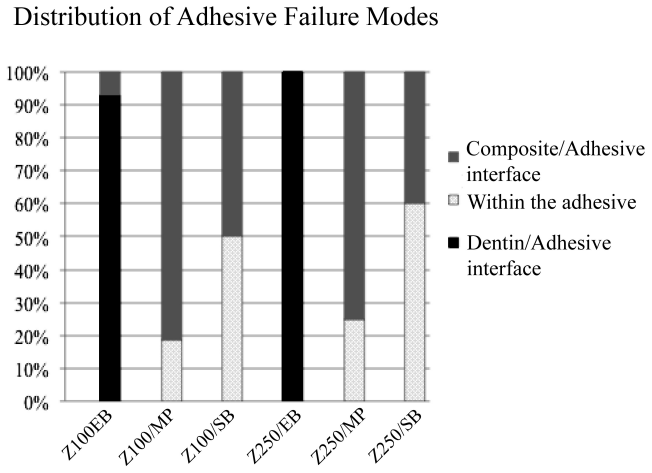

Figure 3.7 Frequency distribution of the modes of adhesive failure for each composite/adhesive combination.

3.5 Discussion

Conventionally, the bond strength at the tooth-resin composite interface is evaluated using direct tensile or shear bond tests. Among these methods, the specimen shape and

experimental fixture used vary considerably, so do the bond strength measurements, even for the same system of materials (209). Note that, in a bi-material system, a stress singularity will always exist at the free edges of the interface, the degree of singularity being dependent on the mechanical properties of the substrates (154). It is therefore not surprising to find that the mechanical properties of the composite, in particular the elastic modulus, can affect the results from bond strength testing (154, 170). In fact, finite element analysis demonstrated that the higher the mismatch in mechanical properties between the substrates the higher the stress concentration at the interface, which results in lower bond strengths (148, 154). Further, for some of the specimens, preparation involves extensive machining in the form of sectioning and trimming, which can lead to a high incidence of pre-test failures (159).

The Brazilian disk test has been used widely for testing the fracture strength of brittle materials. Many authors have described this method and its merits and limitations discussed at length (202, 210, 211). The new variant of the Brazilian disk introduced here was prepared using typical steps in adhesive dentistry, and required much less machining than some micro-tensile test specimens (22). For that reason, we observed negligible pre-test failure. The dentin-restoration interface also formed a closed loop with no free ends, thereby minimizing any stress concentration due to the mismatch in material properties. Again, using the DIC and AE techniques, we demonstrated the viability of the test by showing that failure of the disk was initiated by debonding at the dentin-composite interface. The specimen's shape and size also resembled those of a Class-I restoration, so the measured bond strength should be representative of those of real restorations as correction for the dependence on specimen size (the so-called size effect) would be minimal.

Because the disk specimen resembled a Class-I restoration with a very high level of constraints, the possible effect of shrinkage stress on the measured bond strength cannot be ignored. Care was therefore taken to minimize the shrinkage stress by using an incremental filling technique. The fact that Z100 (which shrinks more than Z250) gave higher bond strength than Z250 indicated that the results were unlikely to have been affected by shrinkage stress.

Statistical analysis of the results showed that both the composite and the adhesive affected the bond strength, but there appeared to be no interaction between the two components. We obtained the same ranking in bond strength for the dental adhesives with either of the two composites used in this study. When data for the two composites were pooled together, EB showed higher bond strength than SB and MP, but no significant differences were detected between SB and MP. When only Z250 was considered, EB showed significantly higher bond strength than SB but not MP. A similar trend was found by da Silva et al. (212) who studied the effect of dentin thickness on the micro-shear bond strength of different bonding systems after 24 hours of water storage. The authors found that the self-etching system EB had the highest median bond strength (21 and 27 MPa) for both of the dentin thicknesses (200 and 500 μm) analyzed, followed by SB (15.6 and 23.4 MPa), and MP (15.2 and 17.9 MPa). Other investigators have also reported that self-etching bonding systems performed better than etch-and-rinse systems (213). Overall, however, results remain contradictory. For example, Dantas et al. (214) found the shear bond strength of two total-etch systems (Single Bond 2 and Multipurpose) to be significantly higher than that of two self-etching systems after 24 hours of water storage. Similar results were found by Mcleod et al. (215) when evaluating the influence of the C-factor on shear bond strength. However, they showed that SB only produced higher bond strength than EB with enamel; no differences in bond strength between the adhesive systems were found with dentin. On the other hand, Perdigao et al. (216) found that MP (65.4 ± 9.5 MPa) resulted in significantly higher micro-tensile dentin bond strength than all the other adhesives tested, including SB and EB, although they did find EB (58.6 ± 6.1 MPa) to perform better than SB (44.7 ± 10.8 MPa). Yet other studies have found no significant differences between the total-etch and self-etch adhesives used in this study (217).

One reason that may explain the better immediate bond strength of self-etch adhesives found in this and other studies (212, 213) is that they reduce the technique sensitivity associated with the application of bonding systems. Self-etch systems simplify the bonding process by eliminating some of the more technique-sensitive steps, such as moisture control, in the use of total-etch systems, which can lead to inadequate

infiltration. Self-etch systems contain hydrophilic and acidic monomers, which are able to simultaneously demineralize and penetrate the dentin, thus reducing the risk of incomplete resin infiltration. Moreover, because of their highly hydrophilic component, the level of moisture in the dentin is not a critical factor in bond formation (96). However, also because of their high hydrophilicity, these adhesives are very permeable and prone to water sorption, which ultimately plasticizes the polymers and lowers their mechanical properties over time (126).

The inconsistent results obtained by the different groups studying the same materials may also be explained by the high variability inherent in the tensile and shear bond tests. In a recent review (209), the coefficients of variation of several bond strength tests were retrieved from 147 articles. The adhesives they assessed included two of those studied here (SB and MP). The review showed a high scatter in the data, with the coefficient of variation ranging from 22% to 49% for the micro-tensile test, 20% to 53% for the tensile test, and 24% to 45% for the shear test. No data was collected for the micro-shear test due to an insufficient number of studies. Possible sources of this variability, as discussed previously, were: variations in dimensions of the specimen, thickness of the adhesive and alignment of the specimen; imprecisely machined jigs; and random inherent flaws in the adhesive or those generated by the preparation procedure, just to name some of them (209). With the modified BDT specimen, the coefficient of variation of the measured bond strengths found in this study ranged between 10% and 22%, which was much lower than the ones reported in the literature for the other types of bond test.

One of the advantages of the modified BDT which may have contributed to the reduced variability in the results is that no fixation of the specimen is required. This, in particular, allows for quick test setup, which avoids dehydration of the specimen, and the elimination of spurious stresses due to specimen misalignment, thus minimizing technique-related errors.

Another reason proposed for the large variability in most bond strength measurement is the high percentage of cohesive failure involving dentin or composite obtained with the tensile and shear bond tests. For example, with the micro-tensile test, the percentage of such cohesive failures ranged from 20% to 39% (209). In the present study, this was 0%

for three of the six groups tested and between 7% and 20% for the other three groups. We therefore had a high incidence of adhesive failures across the groups. As mentioned before, for a bond strength test to be valid, failure must initiate from the interface. Otherwise, the measurement would likely be an underestimate of the true value.

The adhesive failures observed in this study could be subdivided according to which region it occurred in. For example, when MP was used, a higher frequency of composite-adhesive interfacial failure was found; but when EB was used failure mainly occurred at the dentin-adhesive interface; whereas SB showed a combination of cohesive failure in the adhesive and interfacial failure at the composite-adhesive interface. This may explain the higher coefficient of variation seen in the results with SB (Table 3.3). The cohesive failure seen in the SB adhesive could be attributed to the fact that it was applied in two consecutive coatings, between which a weak interface could have formed. Similar results for SB were found by Salvio et al. (213) and Belli et at. (218), who reported a high frequency of failure involving the adhesive layer. A high percentage (~70%) of adhesive failure involving the dentin-adhesive interface has also been reported by others for EB (216), but the same adhesive was found to produce a high incidence of composite cohesive failure (~40%) in other studies (29). Bouillaguet et al. (219) and Perdigao et al. (216) also found a high frequency of adhesive failure for MP; however, the dentin-adhesive interface was mostly involved, which differed from the current study. The inconsistent results observed in the failure mode might be explained by differences in the testing conditions and a lack of standardization among the studies.

The actual mode of failure at the tooth-restoration interface may determine the likelihood of developing secondary caries following interfacial breakdown. For example, with the dentin still fully covered, teeth restored with systems that fail at the composite-adhesive interface may be less likely to develop secondary caries.

3.6 Conclusions

The new variant of the BDT specimen provides several advantages for testing dentin-composite bond strength. These include zero premature failure, simpler testing

procedures, a consistent failure mode involving the adhesive interface, and reduced variation in the measurements.

3.7 Acknowledgement

This study was partially supported by the National Institute of Dental and Craniofacial Research (NIDCR), USA through Grant No. 1 R01 DE021366. The authors of this manuscript declare that no benefits in any form have been received or will be received from a commercial party related directly or indirectly to the subject of this article.

Chapter 4. Degradation in the Dentin-Composite Interface Subjected to Multi-Species Biofilm Challenges

This chapter consists of the manuscript published in Dental Materials. I am the second author of this paper. My role involved participating in discussions to guide the course of the study as well as preparing all samples involved in the experiments. This was a collaborative project between the MDRCBB and Dr. Rudney's laboratory.

Summary

Oral biofilms can degrade the components in dental resin-based composite restorations, thus compromising marginal integrity and leading to secondary caries. In this study, we investigated the mechanical integrity of the dentin-composite interface challenged with multi-species oral biofilms. While most studies used single-species biofilms, we used a more realistic, diverse biofilm model produced directly from plaques collected from donors with a history of early childhood caries. Dentin–composite disks were made using bovine incisor roots filled with Z100™ or Filtek™ LS (3M ESPE). The disks were incubated for 72hr in paired CDC biofilm reactors, using a previously published protocol. One reactor was pulsed with sucrose, and the other was not. A sterile saliva-only control group was run with sucrose pulsing. The disks were fractured under diametral compression to evaluate their interfacial bond strength. Surface deformation of the disks was mapped using digital image correlation (DIC) to ascertain fracture origin. Fracture surfaces were examined using SEM/EDS to assess demineralization and interfacial degradation. Dentin demineralization was greater under sucrose-pulsed biofilms, as the pH dropped below 5.5 during pulsing, with LS and Z100 specimens suffering similar degrees of surface mineral loss. Biofilm growth with sucrose pulsing also caused preferential degradation of the composite-dentin interface, depending on the composite/adhesive system used. Specifically, Z100 specimens showed greater bond strength reduction and more frequent cohesive failure in the adhesive layer. This was attributed to the inferior dentin coverage by Z100 adhesive which possibly led to a higher level of chemical and enzymatic degradation. The results suggested that factors other than dentin demineralization were also responsible for interfacial degradation. We have thus developed a clinically relevant *in vitro* biofilm model which would allow us to effectively assess the degradation of the dentin-composite interface subjected to multi-species biofilm challenge.

4.1 Introduction

The use of resin based dental composites and the associated dentin/enamel bonding adhesives for restoring damaged or decayed teeth have increased significantly in recent years. In 2005, around 77 million composite restorations were placed in the United States, as opposed to 52 million amalgam restorations (220). However, despite its superior aesthetics, low toxicity and ease of handling, composite restorations have higher failure rates and more recurrent caries, requiring as a result more frequent replacement than amalgam restorations (221-224). There is a high likelihood that breakdown of the tooth-composite interface will take place at some point of the restoration's lifetime due to mechanical fatigue caused by mastication. For composite restorations with a high level of shrinkage stress induced by polymerization of the resin matrix, interfacial debonding between the composite and tooth is expected to occur during curing, leading to an early failure. Once interfacial breakdown has taken place, cariogenic bacteria within the oral cavity can invade through the resulting gaps and colonize the subsurface tooth tissues to initiate recurrent caries. Clinically, 80% to 90% of secondary caries was located at the gingival margins of Class II through V restorations, irrespective of the restorative material employed (225, 226); and progression of caries occurs faster in dentin than in enamel. This is because the biofilms grown in these regions are better protected from hygienic procedures.

Oral biofilms are polymicrobial complexes composed of dozens to hundreds of different species (227, 228), and under certain environmental conditions play a critical role in the progression of dental diseases, such as dental caries (227). The fermentable carbohydrates that form part of our food intake are metabolized to polysaccharides by microorganisms from dental plaque. Through nano/micro-leakage, the acids and enzymes produced from the metabolism can demineralize the underlying dental tissues and/or degrade the resin composite and adhesive of a restoration (229). A question of great interest is whether oral biofilms can accelerate the mechanical breakdown of the tooth-composite interface mentioned above by actively degrading the interfacial bond strength, leading to secondary caries.

Oral biofilm models of single-species or defined species consortia are often used in *in vitro* experiments to study the effects of oral biofilms on different substrates. However, such simple models may not be adequate to simulate the complex actions of natural, multi-species oral biofilms on dental restorative materials. Several studies have demonstrated that stable microcosm oral biofilms can be produced from human plaque samples to study microbial effects on the properties of restorative materials (230, 231) or the generation and progression of secondary caries (230-233). In a previous study, we used a CDC biofilm reactor to create a stable oral biofilm community that closely simulates the *in vivo* environment. While the biofilms grown in the CDC reactors underwent significant changes in their microbiological composition, around 60 % of the species were preserved (234). Specimens placed in the reactor can be removed at predetermined time points for assessment of biofilm characteristics, demineralization profiles of dental tissues and degradation of dental materials. Our CDC reactor model also allows for real-time measurement of pH response curves when the reactor is pulsed with sucrose, to simulate acidogenic meals and snacks.

As mentioned above, we are interested in knowing whether oral biofilms can actively reduce the bond strength of the underlying interfaces of a composite restoration. Many mechanical test methods have been used to measure the bond strength between filling materials and tooth tissues, such as the microtensile test, shear test and push-out test (235). In parallel with our development of the CDC reactor model, we also optimized a system for evaluating failure at the dentin - adhesive - composite interface (236), a major component in a composite restoration. In that system, dentin disks are made from bovine incisor roots, and the canal is enlarged and filled with composite (Fig. 4.1). The disk is then subjected to diametral compression, with acoustic emission (AE) and digital image correlation (DIC) being used to determine the time and location at which failure occurs. The disks consistently fail by first debonding at the dentin-composite interface. It is therefore a valid bond test and results have shown that it provides more precise bond strength measurements.

In this study, we combined our previously validated CDC reactor model and dentin-composite disk interfacial failure model to address the following questions: 1.) Does the

presence of a multi-species biofilm lead to degradation of the dentin-composite interface? 2.) Does sucrose-pulsing enhance the effects of biofilm at the interface? 3.) Do biofilm effects at the interface differ between composite-adhesive systems with different chemistries?

4.2 Materials And Methods

Dentin-composite disks

The dentin-composite disks used in this study are illustrated in Fig. 4.1A and B. Bovine incisors were used to prepare the disk specimens. The crowns were cut off at the cemento-enamel junction with a rotary diamond saw (Buehler, USA) under cooling water to provide the portion of root dentin from the incisors. These were then trimmed down into dentin cylinders of 5 mm in diameter using a lathe, and the root canals were enlarged to 2 mm in diameter using Gates-Glidden drills. After that, the dentin cylinders were rinsed with deionized water to remove any remnants. They were then randomly divided into two groups, and filled with one of two composites (Z100™ and Filtek™ LS, both 3M ESPE) using the corresponding adhesives as per the manufacturer's instructions. Z100 and LS were chosen as they represented composites with very different chemistries, bonding systems and shrinkage behaviors. For specimens filled with Z100, the inner dentin surface was etched with 35% phosphoric acid for 20s before rinsing with deionized water. Two consecutive layers of adhesive (Adper™ Single Bond Plus, 3M ESPE) were applied to the etched surface, with each layer being cured for 20s. Z100, a methacrylate-based resin restorative composite, was then applied incrementally to fill the cylinders. Each increment was cured for 40s to ensure adequate curing of the material. For specimens filled with LS, a layer of Self-Etch Primer (LS System Adhesive, 3M ESPE) was first applied and cured for 10s. This was followed by the application of a layer of Self-Etch Bond (LS System Adhesive, 3M ESPE) with 20s of curing. LS, a low-shrinkage silorane-based restorative composite, was then applied incrementally and cured

in the same way as Z100. Finally, the filled cylinders were transversely cut to produce 2-mm thick round disks.

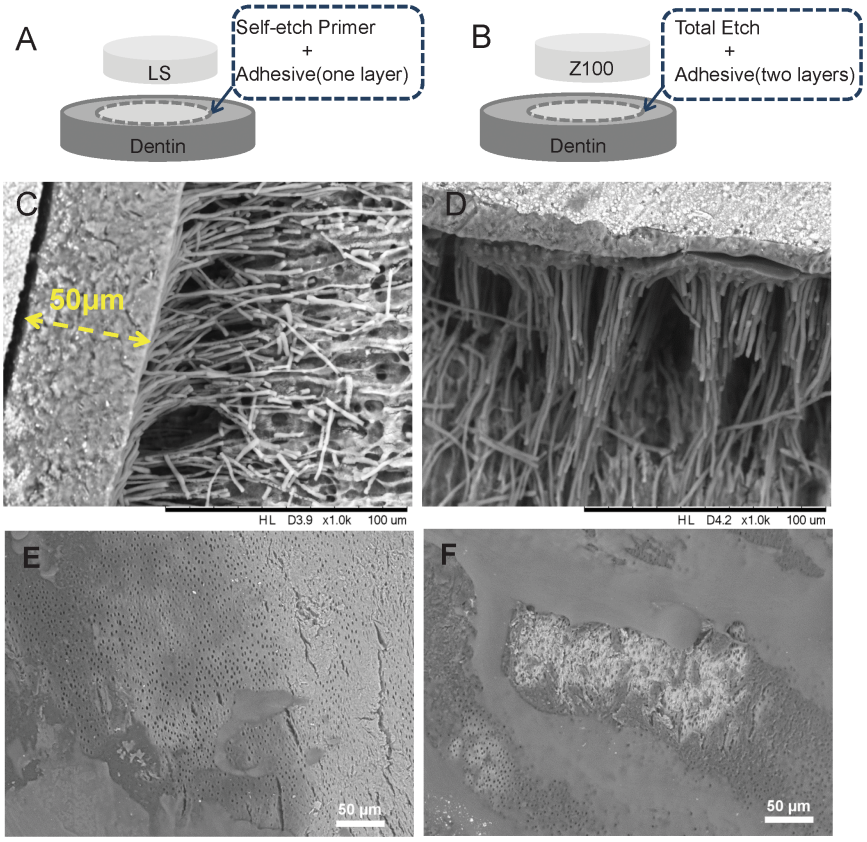

Figure 4.1 Schematic illustrations of dentin-composite disks of LS (A) and Z100 (B). SEM images of LS (C) and Z100 (D) dentin-composite disks after demineralization and deproteinization, showing the adhesive layers and resin tags. SEM images of one layer (E) and two layers (F) of Z100 adhesive applied on etched dentin surfaces showing incomplete coverage.

Human subjects and biofilm stocks

Primary teeth have a higher reported risk of secondary caries with resin-based restorations than permanent dentition since some pediatric dental patients may provide a more challenging oral environment due to their dietary habits (222, 237). Twelve

pediatric dental patients with histories of early childhood caries and a median age of 9 years were recruited as plaque and saliva donors. After explaining the risks and benefits of the study, written consent was obtained from the children's legal guardians for all children enrolled in the study. All procedures involving human subjects were approved by the University of Minnesota Institutional Review Board. A detailed description of the procedures used for sample collection is provided in our previous paper on the CDC reactor model (234). Briefly, subjects were asked to refrain from oral hygiene at bedtime and in the morning before sample collection. A sample of resting whole saliva was collected, centrifuged, filter-sterilized, and stored in aliquots at – 80 ° C. After saliva collection, a sample of dental plaque from either the occlusal or buccal margin of an existing restoration was collected into a vial containing 1ml pre-reduced anaerobic transfer medium (Anaerobe Systems, Morgan Hill, CA, USA) to help preserve the anaerobes also present in supragingival plaque. Biofilm stocks were made by growing microcosms from the plaque of individual subjects, onto hydroxyapatite disks (HA, Clarkson Chromatography, South Williamsport, PA, USA) in the CDC reactor (234). The saliva sample was clarified by centrifugation, diluted twofold in a buffer that simulates the ionic composition of saliva and then sterilized with a 0.2-µm filter. HA discs were precoated with sterilized saliva to form a pellicle. The matching plaque suspension was dispersed by sonification and 30µl of it was applied onto each disc. The disks were then placed immediately into the reactor. After 72 hr of incubation, the biofilms were then removed and pooled, re-suspended in BMM with 20% glycerol, and stored at -80 °C. Stocks were used to provide the inoculum for biofilm challenge in most cases. Fresh plaque was available for a few subjects. In those cases, biofilm challenges were run at the same time that stocks were prepared.

In vitro biofilm challenges

A full description of our CDC Biofilm Reactor based oral microcosm model (238) has been published previously (234). Briefly, it incorporates a lidded vessel through

which growth media can be flowed at a defined rate, and a baffled stir bar to generate shear. Rods inserted through the lid are used to mount samples. Basal Mucin Medium (BMM) containing hog gastric mucin as the primary source of carbohydrate was used as the growth medium (239). Microcosms were incubated aerobically, to better replicate conditions existing in supragingival plaque.

One biofilm challenge was run for every subject. For each challenge, fourteen Z100 and fourteen LS composite-dentin disks were prepared, and stored in 1% (v/v) thymol at room temperature until needed. The disks were coated with acid-resistant nail varnish except one side of the composite filling and a 1 mm perimeter around it, so that the associated interface was exposed. The disks were disinfected with 70% ethanol before mounting and inserting into the reactor. Each exposed surface was coated with 30 µl of sterilized human saliva, and then treated with 30µl plaque/stock from the same donor. Seven disks of each material then were placed into two pre-autoclaved CDC reactors, each containing 350 ml Basal Mucin Medium (BMM), and incubated at 37° C under constant shear (125 rpm) for 24 hr. BMM was then flowed through one reactor at 17 ml/min (125 rpm; 37° C) for another 48 hr. The second reactor was pulsed five times per day (20 v/v%, 43 ml each time) analogous to three meals and two snacks for the 2nd and 3rd days (the flow rate for the second reactor was set at 20 ml min^{-1}, to reduce fouling). Sucrose pulsing was discontinued during the nights. To determine real-time pH, a fitting was machined so that an autoclavable pH electrode could be placed in each reactor. The pH was recorded every 15 min throughout the 72-hr incubation.

Three control experiments were conducted in which disks were coated only with sterilized human saliva and incubated in the CDC bioreactor using the sucrose pulsing protocol described above.

Mechanical tests

After the biofilm challenge, the disks were rinsed with distilled water and the nail varnish removed with a stainless steel spatula. The bond strengths of the disks were

determined by the diametral compression test (Brazilian disk test) using a universal test machine (858 Mini Bionix II, MTS, MN, USA) with two parallel horizontal plates (236). The load was applied in a stroke-control mode at a loading speed of 0.5 mm min^{-1}. Acoustic Emission (AE) and Digital Image Correlation (DIC) were used during the compression tests to monitor the debonding process. Using an AE system (Physical Acoustics Corporation, NJ, USA), acoustic signals produced from microcracking during loading were detected by an AE sensor attached to the lower stationary plate on which the specimens were placed. Data obtained from the AE events were used in combination with the load-displacement histories from the universal test machine to determine when debonding at the tooth-restoration interface occurred. The DIC technique was used to track the change in surface strains on the disks during loading. This was to ensure that interfacial debonding, manifested as high strain concentrations at the dentin-composite interface, occurred before whole disk fracture. A thin layer of white, and then black, paint was sprayed on the surface of the disks facing the CCD camera of the DIC system to facilitate displacement tracking and processing. Photographs were taken continuously at a rate of 30 fps during the compression test and then analyzed by the DIC software (DaVis 7.0, Lavision, Germany) to produce the strain maps.

Scanning electron microscopy (SEM)

SEM was used to examine the morphology of the resin tags, decalcification and fracture modes of the disks. In order to expose the resin tags, a 37% H_3PO_4 gel was applied to freshly prepared dentin-composite disks (Z100 and LS) for 30 minutes, followed by an air-water spray rinse for 15 s. Subsequently, the specimens were immersed in NaOCl (7 ± 2%) for 30 min, followed by rinsing with distilled water for three times. All etched specimens and fractured disks were mounted on aluminum stubs with carbon tape and examined by a tabletop SEM (TM-3000, Hitachi, Japan) operated at a 15-kV accelerating voltage in combo mode, i.e., surface morphology was shown in stereoscopic detail with images in contrast due to different average atomic number

compositions within the sample. Demineralization of the exposed dentin was assessed by an Energy-dispersive X-ray Spectroscopy (EDS) unit (Quantax 70, Bruker, Germany) attached to the SEM.

4.3 Statistical Analysis

The bond strengths for the 7 dentin-composite replicate disks for each of the four conditions within the biofilm trials for each of the 12 subjects were averaged to create within-subjects means for the following groups: Z100 Biofilm No Sucrose (Z100_BNS), Z100 Biofilm With Sucrose (Z100_BWS), LS Biofilm No Sucrose (LS_BNS), and LS Biofilm With Sucrose (LS_BWS). The within-subject means then were analyzed using a two-way repeated-measures Analysis of Variance (ANOVA), with Material and Sucrose as the within-subject factors. Within-run means likewise were generated for each of the three sterile media control runs with sucrose pulsing. The controls were compared to the Z100_BWS and LS_BWS groups using a two–way mixed model ANOVA with Biofilm as the between-group factor and Material as the within-subject factor. Although we did not run controls without sucrose, the same design was used to compare the sucrose controls to the Z100_BNS and LS_BNS groups.

4.4 Results

Composite-dentin interface and resin tag assessment

The adhesive systems for both LS and Z100 produced resin tags of a similar thickness (Fig. 4.1C and D). The self-etching system used in LS yielded an adhesive layer of ~ 50 µm thick without any observable gaps or voids within the layer (Fig. 4.1C). The three-step 'etch and rinse' adhesive system used in Z100 yielded a thinner adhesive layer of 10 to 20 µm, despite the two applications. Delamination between the two sub-layers after demineralization and deproteinization of the dentin could be seen in some locations (Fig. 4.1D). Further examination using SEM of the adhesive layers, without the application of

composites, showed that the Z100 adhesive did not fully cover the dentin surface (Fig. 4.1E). Likewise, the second sub-layer did not fully cover the first (Fig. 4.1F).

Effect of sucrose pulsing on the pH of biofilms

The real-time pH recordings for the biofilms with (WS) and without (NS) sucrose pulsing for each subject are presented in Fig. 4.2. The overall patterns were similar across subjects except during the first day of bacterial inoculation (Fig. S1). The pH of both the NS and WS biofilms remained relatively high during this period, with a generally small reduction from neutral to around 5.5 - 6.5, depending on the subject. On the second and third day, the pH of the biofilms with sucrose pulsing fell rapidly during the first two pulses, and dropped below 5.5. The pH remained below that threshold for several hours after the final pulse of each day. It then rose rapidly back above 6.0. In the corresponding reactor where sucrose was not added, the pH of the biofilms remained above 6.0 at all times. The pH from the control runs without biofilms remained at ~7 throughout the 72-hr incubation, even though sucrose was pulsed on day 2 and day 3.

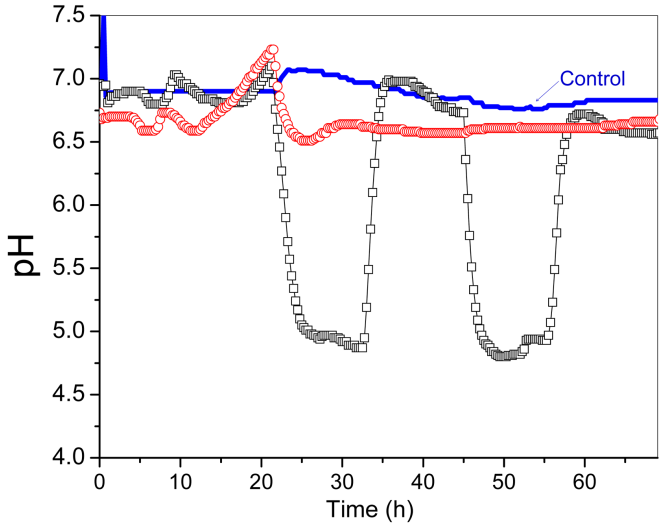

Figure 4.2 Real-time pH recordings from the bioreactors during the 72-hr biofilm challenge (subject #778). (-○-) Biofilm challenge without sucrose pulsing, (-□-)

Biofilm challenge with sucrose pulsing, (---) Control with sucrose pulsing but no biofilms.

Biofilm effects on morphology of exposed dentin

Extensive decalcification occurred in the exposed dentin challenged by biofilms with sucrose pulsing (Fig. 4.3 and Table 4.1). The region of exposed dentin looked darker in the SEM images and had less than 2% of Ca and P in both the LS and Z100 disks, whereas the outer region of dentin protected by the nail varnish showed ~14% of Ca and ~8% of P. On the fractured surfaces, a decalcification depth of ~ 50 μm could be seen as a darker band at the dentin, because of the low mineral content. Closer examination of this region revealed a network of exposed collagen fibrils (Fig. 4.3E and F). Without sucrose pulsing, only a small reduction in Ca and P contents was found in the exposed dentin, even in the presence of biofilms (Fig. 4.3C and D).

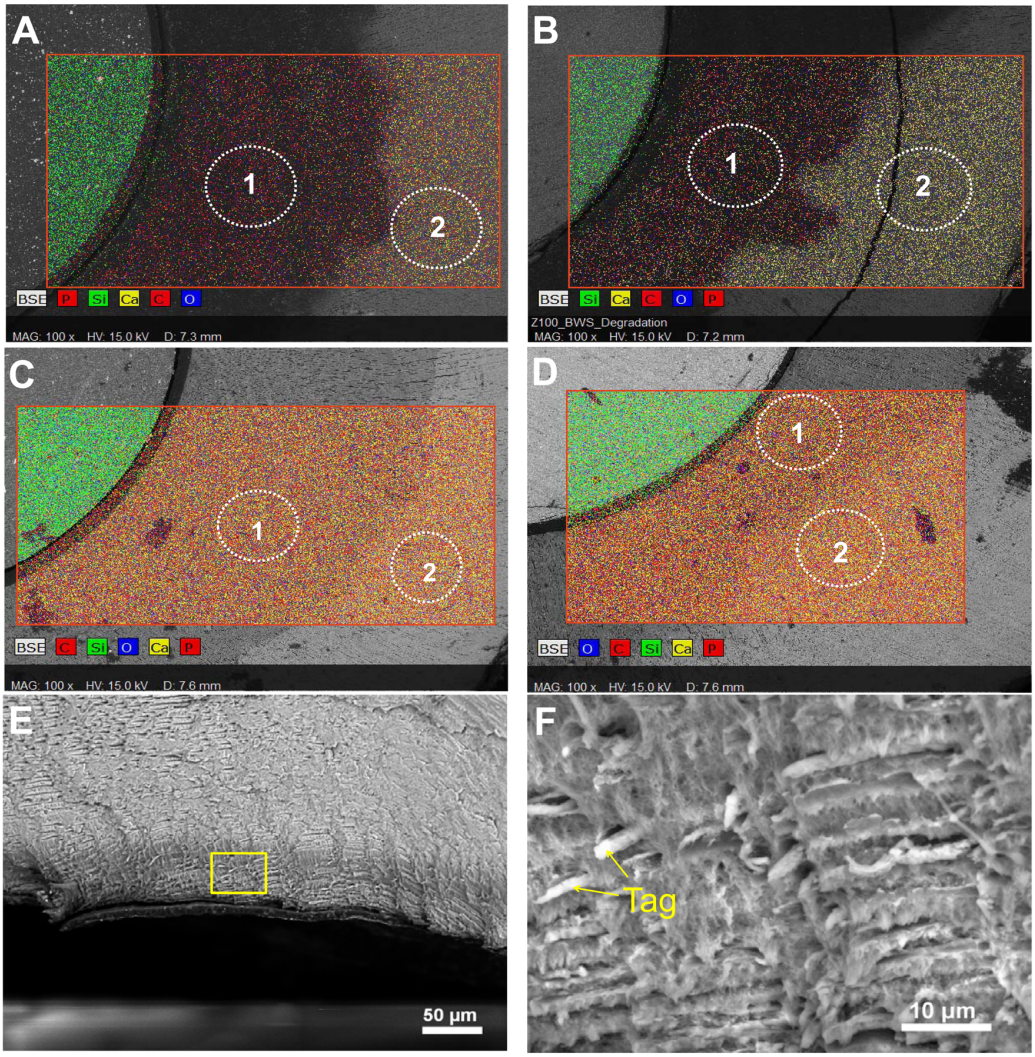

Figure 4.3 SEM, EDS mapping and elemental analysis of dentin-composite disks exposed to biofilm challenges. (A) LS after biofilm challenge with sucrose pulsing. (B) Z100 after biofilm challenge with sucrose pulsing. (C) LS after biofilm challenge without sucrose pulsing. (D) Z100 after biofilm challenge without sucrose pulsing. Regions marked as 1 are exposed dentin and 2 are dentin covered with nail varnish during the biofilm challenge. (E) SEM image of fractured surface of an LS disk specimen after biofilm challenge with sucrose pulsing, showing a dark band of decalcified dentin at the surface. (F) Higher-magnification SEM image of the demineralized dentin showing exposed collagen fibril networks and resin tags.

Table 4.1 Elements distribution of exposed restorations in atomic percentage

Specimen	Region[(a)]	O	C	Ca	P	Si
LS_BWS	1	34.7	62.1	1.8	1.0	0.4
	2	51.5	26.3	14.3	7.7	0.1
LS_BNS	1	46.2	35.6	11.5	6.5	0.2
	2	52.1	24.6	15.3	7.8	0.1
Z100_BWS	1	31.6	63.7	2.7	1.7	0.4
	2	51.7	25.8	14.4	7.9	0.1
Z100_BNS	1	46.5	35.8	10.9	5.6	0.5
	2	51.4	25.5	14.5	8.0	0.1

(a) regions 1 and 2 were labeled in Fig. 4.3 showing the location where EDS was taken from.

Bond strength of dentin-composite disks

Representative load-displacement curves from the diametral compression tests of the four groups of dentin-composite disks after biofilm challenge are shown in Fig. 4.4. Most of the disks deformed rather linearly with increasing load until debonding took place, at which point both a drop in load, as indicated by the arrows, and a significant AE event could be detected. DIC analysis confirmed that debonding occurred at the dentin-composite interface prior to whole-disk fracture, as shown by the high strain concentration (orange color) at the interface where the tensile stress was maximum (inserts in Fig. 4.4, and video). The fracture loads of all the disks after biofilm challenge with the 12 different subjects are shown in Fig. S2. The averaged debonding loads for the four groups (LS_BNS, LS_BWS, Z100_BNS and Z100_BWS) are shown in Fig. 4.5A. The two-way repeat measures ANOVA indicated that the bond strengths for LS were significantly higher than for Z100, when averaged over both the NS and WS

conditions ($p = 0.003$). Bond strengths were significantly reduced by biofilm with sucrose pulsing, when averaged over both materials ($p < 0.001$). The interaction between Materials and Sucrose was not statistically significant. However, the magnitude of the difference between Z100 and LS means was approximately two-fold greater under BWS conditions (24.8 N) relative to BNS conditions (10.2 N). The mixed-model ANOVA comparing controls to sucrose-pulsed biofilms indicated that bond strengths were significantly lower after exposure to sucrose-pulsed biofilms, when averaged over both materials ($p = 0.002$). The difference between bond strengths for LS and Z100 averaged over both the sucrose-pulsed biofilm and control groups verged on significance ($p = 0.055$). The interaction term was not significant, but the magnitude of the mean difference between sucrose-pulsed biofilm and controls was two-fold greater for Z100 (41.1 N) than for LS (21.3 N). When the same model was used to compare the sucrose pulsed controls to biofilms without sucrose, there were no significant differences between biofilms and controls, or Z100 and LS. Collectively, these results suggested that bond strengths for Z100 and LS were essentially similar in the absence of biofilm. In the absence of sucrose pulsing, biofilm appeared to induce a modest reduction in the bond strength of Z100 relative to LS. Sucrose-pulsed biofilms induced reductions in bond strength for both materials, but the magnitude of the change was considerably greater for Z100 than for LS.

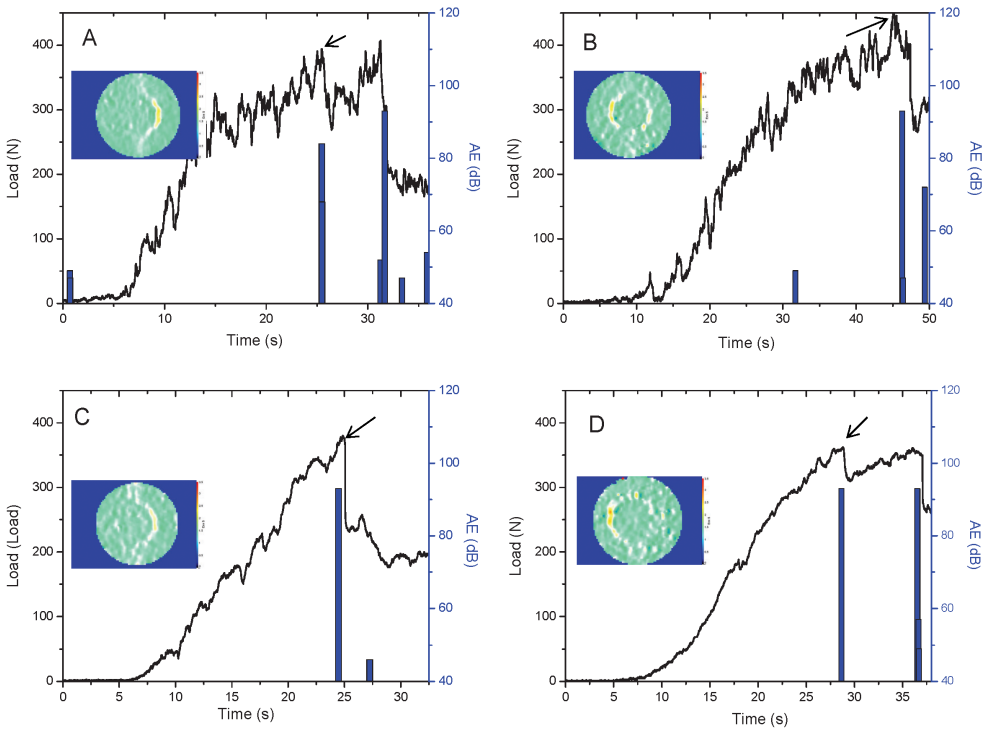

Figure 4.4 Typical load-displacement curves and acoustic emission (AE) signals (bars) from the diametral compression tests of LS and Z100 disks after being subjected to biofilm challenges with or without sucrose pulsing. (A) LS after biofilm challenge without sucrose pulsing. (B) Z100 after biofilm challenge without sucrose pulsing. (C) LS after biofilm challenge with sucrose pulsing. (D) Z100 after biofilm challenge with sucrose pulsing. Inserts are images from digital image correlation showing surface strains on the disks during loading. The arrows indicate load drops due to debonding.

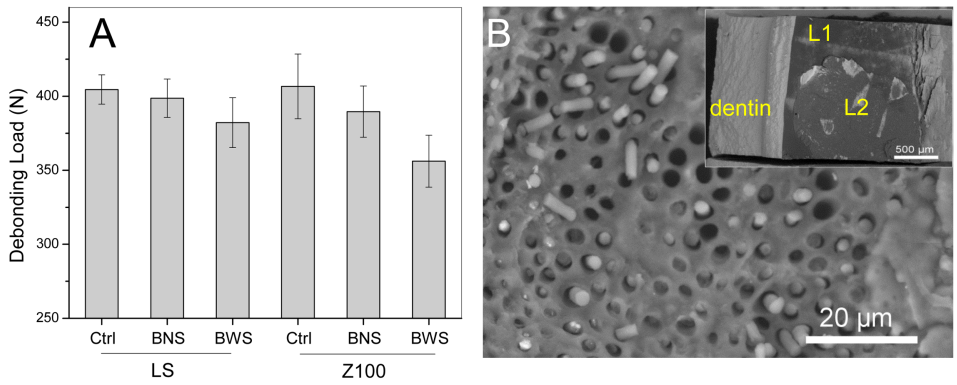

Figure 4.5 (A) Debonding loads averaged over the 12 subjects of dentin-composite disks with different bioreactor conditions. Ctrl: Control with no biofilms; BNS: biofilm without sucrose pulsing; BWS: biofilm with sucrose pulsing. The top of each bar indicates the mean of the values for all 12 subjects, and the error bars are standard deviations. (B) SEM image of the fracture surface of a Z100 disk specimen showing broken resin tags and adhesive. Insert is a lower-magnification SEM image of the same fracture surface: the top layer is the second adhesive layer (L2) debonded from the composite, while another thin layer of adhesive (L1) on dentin can be found below L2. The steps between the two layers indicate that part of the top layer was delaminated from the bottom layer.

Failure analysis

Table 4.2 shows the number and percentage for each of the interfacial failure modes observed in the diametral compression tests of the dentin-composite disks. The LS group exhibited three interfacial failure modes: (1) mixed failure mode including cohesive failure in the resin composite and partial adhesive-composite interfacial failure (C + AC); (2) interfacial failure between the adhesive and composite (AC); and (3) interfacial failure between the adhesive and dentin (AD). The most frequent failure mode for LS was adhesive-composite interfacial failure (50%), followed by mixed failure (30%) and then adhesive-dentin interfacial failure (20%), regardless of the type of biological challenge. In contrast, the failure modes of Z100 at the dentin-composite interface were

predominantly cohesive failure in the adhesive (>80%), again regardless of the type of biological challenge. A small number of interfacial failures between either the adhesive and composite or the adhesive and dentin were observed. Broken resin tags on the dentin side of the fracture surfaces and delamination between the two adhesive layers could also be seen in the Z100 samples (Fig. 4.5B).

Table 4.2 Number (percentage) of specimens failed with a particular fracture mode for LS and Z100 samples under the different experimental conditions

LS	**Control**	**BNS**	**BWS**	**Z100**	**Control**	**BNS**	**BWS**
AC+C	5(29.4)	22(30.6)	26(35.1)	A	13(81.3)	73(96.1)	66(94.3)
AC	8(47.1)	39(54.2)	34(45.9)	AC	1(6.3)	1(1.3)	2(2.9)
AD	4(23.6)	11(15.3)	14(18.9)	AD	2(12.6)	2(2.6)	2(5.8)

Control: specimens coated with saliva only and subjected to sucrose pulsing; **BNS**: biofilm challenge without sucrose pulsing; **BWS**: biofilm challenge with sucrose pulsing. **AC+C**: mixed failure mode includes cohesive failure in resin composite and partial adhesive-composite interfacial failure. **AC**: adhesive-composite interfacial failure. **AD**: adhesive-dentin interfacial failure. **A**: cohesive failure in adhesive layer.

4.5 Discussion

Dental composite restorations reportedly have a shorter lifespan and higher rate of replacement than amalgam restorations due, primarily, to the development of microleakage around the margin of the restorations and subsequent secondary caries in the surrounding tooth tissues (240, 241). Further, 80% to 90% of secondary caries was located at the gingival margins of Class II through V restorations (225, 226). The initiation of marginal failure has been attributed to shrinkage stress caused by the polymerization of the composite resin and cyclic fatigue through mastication. The lifetime of a composite restoration therefore depends strongly on the strength of the restorative and adhesive materials as well as the quality of the integration of the interfacing materials and tissues. Degradation of the tooth-restoration interface can also be caused by the chemical and biological agents that exist in the oral cavity, in particular the cariogenic bacteria that form plaque on the surfaces of teeth and restorations. By using an oral microcosm model together with sucrose pulsing to simulate the conditions present in the mouth, and the modified diametral compression test for bond strength measurement, we investigated the effect of biofilm on the degradation of the dentin-composite interface. It should be emphasized that the disk specimen proposed here is not meant to represent the entire restoration, but only one of its major components; i.e., the dentin-composite interface.

Many mechanical test methods have been used to evaluate the bond strength between filling materials and dentin, e.g. the micro-tensile test and the shear test (235, 242). Because the specimens are small in the micro-tensile test, extensive machining is required which can lead to large amount of premature failure and significant variation in bond strength measurement. It also requires much effort to secure the specimens onto the loading jigs. In contrast, our modified diametral compression discs proposed here require simpler specimen preparation and loading. In the shear test, the interfacial stress distribution is highly non-uniform and in the push-out version the final failure load is affected by the significant friction between the restoration and dentin (243). More importantly, interfacial failure in composite-restored teeth usually happens in an opening (tensile) mode under the occlusal forces or shrinkage stress (244-246). Similar to the

widely used, uniaxial tensile test using bar specimens, the disc in diametral compression is a simple way to induce such type of failure at the interface. Besides, they could be easily fitted into the rods within the CDC biofilm reactor to study both the bond strength reduction and demineralization.

Sucrose is considered the most cariogenic dietary carbohydrate as it leads to the production of organic acids by bacterial fermentation (e.g., lactic, acetic, propionic, succinic or formic), and it is also metabolized to form intracellular and extracellular polysaccharides by microorganisms from the dental plaque. The relationship between sucrose intake and caries development has been demonstrated in several studies (247, 248). The metabolism of sucrose causes a fall in the pH level in the plaque, and dental caries is the direct consequence of the resulting dissolution of mineral. Our biofilm model with sucrose pulsing produced pH - time curves (Fig. 4.2) that were similar to those observed in intraoral studies of plaque pH after sucrose rinsing (249, 250). The pH dropped to a value below 5, and it remained at that level for up to 8 hrs during which sucrose was pulsed 5 times to simulate food intake. Once sucrose pulsing was discontinued and most of the sucrose was consumed, the pH value returned rapidly to the more neutral level of 6 – 7, due to the constant flow of growth medium throughout the night. A slight reduction of the pH to around 5.5 – 6.5 occurred on the first day of bacterial inoculation, which was possibly related to acid production by the bacteria from metabolism of mucin polysaccharides. The same drop in pH on the first day could also be seen in the biofilm without sucrose pulsing.

The CDC biofilm reactor model used in this study has been shown to be able to produce reproducible microcosm biofilms that were representative of the oral microbiota (234). It provides an aerobic environment similar to the human mouth for the growth of oral biofilm. There are over 500 bacterial species identified so far in the dental plaque (251). The Human Oral Microbial Identification Microarray (HOMIM) system detected and evaluated the relative abundance of 272 species and about 60% of species from the original inoculum was detected from microcosms (234). Even though plaques from 12 different subjects were used for this study, the pH-time pattern and bond strength change for each subject were similar.

Enamel demineralization usually occurs when the pH is lower than 5.5 (252) and dentin demineralization can begin at pH 6.7 (253). It therefore was not surprising to see demineralization in the dentin-composite disks where dentin was exposed. The demineralized dentin reached a maximum depth of around 50 μm for both material groups. Assuming the debonding load to be proportional to the thickness of the disk, which was 4 mm originally, a reduction of 50 μm should produce a 2.5% drop in the debonding load. Contrary to expectation, more significant reductions in the debonding load were found for our specimens, especially those prepared with Z100 and subjected to biofilm challenge with sucrose pulsing. This, together with the fact that the two material groups demonstrated different reductions in debonding load despite their similar levels of dentin demineralization, suggested that factors other than surface demineralization were also responsible for the reduction in debonding load.

The adhesive-dentin interface has been shown to be a weak link in the composite restoration (254). It is generally accepted that resin-dentin bonds obtained with contemporary hydrophilic mathacrylate-based adhesives will deteriorate over time even in the absence of mechanical loading (255). In the oral environment, water can enter into the polymer matrix by diffusion, causing a reduction of glass-transition temperature, polymer plasticization and a decrease in thermal stability (256). As a result, this can lead to hygrothermal degradation, hydrolysis and resin leaching (257). Hydrolysis is a chemical process that breaks the covalent bonds within the polymer by addition of water to the ester bonds. It is considered one of the main reasons for resin degradation within the hybrid layer (258, 259). In oral fluids, the ester bonds within the methacrylate polymer matrix are vulnerable to two forms of hydrolytic attack: chemical hydrolysis and enzymatic hydrolysis. Since the bond strength was not significantly affected in the absence of biofilm, or in the presence of biofilm without sucrose, water sorption within polymer by itself is not sufficient to explain the reduction in bond strength caused by sucrose pulsed biofilm. Acids or bases can catalyze the chemical hydrolysis and make the polymer matrix more hydrophilic (254). This may explain the lower bond strength with sucrose pulsed biofilm. Saliva and biofilm contains a variety of enzymes, which may participate in the degradation of the resin. The esterase-catalyzed degradation of

methacrylate esters and commercial dental resins has been documented (260, 261). It is possible that extracellular enzymes released only when sucrose is available might contribute to the degradation of the interface. Such effects might be direct or indirect, since the formation of insoluble glucans by *Streptococcus mutans* has been shown to create zones of intense acidification associated with microcolonies in contact with the HA surface (262). Thus, pH under sucrose-pulsed biofilms might be even lower than the pH in the reactor overall. Furthermore, water sorption can be enhanced by the presence of hydrophilic domains and resin monomers with ionic functional groups (101, 263), which in turn, facilitate ion movement within a polymerized matrix. Water movement promotes hydrolytic degradation and release of the hydrolyzed components of the adhesive layer. This, associated with an increase in permeability of the adhesive layer, creates a vicious cycle that accelerates the deterioration of the mechanical properties of the adhesive layer (264).

The bonding between composite and dentin is of a micromechanical nature, through formation of the resin tags, hybrid layer and adhesive layer, as a result of the acid etching and resin infiltration into the dentinal tubules (265). The adhesive systems for both LS and Z100 were able to infiltrate the etched dentin, forming funnel-shaped resin tags along the entire root canal (Fig. 4.1C and D). Z100 requires a full process of etching and rinsing, and two consecutive coatings of an adhesive that required curing, while LS is intended for use with a self-etching primer and a single coat of adhesive more viscous than that used with Z100. As a result, the LS specimens had a thicker layer of adhesive (Fig. 4.1C). Despite its better handling characteristics, inadequate coverage of the dentin surface by the adhesive was found in the Z100 specimens, and steps could be seen between the two layers of adhesive. These defects in the adhesive layers could have provided channels for water infiltration from the dentin underneath or exposed interface, leading to faster hydrolytic degradation of the adhesive. Similarly, the high shrinkage stress of Z100 could have created partial debonding at the dentin-composite interface to provide more channels for water and acid infiltration. In contrast, dentin in the LS samples was well covered by the thick layer of adhesive, and LS has a very low shrinkage stress. Degradation of the dentin-composite interface in the LS samples was

therefore expected to take place at a slower rate. This may explain why the Z100 samples had a greater reduction in their bond strength after the biofilm challenge and a higher proportion of cohesive failure in the adhesive. In contrast, the LS samples had a more even distribution amongst the different interfacial fracture modes and a lower reduction in the bond strength after biofilm challenge. Incidentally, the reduction in failure load appeared to be uniform across all the fracture modes, i.e. no particular fracture mode had a higher reduction in the failure load than others.

Bovine teeth, instead of human teeth, were used in this study. The use of bovine teeth in dental studies has dramatically increased in the last 30 years since they are easy to obtain in large quantities and good condition. There appear to be small differences in morphology, chemical composition and physical properties between bovine and human teeth. In some bond strength studies, human tissues show higher bond strength than bovine tissues while others show no significant difference between them (266). Another study found no significant difference between human root and bovine root dentin in caries progression, inhibition and composition of biofilm formed (267). On balance, therefore, bovine dentin can be considered a suitable model for human dentin for bond strength and demineralization studies.

In real restored teeth, secondary caries can also occur on occlusal and proximal surfaces that involve enamel and crown dentin. These are different from root dentin in terms of morphology, chemical composition and physical properties. Also, in our disk specimens made with bovine incisor roots, the dentinal tubules were always perpendicular to the dentin-composite interface (Fig. 4.1C and D). The orientations of the dentinal tubules in real life cavities are more varied, especially at the cavity walls. The integrity of the dentin-composite interface here might be more vulnerable to biofilm challenge since resin tags are not fully formed. This, together with the possibility that human dentin may behave differently from bovine dentin, means that caution must be exercised when trying to extend the current results to real life composite restorations in general.

Notwithstanding the limitations mentioned above, our current study demonstrated clearly the effect of microcosm biofilms in degrading dentin-composite interfacial bond.

Future studies will focus on the combined effects of biofilms and cyclic loading on the degradation of dentin-composite interfaces, and will make use of specimens that also include enamel.

4.6 Conclusion

Our *in vitro* investigation has provided the following answers to the questions we posed at the beginning of this paper. 1) The presence of a multi-species biofilm led to degradation of the dentin-composite interface. 2) For the duration of biofilm challenge considered in this study, sucrose pulsing was essential to ensure that the degradation effects were significant. 3) The biofilm effects differed between the restorative systems, with samples prepared with Z100 suffering more degradation. In addition, the results suggested that factors other than dentin demineralization were also responsible for the bond strength reduction.

4.7 Acknowledgement

This work was supported by NIH grant 1 R01 DE021366 from the National Institute for Dental and Craniofacial Research, Bethesda, MD, USA.

Chapter 5. Biological and mechanical degradation of dental composite restoration interface

Summary

The aim of this chapter was to study the combined effect of mechanical loading and microbial challenge on the interfacial integrity of dental composite restorations, and explore whether the effects are modulated by the presence of sucrose. Briefly, standardized MOD class-II restorations were prepared in extracted human third molars. Half of the prepared teeth were subjected to chewing simulation using an artificial oral environment (ATR). Specimens went under 200,000 chewing cycles. After mechanical loading, both groups mechanically challenged or not, were further divided into 3 groups for the microbial challenge: Control (no biofilm), biofilm no sucrose (BNS) and biofilm pulsed with sucrose (BWS)

For biofilm challenge three individual CDC reactors were used. The CDC reactor assigned to the control groups contained nutrient medium only. The samples assigned to BNS and BWS were inoculated with multispecies microbial inoculum from a plaque donor at high caries risk. After inoculation, the specimens were incubated for ~24h under shear but no media flow. On the second day the reactors were flowed with BMM at a rate of 17ml min^{-1}. One of the reactors was pulsed with sucrose 5 times daily, at 2h intervals, to simulate daily meal intake. After 72h the system was taken down and a new cycle was initiated. Real-time pH was recorded for each experimental run. Once twelve biofilm cycles were completed the samples were retrieved and examined for demineralization with Micro-CT and fracture strength by fast fracture test. Fracture loads and failure modes were recorded.

Results showed that only under sucrose pulsing, the pH decrease to values below the critical pH for enamel and even more than the critical pH for dentin. The demineralization in enamel surrounding the restoration was detectable only in the groups where the biofilm was exposed to sucrose pulsing. The fracture loads were significantly reduced by the concomitant presence of biofilm and sucrose, regardless the presence of the mechanical challenge.

5.1 Introduction

One function of a dental composite restoration and the associated dental adhesive is to provide a long-lasting seal between the restorative material and the dental tissues. However, during their lifetime, dental composites restorations are exposed to an array of environmental factors involved in the breakdown of the adhesive interface. Some of these factors act from the installment of the restoration. For instance, when the polymerization shrinkage stress of a dental composite exceeds the interfacial bond strength, delamination and gap formation at the interface occurs (50-52). These open spaces are susceptible to infiltration by oral fluids, acids, metabolites and colonization by oral bacteria (32, 55, 57). Following these initial challenges, additional factors including mechanical, chemical and biological stresses can contribute to interfacial degradation during the service time of a dental restoration. (139). Ultimately, the loss of the marginal sealing perpetuates oral bacteria accumulation at the interface, which may lead to instances of secondary caries around the composite restoration.

Masticatory forces derived from normal chewing and para-functional habits can impose great stress to the adhesive interface. Although the mechanical degradation of dental composites materials has been largely characterized (139, 268-270), much less is known about the effect of mechanical challenge on the interfacial integrity of a dental restoration. Mixed mode mechanical studies, in which samples are subjected to cyclic loading forces (also known as fatigue) followed by fracture toughness or bond strength tests, are useful to study the effect of mechanical loading on the adhesive interface. The few studies published so far showed that regardless the fatigue configuration (i.e. tensile, bending or compression), cyclic loading leads to mechanical weakening of the adhesive interface (143-145). This is demonstrated by an inverse correlation between number of loading cycles and bond strength values, which is independent of the adhesive tested (144). Furthermore, failure at lower cycle number occurred when the cycling load force was between 55% and 99% of the material strength, demonstrating the interplay between static and cyclic loading (145). These data suggest that cyclic mechanical loading can affect the integrity of the bond irrespective of the initial bond strength of the adhesive

interface. Therefore, fatigue is important to consider when exploring interfacial degradation processes.

In addition to mechanical challenge, biological and chemical agents present in oral fluids and food can affect dental composites restorations. Santerre and Finer's research group have demonstrated that esterase activity of saliva promotes the breakdown of condensation bonds present in dental composites polymers (121-123, 271, 272). However, most of the reports focus on the composite material while little information is available about the biological degradation of the adhesive interface. A recent study showed that exposure of model restorations to esterases increased the amount of microbial leakage along the interface (125), suggesting that biological degradation could contribute to the interfacial breakdown.

Lately, oral biofilms have been proposed to have a role in the chemical degradation of the interface (126). Recent data demonstrated that *Streptococcus mutans*, an oral pathogen, possesses esterase activity capable of degrading dental composites and dental adhesives (127) implying a potential microbial mechanism for biological degradation of the adhesive interface.

In the mouth, oral bacteria forms biofilms capable of using fermentable carbohydrates for metabolism and as structural components of the biofilm matrix (76). The production of fermentation byproducts such as organic acids, however, can promote demineralization of hard dental tissues (41). In addition, oral bacteria secrete a large array of enzymes and other metabolic products that might degrade the adhesive interface. To gain insight about the role of oral bacteria in the degradation process, we have investigated the effect of a multiespecies oral biofilm on the interfacial integrity of model dental restorations (273). In our model, dentin-composite disks prepared with two different restorative systems were exposed to oral biofilms and then tested under diametral compression. During the microbial challenge, half of the specimens were exposed to a sucrose-fed biofilm to explore the contribution of sucrose as an environmental factor. A reduction in the debonding load was observed in both groups exposed to biofilm compared to control (no biofilm), but only the reduction seen in the sucrose-fed biofilm group was significant.

These results further support a potential microbial mechanism that in this case was augmented in the presence of sucrose.

Though research efforts have sought to understand the interfacial degradation process, most of the aspects involved in the interfacial breakdown are commonly studied in isolation. In the oral cavity, all these challenging factors are combined and they might contribute to the degradation process in different degrees. The aim of this study is to propose a more comprehensive model to study the combined effect of mechanical loading and microbial challenge on the interfacial integrity of dental composites restorations, and to explore whether the effect of these factors is modulated by environmental factors, such as sucrose.

5.2 Materials And Methods

Specimen preparation

Extracted human third molars were collected upon approval of the University of Minnesota Institutional Review Board. Only teeth free of caries, fractures and cracks were included. The molars were cleaned from soft tissues and hard deposits, if present, and stored in 1% thymol solution. Mesio-occlusal-distal (MOD) class II cavities were prepared using a modified flat end tapered burs (SS White Burs Inc., Lakewood, NY, USA). The dimensions of the cavities were ~2.5mm wide and ~2.5mm deep for the occlusal box, and ~3mm wide and ~1.5mm deep for the proximal box. All teeth were restored using Adper^{TM} Single Bond Plus adhesive system (SB) and Z100^{TM} Restorative (Z100) system (3M ESPE, St. Paul, MN, USA). Briefly, 35% phosphoric acid Scotchbond etchant (3M ESPE, St. Paul, MN, USA) was applied to dentin and enamel for 15s and rinsed with water. Gentle air-drying was used to avoid collagen collapse in dentin. Two consecutive coatings of SB were rubbed on the internal walls of the preparation and polymerized for 20s. The teeth were restored with 2mm thick increments of Z100. Each layer was polymerized for 20s with Elipar^{TM} S10 curing light (1200 mW/cm²). The samples were polished after 24h of water storage. A finishing diamond

stone was used to remove excess material from the restoration margin, polishing was conducted with Progloss™ One Step Composite Polishers (Kerr corporation, Orange, CA, USA). A total of 54 MOD class-II composite restorations were made.

Fatigue (chewing simulation)

Half of the specimens (n=27) were mounted in Teflon rings with self-cured acrylic resin (Dentsply Caulk, Milford, DE, USA). Each mounted specimen was positioned in the mandibular chamber of an artificial oral environment (ART) (274) (Fig. 5.1). A 6mm diameter steatite bead attached to the upper arm was used as the antagonist. The loading target point was located in the functional cusp of the third molars. The artificial mouth was set to simulate 200,000 chewing cycles with a load of 50N at the contact point (275). Throughout the duration of the mechanical challenge the specimens were submerged in deionized water at room temperature. The cycling load was constantly monitored during the loading process.

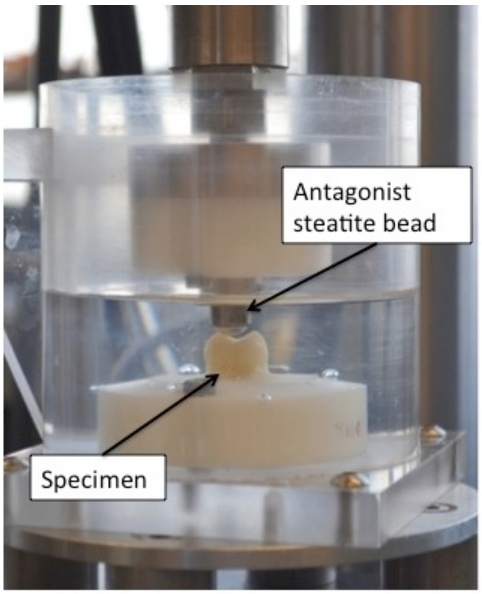

Figure 5.1 Cycling loading set up. Each tooth was mounted and located in the lower chamber of the artificial oral environment.

Preparation of multispecies biofilm frozen stock for inoculation

Frozen multispecies biofilm stock was obtained from a previous study (276). Briefly, plaque and saliva samples were collected from a donor with high caries risk (~9years old). Plaque sample was retrieved from the margin of a dental restoration and immediately transferred into a vial containing pre-reduced anaerobic transfer medium (Anaerobe Systems, Morgan Hill, CA, USA). Whole saliva was collected by expectoration. Immediately after, the collected saliva was centrifuged at 10,000 rpm for 10 minutes, twofold diluted with Gibbon's buffer, filter-sterilized, aliquoted and stored at -80°C (276). A CDC biofilm reactor (BioSurface Technologies, Bozeman, MT, USA) was used to generate biofilm stocks from the plaque inoculum (276). Briefly, hydroxyapatite (HA) disks (Clarkson Chromatography, South Williamsport, PA, USA) were coated on the surface with the filter-sterilized saliva to form the acquired pellicle. 30µl of homogenized matching plaque suspension (same donor as saliva) was used to inoculate each HA disk surface. The disks were then inserted into customized holders and into the CDC reactor containing basal mucin medium (BMM). After 72h of growth at 37°C, the biofilms were removed, pooled, and re-suspended in 20% glycerol BMM and stored at -80 °C (276). Frozen stocks were used to provide the inoculum for the biofilm challenge.

In-vitro biofilm model

We have previously shown that a CDC biofilm reactor can be used to grow a reproducible oral microcosm biofilm, providing an increased microbial diversity (276). Moreover, the CDC reactor model showed to be suitable to study the potential effect of oral bacteria on dental composites (273). For this study, three CDC biofilm reactors were used to carry out the microbial challenge. Each CDC reactor consisted of a 1 liter lidded vessel with an influx port at the top of the vessel and an effluent port at the height of 400 ml approximately. A magnetically driven vaned stir bar provided continuous mixing of the media during the challenge. The lid allowed the incorporation of a pH electrode, a

temperature probe, and six rods that were modified to fit and fix three restored teeth per rod.

Before biofilm exposure, all the restored teeth (Fatigued and non-fatigue) were coated with color-coded acid resistant nail varnish leaving exposed only the composite and the restoration margin. Then, the specimens were further divided into there groups according to the biofilm growth condition in the experiment: Control (no biofilm), biofilm no sucrose (BNS), and biofilm with sucrose (BWS). This originated a total of 6 different groups labeled as follow:

-Fatigue Control (no biofilm)
-Fatigue BNS
-Fatigue BWS
-No Fatigue Control (no biofilm)
-No Fatigue BNS
-No Fatigue BWS

All the specimens were disinfected with 70% ethanol, mounted in the customized rod and coated with 30µl of filtered-sterilized saliva. Only the specimens allocated to BNS and BWS groups were inoculated with 30µl of biofilm stock re-suspended in anaerobic transportation media.

After the inoculation step the samples were incorporated in different reactors according to the growth condition. The non-inoculated specimens (9 Fatigue and 9 No Fatigue) were inserted in a first reactor containing 0.02% sodium azide BMM to inhibit microbial growth during the duration of the experiment (Fig. 5.2a and b). The rest of the samples were allocated in the same manner to a second and third reactor (Fig. 5.2a, b and c). A ~24h incubation period was carried out in all reactors in BMM at 37 °C under constant shear (125 rpm) but with no media flow. This allowed bacteria to attach to the restoration surface (in the case of the inoculated specimens). After the incubation phase, the second and third reactors were connected to the nutrient carboy and BMM was flowed through the system for 48h (Fig. 5.2c and d). The initial rate was set at 17 ml min^{-}

^{1} (125 rpm, 37 °C). In the second reactor, the biofilm was grown in absence of sucrose while in the third reactor sucrose was pulsed five times a day to simulate daily food intake. This was done by adding 42 ml of 40% sucrose into the medium at intervals of 2 hours starting around 8am in the morning. No sucrose pulsing was conducted at night. The flow rate was set at 20 ml min^{-1} during the second day of sucrose pulsing to avoid biofouling and prevent plugging of the efflux tubing. The first reactor (containing the control samples) was not flowed with BMM to minimize the volume of sodium azide hazardous waste produce with each cycle. After 48h, the systems were taken down; the samples were cleaned from biofilm and stored at 4ºC until the next biofilm challenge. For the next cycle of biofilm, the specimens were allocated to their designated reactor (control, BNS and BWS) and the reaction was conducted as mentioned above. A total 12 biofilm challenges were carried out in all the groups.

The whole system was kept under aerobic conditions to simulate the natural succession of supragingival plaque. It was expected that as the thickness of the biofilm increased, a gradient of oxygen generated due to the presence of facultative species, favoring the survival of anaerobic species at the bottom of the biofilm.

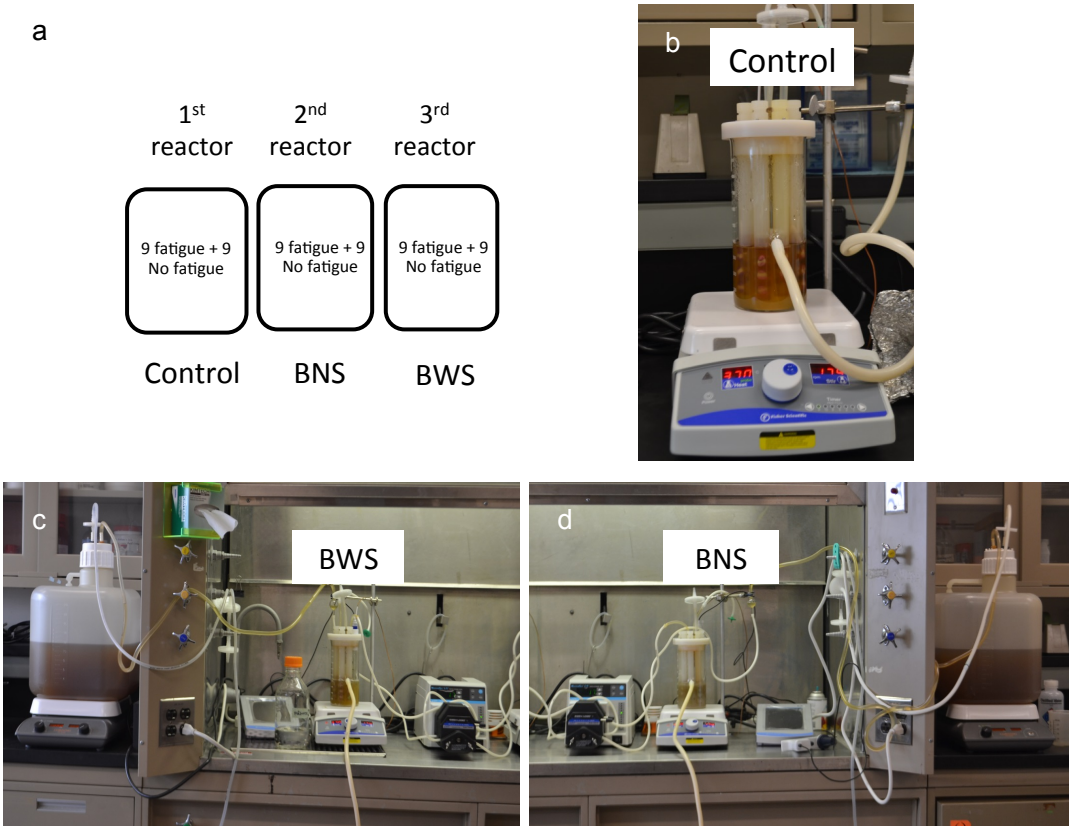

Figure 5.2 (a) Diagram of the specimens' allocation in each CDC reactor. CDC reactor set up for (b) control condition, (c) biofilm with (BWS) condition and (d) biofilm no sucrose (BNS) condition.

pH recording

To determine real-time pH changes in the medium, the CDC vessel's lid was modified to fit an autoclavable pH electrode. The pH was recorded every 15 min throughout the 72h period of experimentation.

Demineralization assessment using Micro-CT

After the twelve cycles of biofilm challenge three specimens from each group were selected and scanned for demineralization around the interface using an X-ray micro-

computed tomography (micro-CT) machine (XT H 225, Nikon Metrology, United Kingdom). The selected teeth were mounted with acrylic resin in Teflon rings and scanned with the following operational parameters: 90 kV, 90 μA, 720 projections and 4 frames per projection. 3D spatial reconstructions were done with CT Pro 3D (Nikon Metrology, Brighton, MI, USA). The processed 3D files were visualized with VG Studio MAX 2.1 (Volume Graphics GmbH, Heidelberg, Germany). For the demineralization analysis, three different landmarks per sample were assessed: occlusal margin, proximal wall and gingival margin. For each chosen region, nine attenuation coefficient profiles were retrieved extending from the surface of the enamel lesion to the deeper sound enamel. The data from the three representative specimens were averaged to obtain a final mineral percentage profile per each group.

Fracture test

Following the biofilm challenge, the restored teeth (including the scanned samples) were disinfected and the protective layer of varnish was removed. Before fast fracture test, the teeth were mounted in Teflon rings with acrylic resin, keeping the occlusal plane facing up. The specimens were fixed in the lower plate of a universal test machine (858 Mini Bionix II, MTS, MN, USA). Each tooth was loaded until fracture with a half sphere loading head (6mm in diameter). The load was applied in a stroke-control mode at a cross-head speed rate of 0.1 mm min^{-1}. The fracture load was recorded. After the test the specimens were scanned with micro-CT to identify the fracture mode. Scanning parameters were: 90 kV, 90 μA, 720 projections and 2 frames per projection.

5.3 Statistical analysis

The mean fracture loads from the different groups were compared using two-way analysis of variance (ANOVA) with biofilm growth condition (Control, BNS, BWS) and fatigue (Fatigue, No Fatigue) as the between-group factors. Multiple comparisons among the different conditions were conducted with Bonferroni *post hoc* test at alpha level of 0.05.

5.4 Results

Effect of sucrose on pH

The pH in the medium was tracked during the duration of each experimental run to study the effect of sucrose pulsing. Similar pH curves were registered among the twelve cycles of biofilm. The pH of the control group was not recorded, as it was known from previous experiments that it remained mostly at 7 during the length of the experiments. In the BWS condition the pH values drastically decreased after the incorporation of sucrose. For this condition, the pH remained at levels below the critical pH for enamel (pH=<5.5) during the sucrose challenge and rose back at levels around 6.5 after the pulse of sucrose was stopped. On the other hand, for the groups exposed to biofilm but with no sucrose pulsing, the pH was relatively stable at values between 6.5 and 7. Figure 5.3 shows the mean pH values over the course of the experiment from the twelve cycles of biofilm.

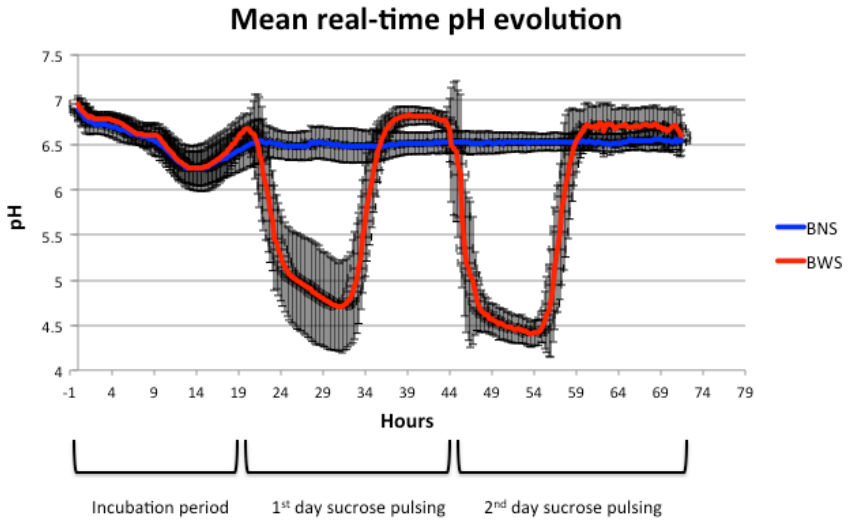

Figure 5.3 Mean real-time pH recording from the twelve-biofilm challenges for BNS and BWS growth conditions. Black bars are the standard deviations.

Effects on enamel demineralization

To study the effect of fatigue and biofilm on the integrity of enamel, three specimens of each group were analyzed with Micro-CT. The cross-sectional and 3D analysis showed no detectable demineralization in Control and BNS conditions for both groups, Fatigue and No Fatigue (Fig. 5.4a, b, c and d). In those groups the enamel surrounding the restorations was mostly intact, except for the samples subjected to fatigue, which presented wear facets at the contact point. Instead, micro-CT images of Fatigue BWS and No Fatigue BWS groups showed enamel demineralization zones next to the restorations (Fig. 5.4e and 4f). The demineralization affected the enamel surrounding the restoration margins with no major differences between the two groups. Interestingly, the enamel demineralization had the pattern of an outer lesion without the presence of a wall lesion. Overall, the demineralized enamel band was parallel to the surface and mostly uniform in thickness within each specimen. Mineral percentage profiles taken from the occlusal surface, proximal wall and gingival margin showed that demineralization was around 200µm deep, regardless of the surface and the fatigue condition (Fig. 5.5a,b and c), although it tended to be deeper at the occlusal surface for both groups (Fig. 5.5a). In some of the specimens the demineralization of the gingival floor reached dentin in cases where the enamel was thin or when the cervical enamel was lost (data not shown).

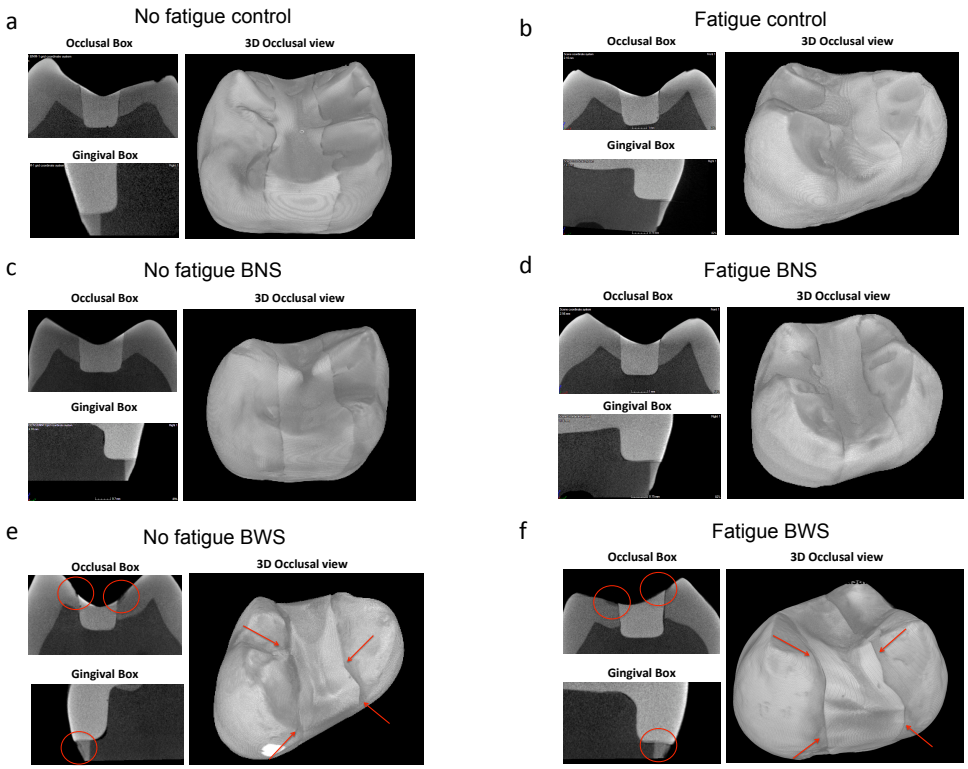

Figure 5.4 Representative Micro-CT cross-sectional images and 3D reconstructions of the restored teeth after fatigue and biofilm challenge. (a) No Fatigue control (no biofilm) (b) Fatigue control (no biofilm). (c) No Fatigue BNS. (d) Fatigue BNS (e) No Fatigue BWS. (f) Fatigue BWS. Red circles and red arrows indicate zones with observed demineralization in the 2D cross-sections and 3D reconstructions, respectively.

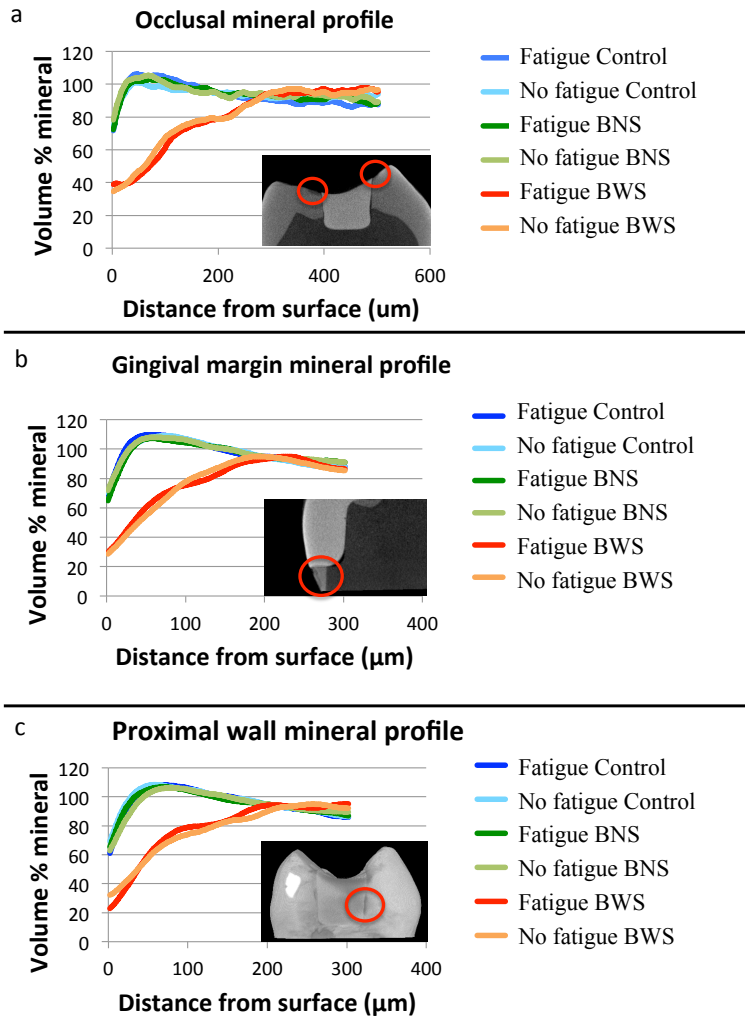

Figure 5.5 Average mineral profiles obtained from three different regions in the teeth for each of the groups. (a) Mineral profile taken from the occlusal margin. (b) Mineral profile taken from the gingival margin. (c) Mineral profile taken from the proximal wall. Inset in each plot is a representative image indicating the approximate locations from where the profiles were obtained.

Effect of fatigue and biofilm on fracture loads and failure modes

To study the effect of fatigue and biofilm exposure on interfacial degradation, the specimens were subjected to fracture test after mechanical and microbial challenges.

Table 5.1 summarizes the mean fracture loads for each group and condition. In general, Fatigue samples displayed slightly lower fracture loads than No Fatigue specimens (Table 5.1, fig. 5.6a and b). However, the main effect for fatigue did not achieve statistical significance, even though the Fatigue groups consistently trended lower ($p = 0.149$). When the biofilm growth conditions were compared, Control showed the highest fracture loads followed by BNS and BWS, for both Fatigue and No Fatigue groups. The main effect for Biofilm was significant ($p = 0.007$). Bonferroni t-tests indicated that the fracture load reduction seen between Control and BWS was statistically significant ($p = 0.006$). Although a profile plot suggested a consistent trend, BNS was not significantly different from either BWS or Control by the Bonferroni test. To explore the nature of the combinatorial effect between fatigue and biofilm, the percentage of load reduction from each group was calculated relative to the mean fracture load of the No fatigue control group (Fig. 5.7). The results showed that Fatigue control generated a reduction of ~16%, whereas No Fatigue BNS and No fatigue BWS displayed a reduction of ~23.5% and ~36.4%, respectively. The reduction generated by Fatigue BNS (30.5%) and Fatigue BWS (52.4%), suggested that combinatorial effects of fatigue and biofilm were mostly additive.

Three main modes of fracture were found: interfacial, cohesive in dental tissue or composite and a mixed mode of fracture (Interfacial and cohesive). In general, the presence of biofilm seemed to produce more cohesive failures in enamel compared to their respective controls in both Fatigue and No Fatigue groups. However, no clear trend was observed for the failure mode and the different conditions.

Table 5.1 Mean and standard deviation (s.d.) of fracture loads (FL) by group and condition

	No fatigue Mean FL (N) ± s.d.	Fatigue Mean FL (N) ± s.d.
Control	1422.4 ± 722.7	1190.6 ± 340.1
BNS	1087.6 ± 444.6	988.8 ± 353.4
BWS	904.3 ± 433.1	678.9 ± 149.5

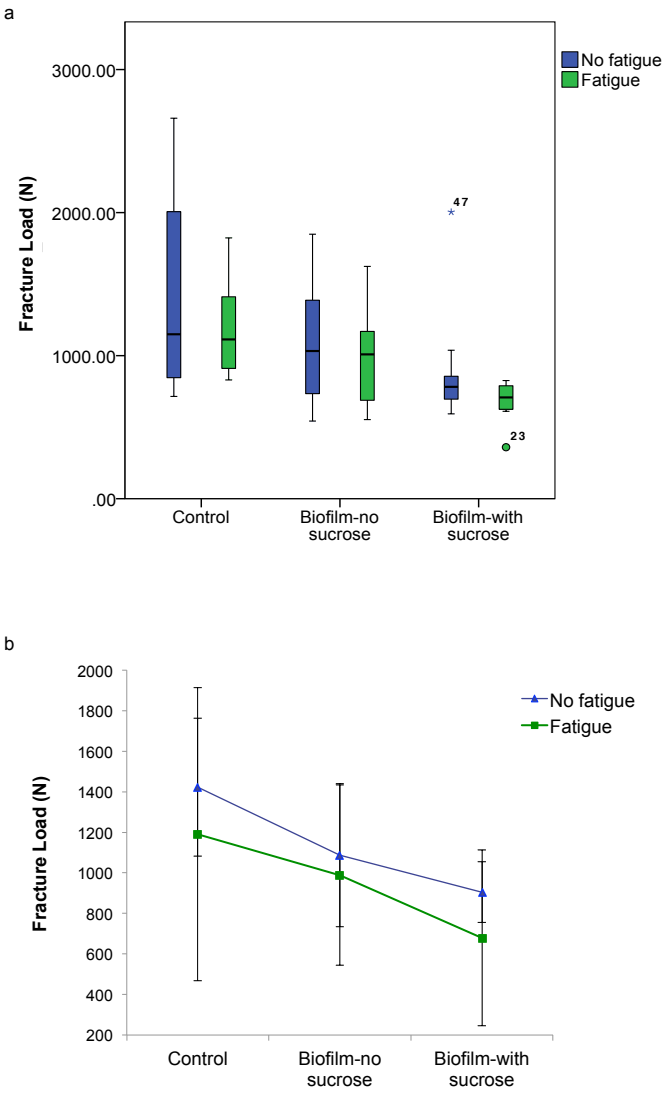

Figure 5.6 Data distribution and mean profile of fracture loads. (a) Box plot displaying the median fracture load value (black bar dividing each box) for each group and condition. Box represents the inter-quartile range. End of whiskers are minimum and maximum load values (except for outliers). (b) Profile plot presenting the mean fracture load values and standard deviation for each group and condition.

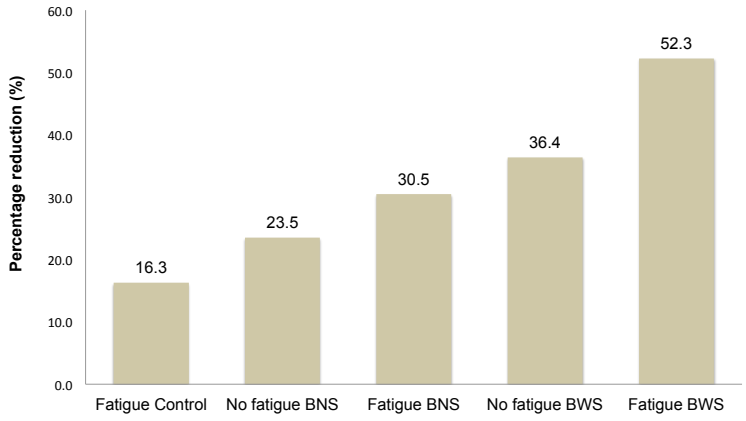

Figure 5.7 Fracture load reduction of each group relative to No fatigue Control group.

5.5 Discussion

Dental composites fail more frequently than amalgams because of higher instances of secondary caries (9, 11). Early breakdown of the interfacial integrity can take place from the first moment that a dental composite is placed in the mouth. Shrinkage stress can lead to the formation of micro-spaces at the interface allowing passage of oral fluids and bacteria (55). Mechanical challenges coming from mastication or para-functional habits can perpetuate the damage to the interface by inducing mechanical weakening of the adhesive bond (143-145). Moreover, chemical and biological challenges can also affect the interfacial integrity of the composite restorations (121, 123, 126). Many of these factors, however, are usually studied in isolation making difficult to determine their relative contribution to the process of degradation. Here, we proposed a more comprehensive model to study the combined effect of mechanical and microbial challenge on the degradation of the adhesive interface.

A multispecies biofilm model was chosen to provide a closer representation of the oral microbial diversity. For many years research focused on *Streptococcus mutans*.

Although valuable knowledge was attained, currently, it is estimated that the oral microbiome is comprised of over 600 predominant species (277). In an earlier study it was demonstrated that by using a CDC reactor and basal mucin media we were able to reproduce a microcosm oral biofilm that retained 60% of the original inoculum at the species level. Furthermore, using this model it was found that multispecies oral biofilms induced interfacial degradation in dentin-composite model restorations (see chapter 4) (273). Here, this CDC reactor biofilm model was combined with mechanical cycling of class-II restorations using an artificial oral environment.

Class-II restorations involve larger removal of tooth tissues reducing the strength of the teeth (278, 279), and have higher failure rates (14-16). High shear and tensile stresses concentrate at the interface of direct composite MOD restoration when subjected to chewing simulations, threating the interfacial integrity (280). Even though interfacial degradation and secondary caries can develop anywhere in the tooth, studies have reported that gingival margin of class-II and class V restoration are largely affected by secondary caries lesions (30, 35, 36). This is probably due to the higher plaque accumulation in these sites, incomplete adaptation of the materials to the restorative margin, and poor adhesion (35, 36). Therefore, a class-II composite restoration provided a convenient model to study the combined effects of mechanical loading and microbial challenge.

Materials or interfaces can fail due to repeated loading with force levels that are unlikely to generate catastrophic failures after just one application (281, 282). Therefore, fatigue challenge is a better tool to understand the *in-vivo* behavior of adhesive systems when subjected to forces. In our study, we simulated chewing cycles using an artificial oral environment. We used 200,000 cycles in order to simulate ~8 month of masticatory function, which was followed by biofilm exposure to explore potential synergistic effect between mechanical and microbial challenge. According to the percentage of fracture load reduction, Fatigue BNS and Fatigue BWS showed greater load reduction compared to No Fatigue BNS, No fatigue BWS or than Fatigue control, yet the magnitude of the drop indicated only additive combined effects between fatigue and the presence of biofilm.

Interestingly, the presence of biofilm lead to more pronounced effect in the reduction of the fracture loads values. When the results were averaged over the Fatigue and No Fatigue groups, the fracture loads decreased by 270N in the case of BNS, and around 515N in the case of BWS compared to the control groups that were not exposed to oral biofilm. Further analysis showed that only the differences between BWS and the control group were statistically significant, suggesting that the presence of sucrose further enhanced any initial biofilm effect. Despite the drop seen in the fracture load values in BNS groups with and without fatigue, no significant differences were found when compared to the Control or BWS groups. Overall, the effect of biofilm, specifically in combination with sucrose, was more pronounced than the effect of fatigue alone on the interfacial degradation of dental composite restorations.

Most of the research investigating mechanical degradation of the adhesive interface use model restorations, such as microtensile beams or small samples of the adhesive interface (143, 145, 275). It is probable that the strong effect of fatigue showed in those studies is less pronounced when a whole restoration is tested under fracture. Others have shown a strong effect of fatigue on class-II composite restorations in terms of gap formation when subjected to a similar cycling regimen. In the study by Frankenberger et al. (146) most of the specimens (~80%) developed significant gaps at the occlusal margin. Though we did not test for marginal gap formation in this study, a reduction in the fracture loads was expected if gaps were formed or enlarged during masticatory challenge. This effect was seen in this study but not to a great extent.

Our pH results showed a great reduction in pH values when the biofilms were pulsed with sucrose. This reduction reached values lower than the critical pH for enamel (pH~5.5) (283) and even more for the critical pH of dentin (pH~6.5) (284). This explains why enamel demineralization was found in both Fatigue and No Fatigue groups exposed to sucrose-fed biofilm. It was expected that the levels of demineralization would be more pronounced in the fatigue group, due to added interfacial breakdown and more penetration of bacteria. However, micro-CT analysis did not show major differences between the two groups. Several reasons could explain this. First, it is possible that demineralization could have been under the detection level of micro-CT. Micro-CT uses

the X-ray attenuation properties of materials, consequently if demineralization changes occurred only at an ultrastructural level without changing enamel density this would not be detectable by X-rays. A second possibility is that the fatigue effect was insufficient to create or enlarge marginal gaps to allow bacteria passage and thus promote additional demineralization along the interface. The fatigue challenge was done at 200.000 cycles which equates to ~8 month approximately (285), whereas the biofilm challenge is estimated to represent between 6 month to one year based on the degree of demineralization reached. A third possibility is that the demineralization event happens independently of the mechanical breakdown of the interface, which supports the idea that secondary caries is a primary lesion next to a dental restoration driven by plaque accumulation. Indeed, micro-CT and microscopy analysis (data not shown) showed demineralization patterns of an outer lesion with no signs of wall lesion formation even though the restorative material used here (Z100) has displayed high levels of microleakage (179). This would support the current argument that the presence of microleakage is less important for secondary caries formation compared to the accumulation of a cariogenic oral biofilm (22). However, it is possible that the number of cycles between biofilm and fatigue were not enough to see this effect, or it is needed to conduct the two challenges simultaneously.

Interestingly, for these experiments the same plaque inoculum was used for the non-sucrose and the sucrose challenge, however a drastic pH reduction was only seen in the presence of sucrose. This highlights the importance of environmental factors in inducing dysbiosis of oral biofilms. Even though recent studies have found that besides mutans streptococci other acidogenic and acid tolerant bacteria might be associated with dental caries (286, 287), others have shown similar microbial composition between caries active and caries free (288). The inconsistency in the results has lead to reevaluation of the role of exact composition of the associated microbiome related to dental caries and other oral diseases. More recent studies have shown conserved metabolic functions in taxonomically diverse oral biofilm communities associated with disease (46, 289),

suggesting that metabolic disruption of oral biofilm will be more associated with the disease than any specific group of oral bacteria.

5.6 Conclusions

In summary, we have presented a more comprehensive model to study the combined effect of mechanical and microbial challenge on the interfacial integrity of dental restorations using a human tooth model. The results showed that when specimens are subjected to both challenges, a greater reduction in fracture strength is seen compared to the effects of fatigue and biofilm alone demonstrating the additive effect of both. The presence of biofilm showed a substantial effect in the degradation of the adhesive interface, which was significant in the presence of sucrose, whereas the effect of fatigue was much less pronounced.

Part II - Antimicrobial containing adhesives

Chapter 6 Short review on antimicrobials-containing dental adhesives

6.1 Introduction

The application of adhesive systems is a critical step in adhesive dentistry. Despite being able to create an immediate effective bond between the tooth structure and the dental restoration, they cannot completely prevent the formation of micro-gaps at the interface (56). Furthermore, their stability and ability to maintain a sealed margin decreases dramatically over time (85, 86). Therefore, microleakage may occur during the time of service of a restoration, with the consequent bacterial invasion through the tooth–restoration margins following their eventual breakdown, which ultimately may lead to the formation of secondary caries (55). The advent of minimal invasive dentistry (MID) makes this unfortunate scenario even more challenging. MID is a new approach in operative dentistry that encourages minimal removal of the dental tissues when preparing a dental restoration. The main goal of MID is the preservation of the dental structure and the protection of the dentin-pulp complex. By applying a conservative technique for caries removal it is likely that viable residual bacteria could remain in the prepared cavity. Furthermore, in some teeth with deep carious lesions, selective excavation is recommended (partial removal of infected dentin), thus contaminated dental tissue is left intentionally beneath the restoration (290). This recommendation relies on the premise that if bacteria are deprived of nutrient sources the lesion would arrest without the need of complete removal of the infected tissue (290). Unfortunately, as mentioned before, composite polymerization shrinkage may result in gaps that prevent the formation of a tight marginal sealing. Recent studies have shown that caries lesions failed to arrest when the interfacial integrity was compromised (291). In addition to this, dental composites lack antimicrobial properties when polymerized, therefore, plaque accumulation at the restoration interface is likely to happen if dental plaque is not properly removed by hygiene procedures. All these clinical challenges have led to the development of restorative materials with antibacterial properties. This is generally achieved by adding antimicrobials to the formulation of dental materials such as composites, cements, glass-ionomers and dental adhesive systems (292-294). The main goal is to limit the effect of bacteria left in the preparation and to prevent future accumulation of plaque at the tooth-restoration interface. Dental adhesives containing antimicrobials can be classified in

antimicrobial-releasing adhesives or antimicrobial-non-releasing adhesives according to the process used to incorporate the antimicrobial into the formulation.

6.1.1 Antimicrobial-releasing adhesives

The initial efforts consisted in adding soluble antimicrobials directly into the formulation of dental adhesives. The antimicrobial agent in this case is continuously released to the oral environment after the dental adhesive is polymerized due of the lack of strong bonding to the adhesive matrix. For adhesive systems the most common agents added to the formulation are glutaraldehyde (GTA), fluoride, chlorhexidine (CHX), benzalkonium chloride (BAC), and chitosan among others (295, 296).

Glutaraldehyde is a common disinfectant that was initially added to adhesive systems to increase the resistance of the hybrid layer to degradation due to its crosslinking capabilities on dentinal collagen (297). When examined by the agar disc diffusion method, the unpolymerized glutaraldehyde-containing adhesives demonstrated a significant inhibitory effect on the growth of several oral bacteria, including streptococci, lactobacilli, and actinomycetes (298-300). However, a high degree of cytotoxicity against rat pulp cells and human fibroblasts has been reported with a commercial product consisting in 5% GTA in combination with HEMA, a common resin monomer utilized in dental adhesive (301).

As another effort to generate an adhesive with antibacterial properties Saito et al. (302) added BAC into an orthodontic dental adhesive to obtain final BAC concentrations of 0.25%, 0.75%, 1.25%, 1.75%, 2.5%, and 5.0% (wt/ wt). The results from the agar disk diffusion test showed that the BAC-polymerized adhesive generated larger halo of inhibition against mutans and sobrinus streptococci with increasing BAC concentration. 2.5% and 5% BAC-containing adhesives displayed the highest antimicrobial activity. However, only the lowest concentration of BAC resulted in low levels of side cytotoxicity. Also, the antimicrobial effect decreased significantly after prolonged water storage, limiting its long-term application (302).

CHX is another antimicrobial added to dental adhesives formulations. CHX is a

cationic bisbiguanide containing chloride with a known broad antibacterial activity. It binds to the negatively charged bacterial cell surface, with specific and strong adsorption to phosphate-containing compounds (303). Once bound to the bacterial membrane it causes leakage of low-molecular-weight components. Usually, with increasing concentrations of CHX the damage is greater, resulting in cytoplasmic leakage and cell death (303). Although the initial purpose of adding CHX was to inhibit collagenolytic activity of endogenous matrix metalloproteases (MMPs), polymerized CHX-containing adhesive has demonstrated antimicrobial activity against planktonic culture of strict anaerobes, such as *Prevotella intermedia*, *Porphyromonas gingivalis* and *Fusobacterium nucleat*um, though no antimicrobial effect was seen against mutans *Streptococcus mutans* or *Lactobacillus casei* (304). Results from another study showed that increasing concentration of CHX generated bigger halos of inhibition when an unpolymerized experimental primer containing 1% and 2% CHX was compared to the control adhesive with no CHX (305). However, the long-term effect in terms of preventing secondary caries is still unknown.

Fluoride has been incorporated into adhesive systems formulations as another alternative to overcome restoration failure. The antimicrobial effect of fluoride is thought to be associated with its weak acidic (pKa 3.5) properties. It has been reported that fluoride can enter bacteria in the form of HF when the external pH is low. After it enters the cell, it can dissociate into H^+ and F^- due to the higher internal pH of the bacteria. This continuous diffusion and dissociation of HF would lead to the acidification of the cytoplasm with the resulting decrease of the proton gradient and enzyme activities (306, 307). Bapna et al (308), tested the antimicrobial effect of fluoride and several other chemical agents incorporated into a common dental adhesive. The results showed that the adhesive containing fluoride at a final concentration of 10% inhibited bacterial growth when the adhesive was exposed to *Streptococcus mutans* culture (308). Even though fluoride release from dental adhesives into the surrounding tooth tissues has shown an anti-cariogenic effect (309, 310), it is unclear whether the this effect of fluoride is related to the inhibition of oral bacteria (311). Also, it is unknown if the effect is sustained over time.

More recently, Chitosan was used to prepare an antimicrobial experimental adhesive. Chitosan is a polycationic biopolymer used extensively in drug delivery applications. It is obtained by alkaline deacetylation of chitin, a natural biocompatible polysaccharide present in marine crustaceans (312). As an antimicrobial, chitosan increases the cell permeability, which results in disruption of the cell membrane and leakage of cell components. The antimicrobial action is thought to be caused by the electrostatic interaction between the NH(3) positively charged groups present in the chitosan molecule and the phospholipids of the bacterial membrane (313). To test the antimicrobial effect of chitosan-incorporated adhesive Elsaka et al. (314) added increasing concentration of chitosan (0.12% to 1%) into single bond dental adhesive. Direct contact method results using the polymerized primer showed that all concentrations displayed significant inhibitory effects on the growth of *Streptococcus mutans* compared to the parental adhesive used as a control. The effect was sustained after 7 days of water storage of the specimens. However, concentrations above 0.12% interfered with the degree of conversion of the adhesive and the tensile dentin bond strength.

Besides soluble antimicrobials, antibiotics have been another alternative to achieve materials with antibacterial properties. Kodou et al (315) studied the antibacterial effect of dentin bonding systems after the incorporation of vancomycin and metronidazole. The adhesive containing metronidazole exhibited inhibition zones against *Streptococcus mutans*, *Streptococcus mitis* and *Actinomyces naeslundii* but not against *Streptococcus sanguis*, *Sreptococcus salivarious* and *Actinomyces viscosus*. On the other hand vancomicin-containing adhesive showed antibacterial effect against all the bacteria tested and the inhibition was greater than the one displayed by metronidazole, however the effect was lost after 30 days of water storage.

In general, many attempts have been made to achieve antibacterial properties in dental adhesives. However, an uncontrolled released of the antimicrobial agents occurs over the course of time due to the lack of covalent bonding. This inevitably leads to a decrease of the initial antimicrobial activity, which limits any long-term benefit.

6.1.2 Antimicrobial Non-releasing materials

To overcome the disadvantage of decreasing antimicrobial activity over time Imazato's group pioneered in the synthesis of an antimicrobial that could be immobilized into dental resin composites and dental adhesives (316). With their method, antibacterial components were stabilized via covalent bonding to the carrier matrix. This approach provided a material loaded with an antimicrobial that does not leach from the bulk of the material, but that can inhibit bacteria by direct contact. The main goal was to provide dental adhesives with a long lasting antimicrobial effect. This system was based in copolymerization of hydroxydodecylpyrimidium bromide (a quaternary ammonium agent) and a methacrylate group, which led to the monomer 12-methacryloyloxydodecyl-pyridinium bromide, mostly known as MDPB. This antibacterial monomer was successfully incorporated into experimental adhesive (317) systems without interfering in mechanical properties such as bond strength (318, 319) or other properties such as the degree of conversion (317) and water sorption (320) of the dental adhesive. Several studies have been conducted to test the antimicrobial activity of the unpolymerized bonding system reporting strong antimicrobial activity against classic dental pathogens when tested by direct contact methods or agar diffusion plates (317, 318, 321-323). These encouraging results led to the commercialization of the MDPB-containing adhesive system under the name of Clearfil SE Protect (Kuraray Medical, Tokyo, Japan). This commercial product has shown inhibitory effects against *Streptococcus mutans, Lactobacillus casei* and *Actinomyces naeslundii* when examined through the agar-disc diffusion method (324).

Although the mechanism of action is not fully elucidated yet, it is speculated that this monomer relies on their quaternary ammonium group to display antimicrobial properties. In general, quaternary ammonium compounds are well known antimicrobials that are used in a large array of clinical situations. Their efficacy is conditioned by the amphiphilic nature of the molecule, having a positively charged quaternary ammonium polar head with one or two apolar chains (325). In solution the polar positive head is readily attracted to the negatively charged cell membrane altering the charge distribution, whereas the apolar chain permeates the membrane and disrupts its physical properties,

causing cell leakage and cell death (326). It is thought that modified monomers, such as MDPB, can cause bacteriolysis when the positive charged quaternary amine gets in contact with the negatively charged bacteria cell membrane, interfering with the electrical balance and ultimately leading to cytoplasmic leakage (327). However the detailed mechanism is still unknown. Because of its interaction with negatively charged surfaces, levels of cytotoxicity have been reported with both experimental MDPB-containing adhesive and commercial product when the unpolymerized state is tested (320, 328).

Following this development several other monomers were developed under the same process of combining quaternary ammonium salts and methacrylates groups, which are under current investigation. Examples of those are: 2- dimethyl-2-dodecyl-1-methacryloxyethyl ammonium iodine (DDMAI) (329); 2-methacryloyloxyethyl dimethylammonium (IDMA1) (330), 2,2-bis(methacryloxyloxyethyl dimethylammonium) (IDMA2) (330), dimethyl amino dodecylmethacrylate (DMADDM) (331), dimethylamino hexylmethacrylate (DMAHM) (332), and methacryloxyl ethylcetyldimethylammonium chloride (DMAE-CB) (333). So far all of them have shown antimicrobial effect to different degrees.

6.2 Problem statement

Overall, immobilized antimicrobial monomers seem to be a promising alternative to provide dental adhesive with long lasting antimicrobial properties. However, a recent systematic review concluded that even though antibacterial-containing adhesives have shown *in vitro* positive antibacterial effect, the clinical performance and the long-term effect is still unclear (334). More importantly, the evidence gathered so far must be taken with caution, as most of the studies evaluating the incorporation of antimicrobial relied on agar disk diffusion test or direct contact methods using single species planktonic cultures and the unpolymerized form of the adhesive. Therefore, the effectiveness of these materials needs to be further studied using methods that better represent the diversity of oral bacteria. In the oral cavity, more than 600 predominant species have been identified (277), of which not only mutans streptococci and lactobacilli are related

with dental caries. Moreover, oral bacteria forms biofilms, which are comprised by interacting microorganisms attached to a surface and embedded in an extracellular matrix consisting mostly of soluble and insoluble polysaccharides. These three-dimensional structures are highly spatially and functionally organized and have shown increased tolerance to antimicrobial agents (77). Therefore, it is clinically relevant to establish representative *in-vitro* models to test the effectiveness of antimicrobial-containing materials aimed to recapitulate the oral microbiota diversity and growing conditions found in the oral cavity.

Chapter 7 deals with testing the antimicrobial effect of a commercially available MPDB-containing dental adhesive system, using a multispecies culture/biofilm model. Both the unpolymerized and the polymerized forms were evaluated. Chapter 8 studies the antimicrobial effect of the polymerized MDPB-containing adhesive, using a Drip Flow Reactor as a model to grow oral biofilms.

6.3 Aims

Aim 1. To test the hypothesis that unpolymerized MDPB-containing dental primer exerts antibacterial effects against multispecies oral bacteria culture (Chapter 7).

- Sub-aim 1. Examine inhibition of multispecies bacterial growth by unpolymerized MDPB-containing primer using agar disk diffusion test.
- Sub-aim 2. Evaluate bactericidal effect of unpolymerized MDPB-containing primer against multispecies oral bacterial planktonic culture using direct contact method.

Aim 2. To test the hypothesis that polymerized MDPB-containing dental adhesive system inhibits growth and metabolism of a multispecies oral biofilm (Chapter 7).

- Sub-aim 1. To test the ability of polymerized MDPB-containing adhesive system to inhibit biofilm biomass formation and metabolic activity in a closed oral multispecies biofilm model.

Aim 3. To test the hypothesis that polymerized MDPB-containing dental adhesive system inhibits growth and metabolism of a more cariogenic sucrose-fed multispecies oral biofilm (Chapter 7).

- Sub-aim 1. To evaluate the ability of MDPB-containing adhesive system to inhibit biofilm biomass formation and metabolic activity in the presence of increasing concentrations of sucrose in the media, using a closed oral multispecies biofilm model.

Aim 4. To develop a method to grow uniform layers of multispecies oral biofilm using a Drip Flow reactor in the absence and presence of sucrose (Chapter 8).

- Sub-aim 1. To evaluate biomass uniformity of multispecies oral biofilm formation over composite specimens in a DFR in the absence of sucrose.
- Sub-aim 2. To quantify the thickness of oral multispecies biofilms grown over dental composite specimen inside of a DFR in the absence of sucrose.
- Sub-aim 3. To evaluate the effect of sucrose on biomass formation and thickness of multispecies oral biofilm grown in a DFR.

Aim 5. To test the hypothesis that polymerized MDPB-containing adhesive system inhibits growth and metabolism of a multispecies oral biofilm when tested in a DFR system in the absence and presence of sucrose (Chapter 9).

- Sub-aim 1. To assess biofilm biomass formation, metabolic activity and viable bacteria in multispecies oral biofilms exposed to MDPB-containing adhesive system.

Chapter 7. Antimicrobial activity of MDPB-containing adhesive system

Summary

The aim of this chapter was to test the antimicrobial effect of the unpolymerized primer containing MDPB against a multispecies oral bacterial culture, as well as testing the ability of the MDPB-polymerized adhesive system to inhibit biofilm formation in the presence and absence of sucrose. Briefly, to test the antimicrobial effect of the unpolymerized form, Clearfil SE Protect primer (SEP)(contains MDPB), Clearfil SE (SE) primer and controls were evaluated through agar diffusion plates and direct contact method. Specimens of the polymerized SEP and SE adhesives system were also prepared and tested for biofilm inhibition in a closed multispecies oral biofilm model. The results showed that the unpolymerized primer displayed a strong antimicrobial activity against a multispecies oral culture. The halo of inhibition generated by the MDPB-containing primer was comparable to that of 2% Chlorhexine. Also, no viable microorganism was recovered after oral multispecies culture was treated with the primer. The polymerized form of SEP adhesive showed reduction of biofilm biomass and metabolic activity compared to SE-control. However, complete inhibition of biofilm formation was not observed. Moreover, the inhibitory effects were only seen in the absence of sucrose.

7.1 Introduction

To prevent plaque accumulation at the adhesive interface and prevent secondary caries, several antimicrobial have been added into the formulation of dental adhesives. Among them, the monomer 12-methacryloyloxydodecyl-pyridinium bromide (MDPB) has been successfully immobilized into the adhesive resin providing an antimicrobial non-releasing material (317). Several studies have evaluated the antimicrobial activity of the unpolymerized state of MDPB-containing showing strong bactericidal effects against several single-species cultures of oral bacteria, including streptococci and lactobacilli (317, 318, 321-323). However, this effect has not been demonstrated against a more complex multiespecies culture. More importantly, even though testing the unpolymerized state (effect of the antimicrobial in solution) is relevant to study its effect as a cavity disinfectant, a better estimation of the long-term antimicrobial effect is obtained by evaluation of the polymerized form. In this regard, the polymerized MDPB-containing adhesive agent has demonstrated some inhibition of bacteria growth (335, 336), but not to the same extent of the unpolymerized form. Moreover, most existing studies have employed single bacterium models often *Streptococcus mutans*, which fail to represent the complexity of oral bacteria populations. In order to evaluate the antimicrobial effectiveness of antimicrobial-containing adhesives, it is necessary to study them under a more representative environment with an increased microbial diversity. In the mouth, oral bacteria form biofilms, which are highly organized communities, composed of many diverse microorganisms acting in concert (41). Only recently was there a study on the effect of MDPB in combination with silver nanoparticles on a static multispecies biofilm model. The combination of these agents showed a strong effect in reducing viability, metabolic activity and acid production of the biofilm (337). However, the commercial product Clearfil SE Protect has not been tested against a more diverse oral biofilm.

Additionally, oral biofilms are affected by environmental factors – some of them coming from our common diet – inducing changes in their composition and metabolism. Frequent fermentation of sucrose by acidogenic bacteria results in low pH levels that trigger an imbalance in the normal microbiota, favoring the growth of more virulent and cariogenic species (41). Moreover, the pH drop tends to be greater and prolonged in time

when higher concentrations and increased frequency of sucrose exposure is used (338, 339). In addition, sucrose can also be utilized for the synthesis of extracellular (EPS) and intracellular polysaccharides (IPS) in the dental plaque. The EPS produced on the tooth and bacterial surfaces enhances initial microbial colonization and the continuous accumulation of EPS enmeshes the microbial cells, creating microcolonies (76). Through *in situ* pH-mapping (77), it has been determined that this complex 3D architecture generates compartmentalized acidic and EPS-rich microenvironments in the biofilm. These acidic compartments, protected by the EPS, showed impaired neutralization by buffer. Furthermore, enhanced resistance to chlorhexidine solution has been found within the EPS-microcolonies compared to those outside such structures within the biofilm.

In general, these two aspects – bacterial diversity and the potent effect that sucrose exerts over oral bacteria – are often ignored when testing antimicrobials. Therefore, the general aim of this study is to assess the antimicrobial effect of MDPB-containing adhesive (unpolymerized and polymerized) against multispecies bacteria culture/biofilms, and to test whether this effect is sustained against a sucrose-fed, more cariogenic biofilm.

We hypothesized that MDPB primer exerts inhibitory effects on multispecies bacterial cultures and inhibits biomass formation and metabolism of oral biofilms when polymerized. Moreover we hypothesized that polymerized MDPB adhesive systems will sustain their effectiveness against a more cariogenic sucrose-fed biofilm.

7.2 Materials and methods

7.2.1 Materials and multispecies inoculum stock

To test the effectiveness of antimicrobial containing adhesives we selected a commercially available adhesive named Clearfil SE Protect bond (SEP) (Kuraray Noritake Dental Inc, Okayama, Japan) that contains MDPB in the primer. An adhesive counterpart manufactured by the same company was chosen as a control for the antimicrobial component, named Clearfil SE bond (SE). SE does not contain antimicrobials but conserves the same main components in the primer formulation (Table 7.1). Both systems are dual component, meaning the primer and bond come separated.

The bond system of SEP contains fluoride, which is reported to have antimicrobial activity besides the remineralizing action. To avoid fluoride as a confounder variable, only the bond of SE was used in combination with the primers when polymerized samples were needed. SE bond has the same composition as the bond for SEP, but with no fluoride (Table 7.2).

In order to generate a clinically relevant biofilm model plaque and saliva samples were collected from a donor with high caries risk (~9years old) (276). Plaque was retrieved from the margin of a dental restoration and immediately transferred into a vial containing pre-reduced anaerobic transfer medium (Anaerobe Systems, Morgan Hill, CA, USA). Whole saliva was collected by expectoration. Immediately after, the collected saliva was centrifuged at 10,000 rpm for 10 minutes, twofold diluted with Gibbon's buffer, filter-sterilized, aliquoted and stored at -80°C (276). Preparation of multispecies biofilm frozen stock for inoculation was done as described in Chapter 5 section 5.2.

Table 7.1 Components in the primer of Clearfil SE (SE) and Clearfil SE Protect (SEP)

Chemical components	SE	SEP
2-hydroxyethyl methacrylate	**X**	**X**
10-Methacryloyloxydecyl dihydrogen phosphate	**X**	**X**
12-Methacryloyloxydocecylpirimidium bromide		**X**
Hydrophilic aliphatic dimethacrylate	**X**	**X**
Water	**X**	**X**
Accelerators	**X**	**X**
Dyes	**X**	**X**
dl-Camphorquinone	**X**	

Table 7.2 Components in the bond of Clearfil SE (SE) and Clearfil SE Protect (SEP)

Chemical components	SE	SEP
Bisphenol A diglycidylmethacrylate	**X**	**X**
2-hydroxyethyl methacrylate	**X**	**X**
10-Methacryloyloxydecyl dihydrogen phosphate	**X**	**X**
Sodium fluoride		**X**
Hydrophilic aliphatic dimethacrylate	**X**	**X**
Colloidal silica	**X**	**X**
Accelerators	**X**	**X**
Initiators	**X**	**X**
dl-Camphorquinone	**X**	**X**

7.2.2 Antimicrobial activity of unpolymerized MDPB-containing primer against multispecies oral bacteria culture

The initial test consisted in exposing oral multispecies bacteria to the unpolymerized primer of SEP (UNSEP). This was carried out based on previous protocols to test MDPB-containing adhesives (304, 317). Unpolymerized SE (UNSE) was used as a control for the antimicrobial component. Saline solution and chlorhexidine were used as internal negative and positive controls for the experiments.

Agar disk diffusion test

Tryptic soy 5% blood agar plates were prepared with Tryptic soy agar (BD Diagnostic Systems Europe, Becton Dickinson, France) and defibrinated sheep blood. 10µL of multispecies frozen stock was diluted for ~6 hours in 10ml of basal mucin medium (BMM) and incubated anaerobically at 37°C under constant shaking (20rpm).

After the incubation period, the optical density (OD) of the multispecies bacteria culture was measured and adjusted to 0.2 (~10^6 CFU/ml). Then 300 µL of the multispecies culture were spread over three Tryptic soy 5% blood agar plates to form a bacterial lawn. Sterile 6mm diameter filter paper disks were soaked in 20µL of either unpolymerized Clearfil SE Protect (UNSEP), unpolymerized Clearfil SE (UNSE), 0.9% sterile saline solution (SS) or 2% chlorhexidine (2%CHX) and then placed in a designated quadrant in each plate. All plates were incubated anaerobically for 24h at 37°C. The major diameter of the halo of inhibition was measured with a ruler. Then, the diameter of the disk was subtracted from the measurements and the resulting values were divided by two. Three individual experiments were conducted in triplicates.

Bactericidal test against oral multispecies planktonic culture

The antimicrobial activity against planktonic culture was tested according to a previous published protocol (304). Briefly, 30µL of unpolymerized SEP primer, unpolymerized SE primer, saline solution, or 2%CHX were mixed with 90µL of multispecies culture at OD 0.2 (~10^6 CFU/ml). After 5 minutes of contact, the mixture was serially diluted and plated on Tryptic soy 5% blood agar plates. The plates were incubated anaerobically for 24h at 37°C. After the incubation period, the presence of colonies was checked by visualization and the number of recovered viable cells was counted with Quantify-one software (Bio-Rad laboratories, Inc., Philadelphia, PA, USA). The test was conducted in triplicates and repeated three times.

7.2.3 Antimicrobial activity test of polymerized MDPB-containing adhesive system against multispecies oral biofilm

The next step was to test the antimicrobial activity of the polymerized form of Clearfil SE protect in a closed oral multispecies biofilm model. The aim of this section was to test whether the polymerized Clearfil SE Protect (SEP) inhibits biofilm formation and metabolic activity compared to the polymerized counterpart (SE) under basal

growing conditions (no sucrose). Unpolymerized primer of both SE and SEP were used as controls.

Sample preparation

All instruments and molds were disinfected with 70% ethanol prior to sample preparation. Polymerized samples were prepared using a circular metallic mold (7mm diameter and 1mm deep) placed against a matrix strip (Patterson® Mylar® Matrix Strips) forming a circular 1mm deep well. 5µL of primer of SEP or SE were deposited at the bottom of the well in contact with the matrix strip; the primer was dried out for 72h to evaporate the water solvent content. After the drying process 5µL of bond were added on top of the primer and cured for 20s. The rest of the mold was filled with Z250 restorative composite and cured for 20s. The samples were removed from the mold and inverted to leave the primer layer as the top surface. The samples were irradiated with UV light for 20 min before the test. The unpolymerized samples were prepared by applying a thin coat of primer on top of polymerized samples, followed by air-drying. After UV irradiation the specimens were allocated in 24 well plates. Each specimen was coated with 5µL of filtered sterilized saliva and then inoculated with 10µL of multispecies stock diluted in anaerobic transportation media (10^5 CFU/ml). After inoculation, 1mL of BMM was added to each well. The plates were incubated for 48h; medium was replenished daily. Then, the specimens were evaluated for biomass formation evaluation and metabolic activity analysis.

Biomass through crystal violet staining

The specimens were washed with 1.0 ml 1xPBS three times. Cells were stained with 0.5ml of 0.1% crystal violet solution for 15 min in an orbital shaker (25 rpm, room temperature). Then the samples were collected into a 2 ml micro tube with 1.0 ml of 30% acetic acid. Solubilization was carried out for 20 min in an orbital shaker (25 rpm, room temperature). After solubilization, 10^{-1} serial dilution was performed. Aliquots of 200µl

of the crystal violet/acetic acid solution were transferred to an optically clear flat-bottom 96-well plate. Optical density was read at 600 nm with a Synergy HT microplate reader (Biotek Instruments, Inc., VT).

Metabolic activity measured by ATP

All specimens were transferred to a new 24 well plate and washed with 0.9% of NaCl three times. Then, each sample was transferred into a 2ml micro tube containing 1ml of 0.9% NaCl, and sonicated for 10 min. After sonication gentle vortexing was performed to ensure biofilm detachment from the disk's surface. 100µl of the bacterial suspension were transferred to an opaque-walled 96-well plate followed by 100µl of BacTiter-Glo™ (Promega, USA) reagent into each individual well. The contents were mixed briefly with an orbital shaker and incubated for five minutes. Luminescence was recorded with a Synergy HT microplate reader (Biotek Instruments, Inc., VT).

7.2.4 Antimicrobial activity test of polymerized primer SEP under increasing concentrations of sucrose.

The aim here is to test whether the polymerized primer of Clearfil SE Protect (SEP) inhibits biofilm formation and metabolic activity compared to the polymerized counterpart (SE) when the oral multispecies biofilm is fed with increasing concentrations of sucrose. Specimens were prepared as mentioned above (section 6.2.2). After UV irradiation the specimens were allocated in 24 well plates. Each specimen was coated with 5µL of filtered sterilized saliva and then inoculated with 10µL of multispecies stock diluted in anaerobic transportation media (~10^5 CFU/ml). After inoculation, 1ml of BMM was added to each well. The plates were incubated for 24h. On the second day the medium was replenished with BMM only, or 1% sucrose BMM, or 5% sucrose BMM or 10% sucrose BMM according to the group. The specimens were incubated for another 24h. After the incubation period the samples were collected and assessed for biomass through crystal violet staining and metabolic activity through ATP assay as described

above (section 6.2.2).

7.3 Statistical Analysis

The results were analyzed by one-way analysis of variance (ANOVA), followed by Tukey HSD post-hoc test at a significant level of 0.05. In cases where the equal variance assumption was violated Dunnett's T3 post-hoc test was used. For the experiments with increasing concentration of sucrose, two-way ANOVA was utilized with sucrose and the presence of antimicrobial as the in between subject factors. Analysis was conducted with IBM SPSS statistics Grad Pack 23.0.

7.4 Results

Unpolymerized SEP exerts inhibitory effects on oral multispecies bacteria

Unpolymerized MDPB-containing adhesive system has been mostly tested against single species culture of specific oral bacteria. We wanted to test if the unpolymerized SEP displayed antimicrobial activity against an oral multispecies bacteria culture originated from plaque samples of children with high caries risk. The agar diffusion test showed that the unpolymerized form of SEP displayed similar halos of inhibition compared to 2% CHX (Fig. 7.1a and b), which is a strong and well known antimicrobial. Interestingly, the unpolymerized control SE also display levels of antimicrobial activity as smaller halos of complete inhibition surrounded by a second halo of partial inhibition was observed (Fig. 7.1a), though the inhibition by UNSEP was significantly greater than UNSE (p=0.00006). SS (negative internal control) as expected, did not generate any halo of inhibition. The results of the bactericidal test showed that both unpolymerized primers SE and SEP have a strong bactericidal effect against oral multispecies planktonic culture as no viable cells were recovered (Table 7.3). Same results were observed for 2% CHX.

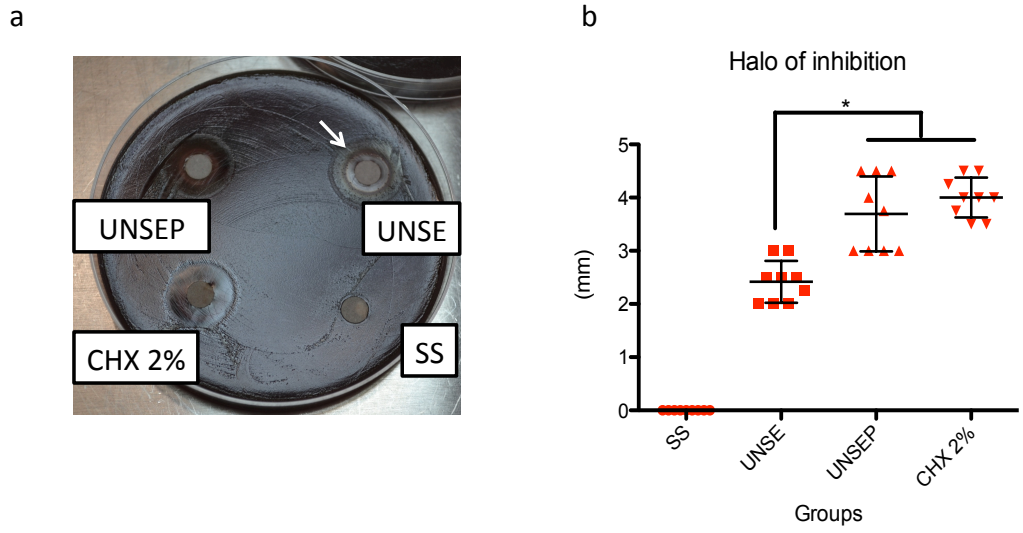

Figure 7.1 Antimicrobial activity of unpolymerized primer against multispecies bacteria. a) Representative image of agar disk diffusion test. b) Halo of inhibition generated by the different groups.

Table 7.3 Number of total viable cells recovered after bactericidal test

Groups	Viable cells recovered	Log_{10} CFU/ml Mean ± s.d
SS (negative control)	+	7.32 ± 0.26
UNSE	-	n.a
UNSEP	-	n.a
CHX 2% (positive control)	-	n.a

SS= saline solution
UNSE= unpolymerized Clearfil SE
UNSE= unpolymerized Clearfil SE Protect
CHX 2%= chlorhexidine 2%
s.d= standard deviation of the mean
n.a=non aplicable

Polymerized SEP reduces oral multispecies biofilm formation and metabolic activity

The assessment of the antimicrobial activity of the polymerized form of MDPB-containing adhesive is critical to estimate the ability of this adhesive to prevent secondary caries formation. We tested whether the polymerized SEP adhesive system had an antimicrobial effect against an oral multispecies biofilm model. Polymerized SEP showed a significant reduction in total biomass formation (p=0.016) compared to the counterpart SE after 48h of growth. The metabolic activity was also reduced but the difference was not statistically significant (p=0.216) (Fig. 7.2 and 7.3a). However, complete inhibition of biofilm formation was not observed (Fig. 7.2 and 7.3a). The unpolymerized controls SE and SEP displayed a significant reduction in biofilm formation and metabolic activity, with UNSEP showing lower levels than UNSE in metabolic activity values.

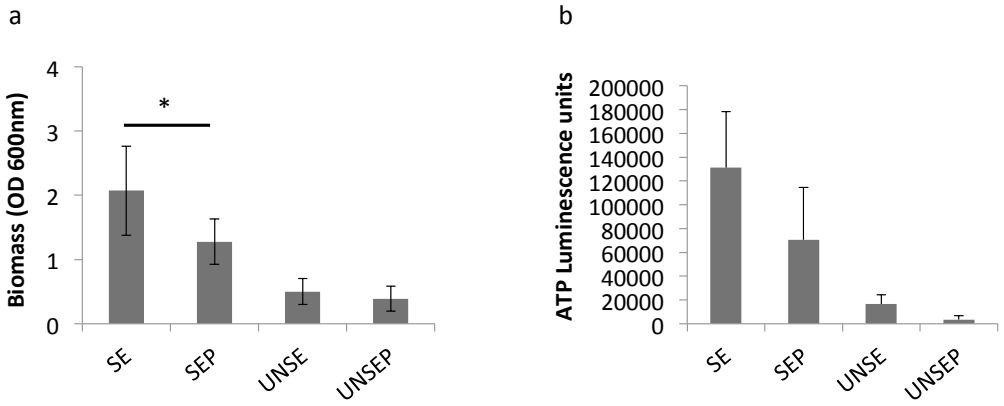

Figure 7.2 Antimicrobial effect of polymerized SEP under basal conditions. (a) Quantification of biofilm biomass formed over the surfaces of SE, SEP, UNSE and UNSEP specimens through crystal violet staining. (b) Metabolic activity of the same groups measured by ATP assay.

Presence of sucrose abolished antimicrobial activity

Sucrose is a fermentable carbohydrate that induces the production of EPS. It has been reported that sucrose-fed biofilms show increased resistance to antimicrobials. We

assessed the ability of SEP adhesive system to sustain an antimicrobial effect against an oral multispecies biofilm in the presence of sucrose. Total biomass and metabolic activity results showed that in the presence of increasing concentrations of sucrose the antimicrobial effect is lost as no significant differences are detected between the SE and SEP (Fig. 7.3 and 7.4). Two-way ANOVA analysis showed no interaction between the presence of sucrose and the presence of antimicrobial in the dental adhesive. However, the main effect of sucrose was statistically significant (p<0.001). The values of biomass and metabolic activity were higher with the increasing sucrose concentration.

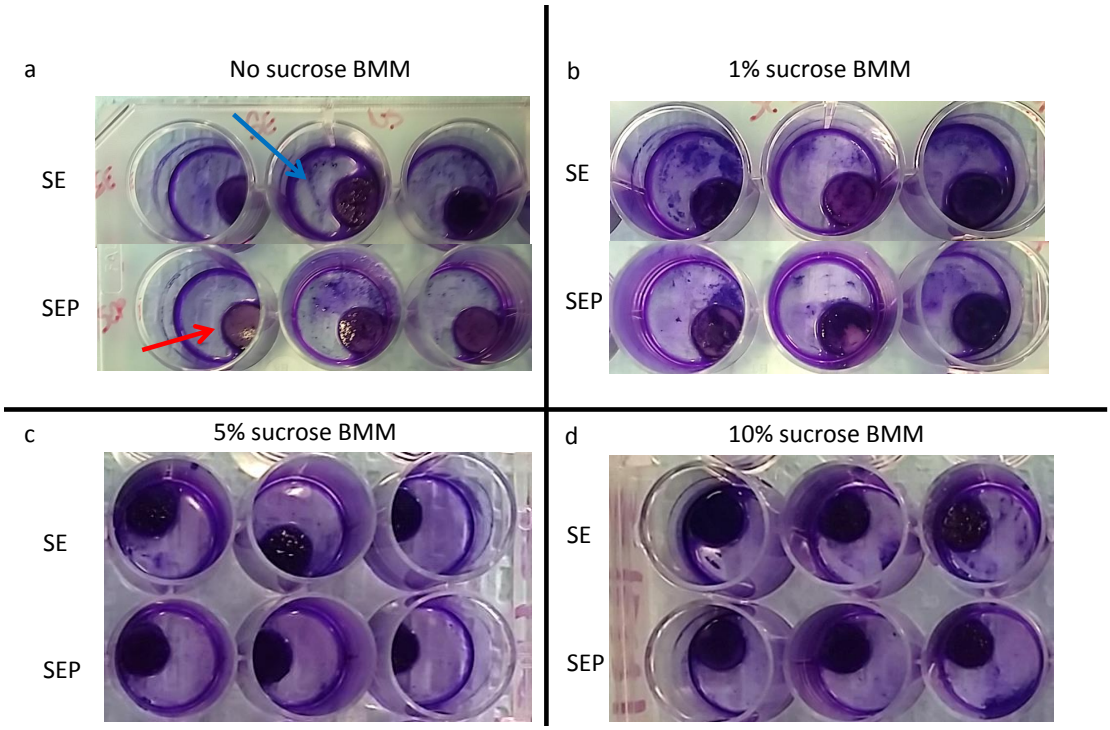

Figure 7.3 Crystal violet staining of oral biofilm formed over the surface of SE and SEP specimens after 48h of growth under (a) no sucrose, (b) 1% sucrose BMM, (c) 5% sucrose BMM and (d) 10% sucrose BMM.

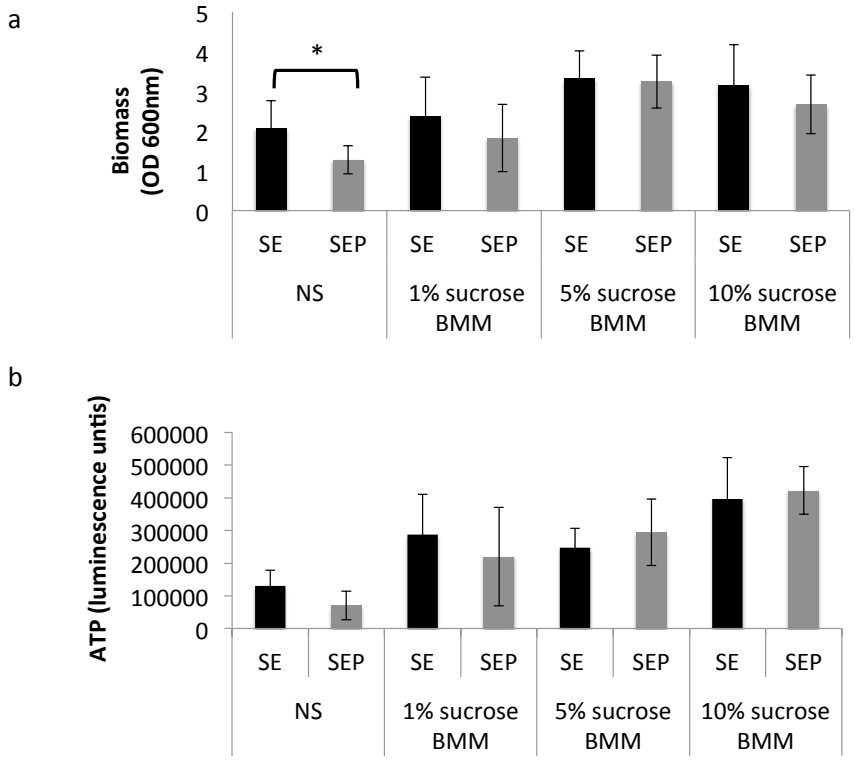

Figure 7.4 Crystal violet staining of oral biofilm formed over the surface of SE and SEP specimens after 48h of growth under (a) basal conditions, (b) 1% sucrose BMM, (c) 5% sucrose BMM and (d) 10% sucrose BMM.

7.5 Discussion

Antimicrobials immobilized to the matrix of dental adhesives seem to be promising to prevent the formation of secondary caries at the restoration interface. MDPB-containing systems have shown strong antimicrobial activity against certain oral bacteria when tested in the unpolymerized state. However, the antimicrobial activity of the polymerized adhesive seems to be to a lesser extent of that the unpolymerized form (335, 336). In general, this antimicrobial adhesive has been tested using agar disk diffusion test, direct contact method, or using a biofilm model of *S. mutans*. Even though valuable preliminary

information is obtained with these methods, they fail to recapitulate the diversity and growth of oral biofilms. It has been reported that due to site-specific environmental conditions, the composition of the oral microbiota varies significantly with the different regions within the mouth (eg, tongue, buccal mucosa, and teeth). Therefore, for the study of dental materials and oral bacteria interactions it is clinically relevant to develop a model that closely represents the microbiota associated with the dental material. We decided to use a microcosm approach to develop a multispecies oral biofilm. For this study plaque samples were taken from composite restoration margins of children at high caries risk. The use of this microcosm technique maintained the complexity and heterogeneity of the *in vivo* dental plaques associated with dental composite restorations (276).

The antimicrobial activity of the unpolymerized MDPB-containing primer showed a strong effect against an oral multispecies culture. These data complement previous observations in which the Clearfil SE protect primer was tested against streptococci, lactobacilli and actinomycetes (324). This strong antimicrobial effect is not surprising as before polymerization the MDPB monomer acts as a free antimicrobial. Due to its positive charge polar head, MDPB can interact with the negatively charged bacteria in a very rapid manner exerting antibacterial effects. For a clinical application, having a strong antimicrobial effect during the unpolymerized state can be advantageous to inhibit residual bacteria left at the restoration walls. In this line of research, Imazato et al. (324) showed that MDPB-containing primer generated a 2 log cell reduction after being applied to infected demineralized dentin surface (10^6 *Streptococcus mutans* cells) for 10 minutes. Also, another study reported that no viable bacteria were recovered after MDPB-containing primer was in contact with planktonic culture of residual cariogenic oral bacteria (323). Those data indicate that the application of the unpolymerized MDPB-containing primer can be beneficial after caries removal, especially when partial excavation is recommend. However, proximity with the dental pulp must be considered as levels of cytotoxicity have been reported with both experimental and commercial product (321, 328). In addition, for this specific application other factors need to be further evaluated, such as the bonding ability to infected substrates. Interestingly, the

control primer without MDPB also showed strong antimicrobial activity when the unpolymerized state was tested against a multispecies planktonic culture, although a lesser degree of effect was found with the agar disk diffusion test. A main explanation for this observation might be the presence of acidic adhesion-promoting monomers in the composition of the dental primer. It has been reported that unpolymerized dental adhesives without any added antimicrobial can display some degree of antimicrobial activity depending on their formulations (298, 340, 341). In specific, self-etching systems usually contain highly acidic monomers in the primer yielding to lower pH values than conventional etch-and-rinse adhesive systems (296). Protons ions can destroy the amino – acid bond in nucleic acids, modify the cytoplasmic pH and precipitate proteins. It has been demonstrated that low pH adhesives display antimicrobial activity against oral streptococci similar to that of chlorhexidine (342) but not to acid tolerant bacteria such as Lactobacilli (343).

This also might explain the results seen with the agar disk diffusion test, in which a second partial inhibition zone was observed. Considering this aspect, the inhibition generated herein by the MDPB-containing primer cannot be completely attributed to the presence of the antimicrobial monomer.

As mentioned above, many studies have concentrated on the effect of the unpolymerized form of MDPB-containing adhesive, while much less is known of the antimicrobial activity of the polymerized state. Here, we presented a closed biofilm model using a composite-associated microcosm inoculum to test the effect of the polymerized Clearfil SE protect at inhibiting oral biofilm formation. The results showed that the polymerized MPDB-adhesive system significantly reduced the amount of biomass formed when compared to the control SE, which generated a thicker layer of biofilm over the surface of the specimens. Also, the ATP activity assay showed reduction on the metabolic activity in specimens prepared with MDPB-containing adhesive system compared to control. However, complete inhibition of biofilm formation was not observed. It is possible that because MDPB is immobilized into the adhesive matrix, there are not enough available cationic groups on the surface of the specimens after polymerization. It has been shown that for bactericidal cationic surfaces a certain charge

density threshold must be achieved to display rapid bactericidal effects (344). Also, in our study we simulated acquired salivary pellicle formation prior to inoculation with oral bacteria, which might have influenced the antimicrobial effect. Muller et al (345), while investigating the influence of prior protein adsorption on the antimicrobial activities of positively charged MDPB-coated silicon wafers found that the original bactericidal activity of the pyridinium-coated surface was greatly reduced upon adsorption of a protein film. Thus, a limitation of surfaces with cationic groups is their susceptibility to adsorb proteins present in body fluids due to electrostatic interactions, which can hinder the antimicrobial functional groups. This must be taken into consideration when developing new antibacterial materials as dental restorations are constantly exposed to saliva.

Another important aspect evaluated in this study was the effect of sucrose on the antimicrobial activity of the polymerized MDPB-containing adhesive system. In secondary caries (as in primary caries) the process of degradation of dental tissues by oral bacteria is triggered by a metabolic deregulation of the oral biofilm. It is known that in the presence of high concentration or frequent consumption of fermentable carbohydrates, such as sucrose, fermentation byproducts lead to acidification of the milieu generating an imbalance in the normal microbiota, which favors the growth of more virulent and acid-tolerant cariogenic species (41). In the model presented here, increasing concentrations of sucrose, spanning from 1% to 10% were added after the first 24h of biofilm growth to simulate a cariogenic challenge. The results demonstrated that the ability to reduce biofilm formation and metabolic activity was lost when sucrose is present in the media, regardless the concentration of sucrose, although more biomass and higher metabolic activity was seen with increasing concentration. In a similar line of research, Lobo et al. (346) and de Carvalho et al. (347) demonstrated that Clearfil SE Protect system failed to prevent demineralization next to a composite restoration when the restorations were challenged with a cariogenic *Streptococcus mutans* biofilm (346, 347). These results highlight the relevance of incorporating factors associated with dysbiosis of the oral biofilm when studying dental materials with antibacterial properties. This becomes even more important when considering that composite restorations display

higher failure rates in patients at high caries risk (14).

Reports of new prototypes for dental materials with antibacterial properties are increasing at a fast pace in the literature. Here we presented a more representative *in vitro* model for the screening of these products prior the assessment with clinical trials or their eventual commercialization.

7.6 Conclusion

Commercially available MDPB-containing primer showed strong antimicrobial activity against multispecies bacteria culture when tested in the unpolymerized state. The polymerized antimicrobial adhesive reduced biofilm formation and metabolic activity when tested in a closed multispecies biofilm model; however complete inhibition of oral biofilm formation was not observed. The presence of sucrose in the media abolished the antimicrobial effect seen under basal growing conditions.

Chapter 8. Testing antimicrobial activity of MDPB-containing adhesive system using a Drip Flow Reactor

Summary

The aim of this chapter was to study the antibiofilm effect of an MDPB-containing adhesive using Drip flow reactor model to simulate oral conditions. Initial work was done to optimize the DFR for antimicrobial testing. Uniform biofilm growth over dental composites specimens was analyzed through biomass formation and biofilm thickness. The antimicrobial activity was tested after the system was optimized. Briefly, specimens prepared with Clearfil SE (SE) and Clearfil SE Protect (SEP) were allocated in a designated DFR channel and coated with 5µl of filtered-sterilized saliva. Each individual DFR channel was inoculated with 16ml of oral multispecies inoculum and incubated anaerobically for 12h at 37°C under shear condition. After the incubation phase, DFR was transferred to a modified incubator and connected to nutrient flask containing Basal Mucin Media (BMM) or 1% sucrose BMM. Flow rate was set at 0.5 ml/min. Biofilms were grown for 24 at 37°C. After the growth phase the biofilms grown over the specimens were assessed for biofilm biomass, metabolic activity and recoverable viable cells. The optimization phase showed that oral biofilms could be grown in a uniform manner inside a DFR. However, it was critical to control the inoculum concentration to avoid overgrowth.

The results for the antimicrobial testing showed that the MPDB-containing adhesive (SEP) did not prevent biofilm formation, neither reduced metabolic activity nor viable cell count compared to SE-control. The lack of antimicrobial activity was seen in both conditions, with and without sucrose.

8.1 Introduction

To evaluate the effectiveness of antimicrobial-containing bonding systems against oral bacteria, it is necessary to generate representative models of the oral environment. Most studies utilize bacterial culture or single-species biofilms models based on historically defined cariogenic pathogens, which fail to portrait the complexity of the oral microbiota. Moreover, the advent of molecular technologies revealed that not only mutans streptococci or lactobacilli species are related with dental caries. We have shown previously an *in vitro* approach for recapitulating the complex bacterial population associated with dental composites (Chapters 4-5 and 7). In that system, oral bacterial samples were obtained from composite restorations of patients at high caries risk and grown in a bioreactor to generate oral biofilms that were associated with dental composites and with an increased microbial diversity.

Besides the use of a relevant microbial population, it is also important to recreate other environmental conditions that can influence biofilm formation. It has been reported, for example, that fluid flow over biofilms not only provides nutrient transport, but also induces fluctuating mechanical pressures that causes alterations in the biofilm architecture (348). Indeed, oral biofilms may experience diverse mechanical challenges, since they form under highly different shear rates coming from exposure to saliva or the crevicular fluid. Paramona et al. (349) showed that oral multispecies biofilms grown at lower shear rates were more carpet-like, homogeneous, and thinner compared with biofilms grown at higher shear rates, which were more "fluffy", heterogeneous, and thicker.

Our study proposes the use of a drip flow bioreactor (DFR) to recreate the mechanical challenges induced by fluid flow. A DFR has the advantage of growing biofilms under low/mild shear and close to the air-liquid interface (350), resembling what occurs in the oral cavity. In this chapter a DFR is used in combination with an oral multispecies inoculum to generate an oral biofilm model for studying effectiveness of antimicrobial-containing bonding systems. This model was also used to test whether the antimicrobial effect is sustained against a sucrose-fed, more cariogenic biofilm.

The initial goal was use the DFR to grow uniform layers of multispecies oral biofilm over dental materials specimens in the presence and absence of sucrose. We hypothesized that polymerized MDPB-containing adhesive system inhibits growth and metabolism of a multispecies oral biofilm when tested in a DFR system in the absence and presence of sucrose.

8.2 Materials and methods

8.2.1 Drip Flow Reactor system and optimization

The goal of this section was to grow multispecies biofilms from frozen stocks over dental specimens in a uniform and repeatable manner, using a DFR (BioSurface Technologies, Bozeman, MT, USA) (350). These frozen stocks were derived from plaque samples taken from composite restorations. Composite resin disks with no antimicrobial properties were used as substrates to verify uniform biofilm formation along the DFR channels, when different inoculum concentrations and increasing concentrations of sucrose were used.

DFR device

The DFR system consisted of a polysulfone base with four 2.55 cm x 10.16 cm x 1.99 cm channels and four 1.27-cm barbed effluent ports (one at the end of each channel) (Fig. 8.1), which connect through tubing with the waste collection carboy. Each channel is covered by polycarbonate covers 3.44 cm × 12.7 cm × 1.22 cm) and secured with nylon screws to the reactor base. Each of the cover contains two ports, one for the influent media and another one for bacterial air vent attachment (used to allow for the sterile air and gas exchange). Mininert valves are inserted in each of influent ports allowing the passage of a needle connected the nutrient tubing (Fig. 8.1a). O-rings are fitted underneath to seal cover to base during the experimental run. To provide media flow the device is set on a 10° base (Fig. 8.1b).

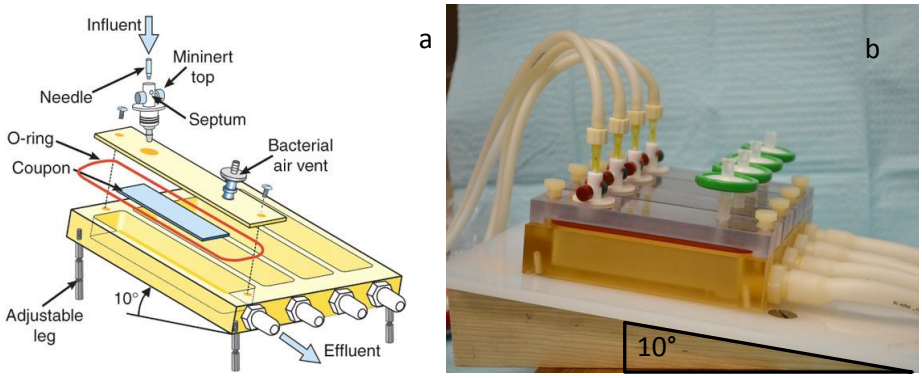

Figure 8.1 (a) Schematic representation DFR taken from (350). (b) DFR used in the experiments showing a 10° base used to reached the desired inclination.

Sample preparation

Composite disks made with Z250 (3M ESPE, St. Paul, MN, USA) were prepared using a metallic mold (7mm diameter and 1mm deep). Briefly, the mold was put against a flat matrix strip and then filled with Z250 composite, a glass slide was placed on top of the mold to obtain a smooth and leveled surface of the specimen. Each composite disk was cured for 40 sec with a curing light unit (Elipar, 3M ESPE, St. Paul, MN, USA). After polymerization, the specimens were irradiated with U.V. light for 20 min before inoculation.

Modifications to DFR

The original DFR design was modified to fit specimens made with dental adhesives/composite materials. Customized rectangular coupons were designed to hold composite specimens inside each channel (Fig. 8.2). Each coupon contained seven wells (7mm diameter and 1mm deep) aligned at the center of the rectangle. The position of the wells was defined as 1 to 7 within each channel, where 1 was the top position and 7 the one at the bottom of the coupon. Two screw-retained beveled bars were used to keep the specimens in place and to channel the medium flow to the center of each holder (Fig. 8.2). This last step ensured that all the specimens were covered by the medium during the

experimental run.

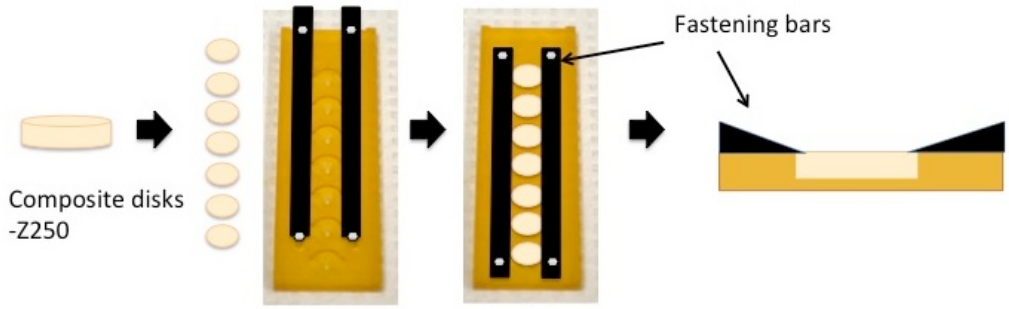

Figure 8.2 Modified coupons to allow the incorporation of round samples made out of dental adhesive/composite materials. Beveled fastening bars to avoid sample movements and to channel medium flow are shown in black.

Biofilm biomass assessment generated with different inoculum concentrations

Frozen stocks were prepared as explained before (see details in chapter 5 section 5.2). After U.V. irradiation, the composite disk specimens were positioned in the customized holders (Position 1-top to 7-bottom) and coated with 5µl of filtered-sterilized saliva. Multispecies culture was grown from frozen stock until early log phase (OD ~0.2; ~10^6 CFU/ml). Multiple dilutions for inoculation were prepared from the original inoculum (1:10, 1:25, 1:50 and 1:100). Each individual DFR channel was inoculated with 16ml of either original or diluted inoculum and incubated for 16h inside an anaerobic chamber at 37°C in an orbital shaker at 20rpm. After the incubation phase, the DFR was moved to a modified incubator (Fig. 8.3) and connected to the nutrient flask containing Basal Mucin Medium (BMM). DFR inclination was set at 10 degrees. Flow medium rate was set at 0.5 ml min^{-1}. Biofilms were grown aerobically for 24h at 37°C (Fig. 8.3). DFR was disconnected after 24h of media flow and the specimens were transferred to a 24 well plate for analysis by crystal violet staining. The staining was performed as described above in chapter 7 section 6.6.2.

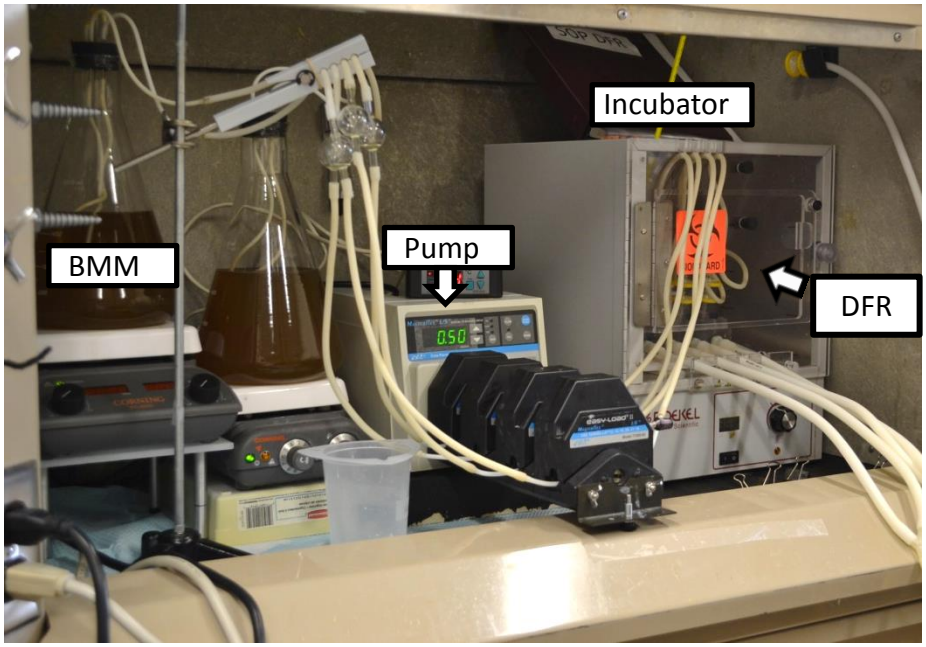

Figure 8.3 DFR experimental set up. The DFR was located inside a modified incubator to keep the temperature at 37º during the medium flow phase.

Evaluation of biofilm thickness with different inoculum concentrations

1:0, 1:25 and 1:50 dilutions from the original inoculum were selected to evaluate whether the inoculum concentration influenced the biofilm thickness after 24h of growth. Composite disks were inoculated and incubated in a DFR following the same steps mentioned above. Two runs of experiments were performed. After 24h, three disk specimens from each inoculum concentration were recovered for analysis. Near infrared cross-polarization optical coherence tomography (CP-OCT) system (IVS-200-CPM; Santec Co., Komaki, Japan) was used for real-time imaging of biofilm grown on dental composite material discs. The CP-OCT system used a high swept rate (30 kHz) continuous wavelength scanning laser centered near 1310 nm with a bandwidth of 104 nm. The axial resolution for structures in the biofilm was 8.5 μm whereas the lateral resolution of the system was approximately 80 μm (351). The recovered specimens were positioned in a 7-mm diameter customized holder containing 1xPBS. This allowed keeping the biofilms hydrated during the image acquisition. For each biofilm three cross-

sectional images were selected, and three thickness measurements of the biofilm (left, middle and right) were taken in real time. A total of 9 measurements were obtained per sample.

Evaluation of biofilm thickness and biomass with increasing sucrose concentration in the media

To evaluate the influence of increasing concentration of sucrose on the biofilm growth a 1:25 dilution (~10^4 CFU/ml) from a 0.2 OD original multispecies inoculum was prepared. Seven composite disks were inoculated in each channel and incubated in a DFR as mentioned above. After the overnight incubation, the channels were connected to four different nutrient flask containing no sucrose BMM, 0.1% sucrose BMM, 0.5% sucrose BMM, and 1% sucrose BMM. Flow rate was set at 0.5ml min^{-1} for the following 24 hours. DFR was disconnected after 24h of media flow and the specimens were retrieved for thickness evaluation through Optical Coherence Tomography (OCT) imaging analysis. A separated run using the same inoculum concentration was done to compare biofilm biomass between BMM no sucrose and 1% sucrose BMM.

8.2.2 Antimicrobial activity of antimicrobial-containing dental adhesive tested in a DFR

Once it was confirmed that uniform biofilm formation over dental specimens could be obtained along and across the channels, we proceeded to test the antimicrobial effect of an MDPB-containing adhesive over a multispecies biofilm using a DFR.

Sample preparation

Polymerized samples were prepared using a circular metallic mold (7mm diameter and 1mm deep) that at the bottom was facing a matrix strip (Patterson® Mylar® Matrix Strips) while the top was open forming a circular 1mm deep well. 5µL of primer of SEP or SE were deposited inside the well in contact with the matrix strip; the primer was dried

out for 72h to evaporate the water solvent. After the drying process 5µL of bond were added on top of the primer and cured for 20s. The rest of the mold was filled with Z250 restorative composite and cured for 20s. The samples were removed from the mold, and then inverted to leave the primer layer as the top surface. The samples were irradiated with UV light for 20 min before the test.

DFR challenge

Drip flow reactor was used to simulate oral conditions. After UV radiation the polymerized SE and SEP specimens were located in the DFR customized holders and coated with 5µl of filtered-sterilized saliva. Multi-species culture was grown from frozen stock until early log phase (OD ~0.2) and diluted 1:25 (~10^4 CFU/ml). Each individual DFR channel was inoculated with 16ml inoculum and incubated for 12h inside of an anaerobic chamber under constant shaking (20 rpm at 37°C). After the incubation phase, DFR was moved to a modified incubator and connected to nutrient flask containing no sucrose BMM or 1% sucrose BMM. Flow rate was set at 0.5 ml min^{-1}. Biofilms were grown aerobically for 24h at 37°C. DFR was disconnected after 24h of media flow and the specimens were retrieved for biomass formation analysis through crystal violet, metabolic activity and colony forming units counting. Three experimental runs were conducted for each condition, no sucrose and 1% sucrose. Unpolymerized SEP was used as positive control for biofilm inhibition.

Biomass through crystal violet staining

Three specimens of each channel (group) were transferred to a new 24 well plate and stained as mentioned before (Chapter 6 section 6.6.2).

Metabolic activity measured by ATP

Three specimens from each group were transferred to a new 24 well plate and washed

with 0.9% NaCl three times. Then each sample was transferred into a 2ml micro tube containing 1ml of 0.9% of NaCl and sonicated for 10 min. After sonication, gentle vortexing and pipette mixing was performed to ensure biofilm detachment from the disk surface. 100µl of the bacterial suspension was transferred into an opaque-walled 96-well plate (Costar) and then 100µl of BacTiter-Glo™ reagent were added to each individual well. The contents were mixed briefly on an orbital shaker and incubated for five minutes. Luminescence was recorded with a Synergy HT microplate reader (Biotek Instruments, Inc., VT).

Colony forming units (CFU)

In order to study the viability of the biofilm after the exposure to the antimicrobial containing adhesives, plating and CFU counting was carried out. Briefly, specimens with 24h biofilms were washed with 0.9% NaCl to remove loose bacteria. The biofilms were suspended in 1 ml 0.9% NaCl and harvested by sonication for 10 min, followed by gentle vortexing and pipetting. An aliquot of 100 µl of the suspension was diluted in 0.9% NaCl in series up to 10^{-7} and plated into Tryptic soy 5% blood agar culture plates. The plates were incubated for 24h in an anaerobic chamber. Colonies were counted with Quantify-one software (Bio-Rad laboratories, Inc., Philadelphia, PA, USA).

8.3 Statistical Analysis

One-way analysis of variance (ANOVA) at a significant level of 0.05 was used to analyze the results from: biomass formation with different concentrations of multispecies inoculum, biomass formation along the positions in the DFR channel, thickness results from different inoculum concentration and increasing concentration of sucrose. Tukey's HSD was used as a post-hoc test when ANOVA was significant. Dunnett's T3 was used when equal variance assumption was violated. Student's t test was used to compare the mean biomass values between no sucrose condition and 1% sucrose BMM ($p<0.05$). Two-way ANOVA was used to analyze the results from biomass, metabolic activity and

CFU when the antimicrobial-containing adhesive was tested. The presence of antimicrobial and sucrose conditions was considered as the between-subject factors. Analysis was conducted with IBM SPSS statistics Grad Pack 23.0.

8.4 Results

Effect of multispecies inoculum concentration on biofilm biomass and biofilm thickness

The first goal was to evaluate if a DFR was suitable to grow a uniform biofilm layer over the surface of dental materials. All different concentrations of inoculum were able to generate thick biofilms, however the original inoculum and 1:10 dilution induced overgrowth. At these concentrations, it was observed that the top layer of the biofilm was loosely attached and it was easily washed away after rinsing with 1xPBS. In addition, crystal violet staining quantification showed different amounts of biomass from position 1 to 7 when samples were inoculated with either original inoculum or 1:10 dilution (Fig. 8.4a). With further dilution the biomass detected by the staining seemed to be more uniform along the positions in the channels. An interesting observation was that for all dilutions, the biofilm formed in position 7 was usually very loose and large parts were lost during the analysis procedure, yielding to reduced biofilm attachment in position 7 (p=0.00062) (Fig. 8.4a). The mean biomass formation per channel was very similar among all the concentrations tested, with no significant differences (p=0.846)(Fig. 8.4b). However, as mentioned before parts of biofilms could not be analyzed with original inoculum or 1:10 dilution.

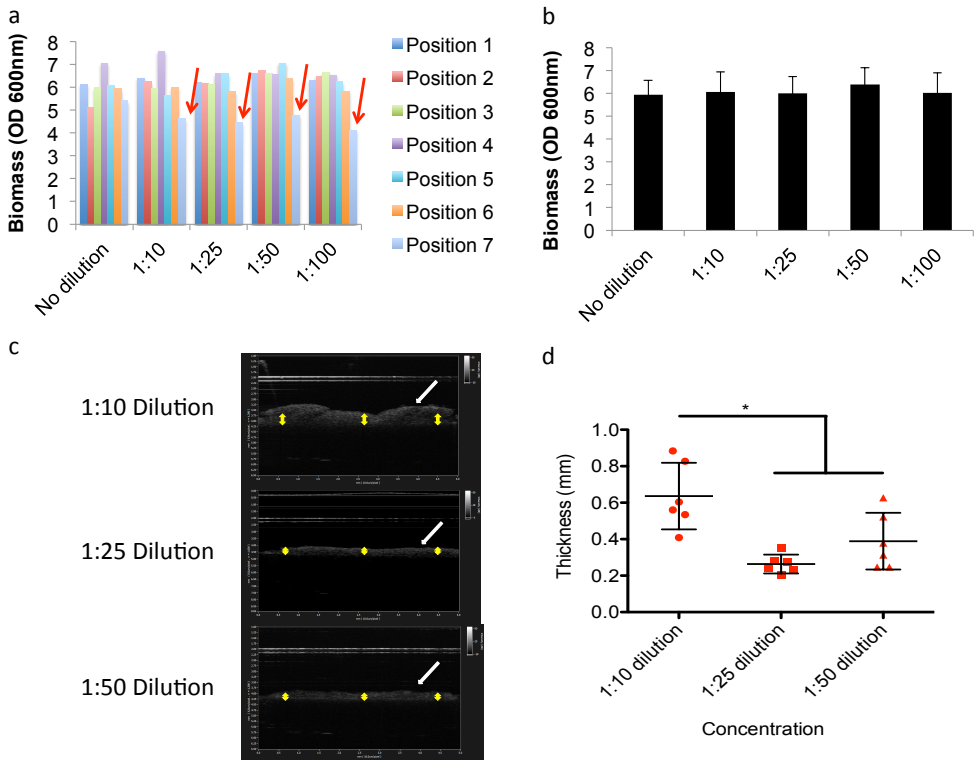

Figure 8.4 Biofilm biomass and thickness with different inoculum concentrations. (a) Biomass quantification in each channel per sample position and inoculum concentration. Red arrow points the reduced biofilm attachment found in position seven. (b) Mean and standard deviation of biomass quantification per channels with different inoculum concentration. (c) CP-OCT images showing the biofilm thickness with 1:10, 1:25 and 1:50 dilution from the original multispecies inoculum. White arrow indicates the layer of oral biofilm formed over the dental composite specimens. Yellow arrows indicate the approximate positions where real-time thickness measurements were taken. (d) Mean and standard deviation of biofilm thickness with decreasing concentration of inoculum.

Real-time thickness analysis revealed that thickness was influenced by the inoculum concentration (p=0.01). 1:10 dilution led to thicker biofilm formation compared to 1:25 and 1:50 dilution, but only 1:25 comparison showed statistically significant differences (p=0.009). It is possible that the crystal violet staining could not capture such differences

in thickness, as usually the top layer of the biofilm was lost during the analysis procedure. Due to these results the next set of experiments used 1:25 dilution of the original inoculum to inoculate the specimens, and also position 7 was removed from the analysis.

Effect of sucrose concentration on biofilm biomass and biofilm thickness

Figure 8.5a shows representative CP-OCT cross-sectional images of oral biofilms grown in the absence of sucrose or with increasing concentrations of sucrose. The incorporation of sucrose in the media led to thicker biofilms (p=2.975^{-10}) that presented a bulky morphology compared to the samples in no sucrose condition, which tended to be much flatter and uniform (Fig. 8.5a and b). The thickness of the biofilms was larger with 0.5 % and 1% of sucrose in the media (Fig. 8.5a and b). Also the biofilms grown in the presence of sucrose tended to be orange in color compared to the no sucrose group (Fig. 8.5c). 1% of sucrose in the media generated more biofilm biomass (p=0.01) ((Fig. 8.5d and e) and the thickest biofilms compared to lower concentrations and no sucrose condition (Fig. 8.5a and b). The biofilm biomass tended to be uniform along the positions in the DFR (Fig. 8.5e)

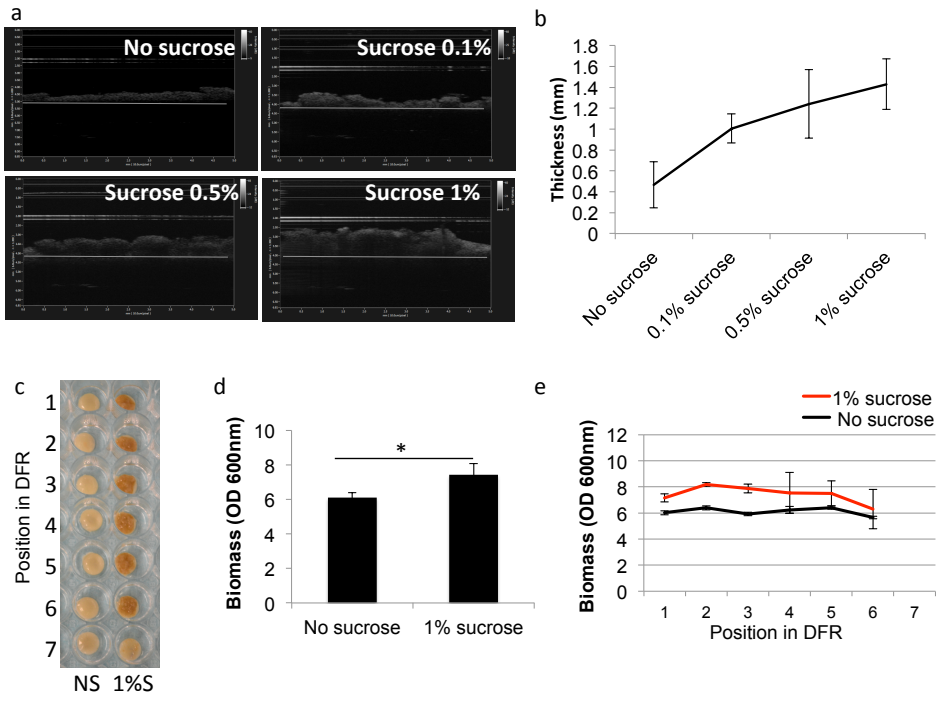

Figure 8.5 Effect of sucrose concentration on biofilm biomass and biofilm thickness. (a) Cross-sectional CP-OCT images of oral biofilms grown under no sucrose and increasing concentrations of sucrose. (b) Mean and standard deviation of biofilm thickness per channel, under no sucrose and increasing concentrations of sucrose. (c) Retrieved composite disk specimens with biofilm formed on the surface. NS= biofilm grown without sucrose. 1%S= biofilms grown in 1% sucrose BMM. (d) Mean and standard deviation of the biofilm biomass of specimens under no sucrose condition and 1% sucrose BMM. d) Biofilm biomass formed under no sucrose and 1% sucrose BMM from DFR position 1 to 6.

Antimicrobial activity of dental adhesives tested in a DFR

After optimizing the DFR for multispecies biofilm growth, the next step was to use this model to compare the antimicrobial activity of MDPB-containg adhesive systems in the presence and absence of sucrose. The results showed that the MDPB-containing adhesive, SEP, failed to prevent biofilm formation, as the amount of biomass was very

similar to one formed over specimens without MDPB (SE) (Fig. 8.6a-e). This tendency was observed for both no sucrose (p=0.931) and 1% sucrose (p=0.531) conditions. Also, no differences were observed for metabolic activity (p=0.497 no sucrose; p=0.055 1% sucrose), and viable bacteria (p=0.768 for no sucrose and p=0.488 for 1% sucrose BMM). During the course of these experiments, the unpolymerized form of SEP used as a positive control for biofilm inhibition (internal control of the experiment). UNSEP showed reduction of biofilm formation in both growing conditions, but the effect was less pronounced in the presence of sucrose for biomass formation. As occurred during the optimization phase of the DFR and the experiments performed in the closed biofilm model (Chapter 7), the main effect of sucrose was statistically significant (p<0.001), generating an increased amount of biomass and higher metabolic activity. Interestingly, a decrease in the number of recoverable viable bacteria was also induced by the presence of sucrose (p=0.01).

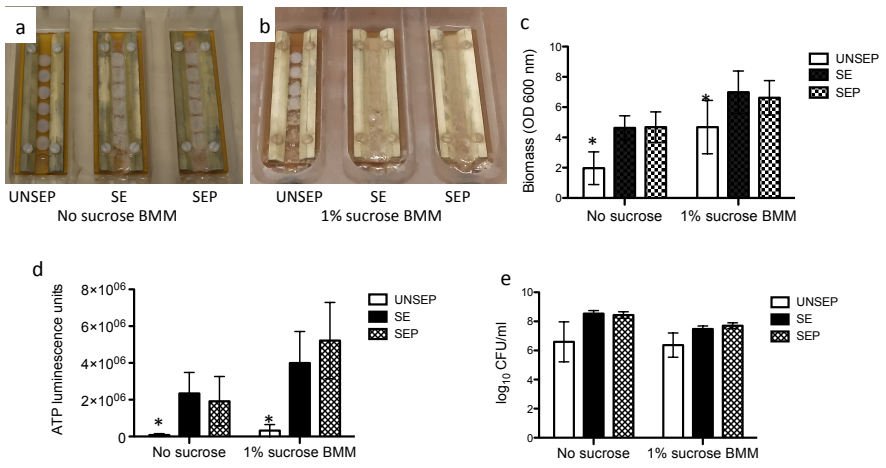

Figure 8.6 Polymerized MDPB containing adhesive effect on biofilm growth and metabolic activity of a multispecies oral biofilm. (a) 24h multispecies biofilms exposed to the different groups in the absence of sucrose. (b) Same as (a) but in the presence of 1% sucrose BMM. (c) Biofilm biomass formation over SE, SEP and control UNSEP groups. (d) Metabolic activity measured by ATP assay of biofilm

grown over SE, SEP and control UNSEP specimens. (e) Viable recovered bacteria from biofilms exposed to each group.

8.5 Discussion

Immobilized antimicrobials in the matrix of adhesive systems seemed to be a viable alternative to prevent the formation of secondary caries (334). An effective antimicrobial-containing adhesive should inhibit the growth of invading bacteria and subsequently reduce bacterial leakage even when marginal sealing is not complete after the placement of a restoration. Even though data supports the strong antimicrobial effect of unpolymerized MDPB-containing adhesive, the effectiveness of the polymerized form is not clearly supported, and neither is the long-term effect. Moreover, most studies rely on disk diffusion test or single species models, which do not recapitulate the complexity of oral biofilms. Therefore, *in vitro* models that simulate the growth conditions and diversity of oral biofilms are needed to test the effectiveness of antimicrobial adhesive systems. Here we presented a model based on the combination of a dental composite-associated multispecies inoculum with a DFR system to grow oral biofilms under similar conditions to the oral cavity.

The DFR provided a suitable model to grow a multispecies oral biofilm, however several modifications were done to ensure that biofilms grew uniformly along each channel. Higher inoculum concentrations generated biofilm overgrowth, whereas 1:25 and further dilutions tended to generate more uniform layers of biofilm. For future experiments 1:25 dilution of the original inoculum was used to minimize sampling errors generated by the dilution procedure. In addition, the DFR generated thinner and flatter biofilms in the absence of sucrose, while bulkier and thicker biofilms were observed with 1% sucrose in the media. For both conditions, it was common that biofilms grown at the bottom of the channel (position 7) were loosely attached to the surface of the specimens, and were constantly lost during the examination procedure. For this reason, only biofilm grown from position 1 to 6 were considered for the rest for the experiments.

This model was used to test the antibiofilm effect of the polymerized MDPB-containing adhesive. The results showed that SEP was unable to inhibit biofilm

formation. The levels of biomass, metabolic activity and viable counts were almost the same as the control adhesive SE. Compared to the model presented in Chapter 6 it is possible that the DRF model is a challenging system for antimicrobial surfaces as large amounts of biofilm are produced. However, other research groups have shown successful reduction of biofouling by cationic surfaces based in quaternary ammonium after 3 days of bacterial challenge using a DFR, although only single species biofilms were used (352).

Another explanation for these results is that this cationic monomer is covalently bound to the resin matrix, therefore the antimicrobial effect depends on how many cationic heads are exposed in the surface on the material. Indeed, it has been reported that immobilized cationic agents need to achieve a charge density threshold to exert antimicrobial effects (344). During the polymerization process the distribution of cationic heads is not controlled and they might not end up facing the surface of the specimen. This might yield an insufficient number of exposed groups to induce antimicrobial effects. Also as explained in Chapter 7, the samples were coated with filtered-sterilized saliva to simulate acquired salivary pellicle, which might have interacted with the cationic heads, reducing the overall antimicrobial potential. Nevertheless, dental materials are constantly exposed to saliva and crevicular fluid, thus a reduction of antibacterial activities by salivary protein coatings (345) is a possibility that must be considered when testing cationic antimicrobial materials.

The incorporation of sucrose did not change the trend observed with SEP in the absence of sucrose, but it increased the amount of biofilm formed and the metabolic activity, while reducing the number of viable cells. This can be explained by the production of exopolysaccharides (EPS) induced by sucrose (77), which generates an increase of the overall biomass and activity. The reduction on viable cell counts might be related with the selection process generated by the acidification of the local environment favoring the survival of aciduric species (41). For both conditions, no sucrose and 1% sucrose, the amount of biofilm biomass was larger than in the closed biofilm model presented in Chapter 6. It is possible that negatively charged EPS had electrostatically interfered with the cationic monomers and also acted as a physical barrier that restricted

the access to the bacterial cell wall (77), which might explain the differences in the results.

In summary, it is important that the model used to test the antimicrobial effect of antimicrobial-containing adhesive reflects the growing conditions of oral bacteria in the mouth. As seen here, different models might yield to different outcomes.

8.6 Conclusions

A DFR was optimized to test antimicrobial effect of antimicrobial-containing dental adhesives. The results showed that polymerized MDPB-containing adhesive failed to inhibit multispecies oral biofilm formation in the absence and presence of sucrose when tested in a DFR. Immobilized antimicrobial agents into dental adhesives might not provide protection against secondary caries.

Chapter 9. Conclusions

The breakdown of the adhesive interface in dental composite restorations might lead to higher incidence of secondary caries. Each of the components of the interface is susceptible to failure by many different factors. Better tools to study the interfacial integrity of dental composites and the factors associated with its eventual breakdown are needed.

We presented a more comprehensive method to study interfacial leakage. Using silver nitrate infiltration and image subtraction, we were able to use micro-CT to quantify leakage in 3D, overcoming previous limitations with this technique. Our results confirmed that leakage had an uneven distribution around the restorations. Also, for the set of adhesives included in the study, leakage at the interface mostly occurred between the adhesive system and the tooth structure. The same technique can be used to analyze leakage in other restorations types.

A new variant of the Brazilian Disk Test specimen was developed for testing dentin-composite bond strength. This novel test provided several advantages including: zero premature failure, simpler testing procedures, a consistent failure mode involving the adhesive interface, and reduced variation in the measurements.

Also, we presented a more comprehensive system to study the combined effect of mechanical and microbial challenge on the interfacial integrity of dental restorations in a human tooth model. Dental composites restorations were subjected to fatigue and to a multispecies oral biofilm to induce effects on the adhesive interface. The results showed that when specimens are subjected to both challenges, a greater reduction in fracture strength is seen compared to the effects of fatigue and biofilm alone demonstrating the additive effect of both. The presence of biofilm showed a substantial effect in the degradation of the adhesive interface, which was significant in the presence of sucrose, whereas the effect of fatigue was much less pronounced.

A multispecies oral biofilm/culture model was presented to test the effectiveness of commercially available MDPB-containing adhesive system. The unpolymerized dentin primer showed strong antimicrobial activity against multispecies bacteria. The polymerized antimicrobial adhesive reduced biofilm formation and metabolic activity when tested in a closed multispecies biofilm model; however complete inhibition of oral biofilm formation was not observed. The presence of sucrose in the media abolished the antimicrobial effect seen under basal growing conditions.

A DFR was optimized to test antimicrobial effect of antimicrobial-containing dental adhesives. The results showed that polymerized MDPB-containing adhesive failed to inhibit multispecies oral biofilm formation in the absence and presence of sucrose when tested in a DFR. Immobilized antimicrobial agents into dental adhesives might not provide protection against secondary caries.

Bibliography

1. Beazoglou T, Eklund S, Heffley D, Meiers J, Brown LJ, Bailit H. Economic impact of regulating the use of amalgam restorations. *Public Health Rep* 2007;**122**(5):657-63.
2. Mjor IA, Toffenetti F. Placement and replacement of resin-based composite restorations in Italy. *Oper Dent* 1992;**17**(3):82-5.
3. Mjor IA, Toffenetti F. Placement and replacement of amalgam restorations in Italy. *Oper Dent* 1992;**17**(2):70-3.
4. Gordan VV, Riley JL, 3rd, Geraldeli S, Rindal DB, Qvist V, Fellows JL, et al. Repair or replacement of defective restorations by dentists in The Dental Practice-Based Research Network. *J Am Dent Assoc* 2012;**143**(6):593-601.
5. Murray PE, Windsor LJ, Smyth TW, Hafez AA, Cox CF. Analysis of pulpal reactions to restorative procedures, materials, pulp capping, and future therapies. *Crit Rev Oral Biol Med* 2002;**13**(6):509-20.
6. Roberts HW, Charlton DG. The release of mercury from amalgam restorations and its health effects: a review. *Oper Dent* 2009;**34**(5):605-14.
7. Forss H, Widstrom E. Reasons for restorative therapy and the longevity of restorations in adults. *Acta Odontol Scand* 2004;**62**(2):82-6.
8. Vidnes-Kopperud S, Tveit AB, Gaarden T, Sandvik L, Espelid I. Factors influencing dentists' choice of amalgam and tooth-colored restorative materials for Class II preparations in younger patients. *Acta Odontol Scand* 2009;**67**(2):74-9.
9. Bernardo M, Luis H, Martin MD, Leroux BG, Rue T, Leitao J, et al. Survival and reasons for failure of amalgam versus composite posterior restorations placed in a randomized clinical trial. *J Am Dent Assoc* 2007;**138**(6):775-83.
10. Mannocci F, Qualtrough AJ, Worthington HV, Watson TF, Pitt Ford TR. Randomized clinical comparison of endodontically treated teeth restored with amalgam or with fiber posts and resin composite: five-year results. *Oper Dent* 2005;**30**(1):9-15.
11. Soncini JA, Maserejian NN, Trachtenberg F, Tavares M, Hayes C. The longevity of amalgam versus compomer/composite restorations in posterior primary and permanent teeth: findings From the New England Children's Amalgam Trial. *J Am Dent Assoc* 2007;**138**(6):763-72.
12. Kopperud SE, Tveit AB, Gaarden T, Sandvik L, Espelid I. Longevity of posterior dental restorations and reasons for failure. *Eur J Oral Sci* 2012;**120**(6):539-48.
13. Opdam NJ, Loomans BA, Roeters FJ, Bronkhorst EM. Five-year clinical performance of posterior resin composite restorations placed by dental students. *J Dent* 2004;**32**(5):379-83.
14. Opdam NJ, Bronkhorst EM, Roeters JM, Loomans BA. A retrospective clinical study on longevity of posterior composite and amalgam restorations. *Dent Mater* 2007;**23**(1):2-8.

15. Opdam NJ, van de Sande FH, Bronkhorst E, Cenci MS, Bottenberg P, Pallesen U, et al. Longevity of posterior composite restorations: a systematic review and meta-analysis. *J Dent Res* 2014;**93**(10):943-9.
16. Van Nieuwenhuysen JP, D'Hoore W, Carvalho J, Qvist V. Long-term evaluation of extensive restorations in permanent teeth. *J Dent* 2003;**31**(6):395-405.
17. Hunter AR, Treasure ET, Hunter AJ. Increases in cavity volume associated with the removal of class 2 amalgam and composite restorations. *Oper Dent* 1995;**20**(1):2-6.
18. Millar BJ, Robinson PB, Davies BR. Effects of the removal of composite resin restorations on Class II cavities. *Br Dent J* 1992;**173**(6):210-2.
19. Gordan VV, Mondragon E, Shen C. Replacement of resin-based composite: evaluation of cavity design, cavity depth, and shade matching. *Quintessence Int* 2002;**33**(4):273-8.
20. Mjor IA, Toffenetti F. Secondary caries: a literature review with case reports. *Quintessence Int* 2000;**31**(3):165-79.
21. Hals E, Nernaes A. Histopathology of in vitro caries developing around silver amalgam fillings. *Caries Res* 1971;**5**(1):58-77.
22. Kidd EA, Fejerskov O. What constitutes dental caries? Histopathology of carious enamel and dentin related to the action of cariogenic biofilms. *J Dent Res* 2004;**83 Spec No C**:C35-8.
23. Hals E, Andreassen BH, Bie T. Histopathology of natural caries around silver amalgam fillings. *Caries Res* 1974;**8**(4):343-58.
24. Kidd EA. Microleakage: a review. *J Dent* 1976;**4**(5):199-206.
25. [cited; Available from: http://pocketdentistry.com/7-the-tooth-coloured-restorative-materials-i-resin-composites/
26. Hals E, Kvinnsland I. Structure of experimental in vitro and in vivo lesions around composite (Addent XV) fillings. *Scand J Dent Res* 1974;**82**(7):517-26.
27. Hals E, Laegreid O. Experimental in vitro lesions adjacent to composite restorations in etched cavities. *Oral Surg Oral Med Oral Pathol* 1976;**41**(2):225-34.
28. Kidd EA. Microleakage in relation to amalgam and composite restorations. A laboratory study. *Br Dent J* 1976;**141**(10):305-10.
29. Jokstad A. Secondary caries and microleakage. *Dent Mater* 2016;**32**(1):11-25.
30. Mjor IA. Frequency of secondary caries at various anatomical locations. *Oper Dent* 1985;**10**(3):88-92.
31. Thomas RZ, Ruben JL, ten Bosch JJ, Fidler V, Huysmans MC. Approximal secondary caries lesion progression, a 20-week in situ study. *Caries Res* 2007;**41**(5):399-405.
32. Diercke K, Lussi A, Kersten T, Seemann R. Isolated development of inner (wall) caries like lesions in a bacterial-based in vitro model. *Clin Oral Investig* 2009;**13**(4):439-44.
33. Nassar HM, Gonzalez-Cabezas C. Effect of gap geometry on secondary caries wall lesion development. *Caries Res* 2011;**45**(4):346-52.
34. Nedeljkovic I, Teughels W, De Munck J, Van Meerbeek B, Van Landuyt KL. Is secondary caries with composites a material-based problem? *Dent Mater* 2015;**31**(11):e247-77.

35. Mjor IA. The location of clinically diagnosed secondary caries. *Quintessence Int* 1998;**29**(5):313-7.
36. Mjor IA. Clinical diagnosis of recurrent caries. *J Am Dent Assoc* 2005;**136**(10):1426-33.
37. Light curing. [cited; Available from: http://pocketdentistry.com/composite-resin-fundamentals-and-direct-technique-restorations/
38. Gingival margin in this class II composite demonstrates the pervasive problem of microleakage. [cited; Available from: http://www.dentistrytoday.com/restorative-134/1799--sp-118036882
39. Nyvad B, Crielaard W, Mira A, Takahashi N, Beighton D. Dental caries from a molecular microbiological perspective. *Caries Res* 2013;**47**(2):89-102.
40. Takahashi N, Nyvad B. Caries ecology revisited: microbial dynamics and the caries process. *Caries Res* 2008;**42**(6):409-18.
41. Marsh PD. Microbiology of dental plaque biofilms and their role in oral health and caries. *Dent Clin North Am* 2010;**54**(3):441-54.
42. Gonzalez-Cabezas C, Li Y, Gregory RL, Stookey GK. Distribution of cariogenic bacteria in carious lesions around tooth-colored restorations. *Am J Dent* 2002;**15**(4):248-51.
43. Splieth C, Bernhardt O, Heinrich A, Bernhardt H, Meyer G. Anaerobic microflora under Class I and Class II composite and amalgam restorations. *Quintessence Int* 2003;**34**(7):497-503.
44. Mo SS, Bao W, Lai GY, Wang J, Li MY. The microfloral analysis of secondary caries biofilm around Class I and Class II composite and amalgam fillings. *BMC Infect Dis* 2010;**10**:241.
45. Peterson SN, Snesrud E, Schork NJ, Bretz WA. Dental caries pathogenicity: a genomic and metagenomic perspective. *Int Dent J* 2011;**61 Suppl 1**:11-22.
46. Rudney JD, Jagtap PD, Reilly CS, Chen R, Markowski TW, Higgins L, et al. Protein relative abundance patterns associated with sucrose-induced dysbiosis are conserved across taxonomically diverse oral microcosm biofilm models of dental caries. *Microbiome* 2015;**3**:69.
47. Ferracane JL. Resin composite--state of the art. *Dent Mater* 2011;**27**(1):29-38.
48. Peutzfeldt A. Resin composites in dentistry: the monomer systems. *Eur J Oral Sci* 1997;**105**(2):97-116.
49. Ferracane JL, Hilton TJ. Polymerization stress - Is it clinically meaningful? *Dent Mater* 2016;**32**(1):1-10.
50. Boaro LC, Froes-Salgado NR, Gajewski VE, Bicalho AA, Valdivia AD, Soares CJ, et al. Correlation between polymerization stress and interfacial integrity of composites restorations assessed by different in vitro tests. *Dent Mater* 2014;**30**(9):984-92.
51. Yamamoto T, Ferracane JL, Sakaguchi RL, Swain MV. Calculation of contraction stresses in dental composites by analysis of crack propagation in the matrix surrounding a cavity. *Dent Mater* 2009;**25**(4):543-50.

52. Yamamoto T, Nishide A, Swain MV, Ferracane JL, Sakaguchi RL, Momoi Y. Contraction stresses in dental composites adjacent to and at the bonded interface as measured by crack analysis. *Acta Biomater* 2011;**7**(1):417-23.
53. Hilton TJ. Can modern restorative procedures and materials reliably seal cavities? In vitro investigations. Part 2. *Am J Dent* 2002;**15**(4):279-89.
54. Hilton TJ. Can modern restorative procedures and materials reliably seal cavities? In vitro investigations. Part 1. *Am J Dent* 2002;**15**(3):198-210.
55. Cenci MS, Pereira-Cenci T, Cury JA, Ten Cate JM. Relationship between gap size and dentine secondary caries formation assessed in a microcosm biofilm model. *Caries Res* 2009;**43**(2):97-102.
56. Loguercio AD, Reis A, Bortoli G, Patzlaft R, Kenshima S, Rodrigues Filho LE, et al. Influence of adhesive systems on interfacial dentin gap formation in vitro. *Oper Dent* 2006;**31**(4):431-41.
57. Totiam P, Gonzalez-Cabezas C, Fontana MR, Zero DT. A new in vitro model to study the relationship of gap size and secondary caries. *Caries Res* 2007;**41**(6):467-73.
58. Kuper NK, Opdam NJ, Ruben JL, de Soet JJ, Cenci MS, Bronkhorst EM, et al. Gap size and wall lesion development next to composite. *J Dent Res* 2014;**93**(7 Suppl):108S-13S.
59. Montagner AF, Kuper NK, Opdam NJ, Bronkhorst EM, Cenci MS, Huysmans MC. Wall-lesion development in gaps: The role of the adhesive bonding material. *J Dent* 2015;**43**(8):1007-12.
60. de Fucio SB, Puppin-Rontani RM, de Carvalho FG, Mattos-Graner Rde O, Correr-Sobrinho L, Garcia-Godoy F. Analyses of biofilms accumulated on dental restorative materials. *Am J Dent* 2009;**22**(3):131-6.
61. Svanberg M, Mjor IA, Orstavik D. Mutans streptococci in plaque from margins of amalgam, composite, and glass-ionomer restorations. *J Dent Res* 1990;**69**(3):861-4.
62. Padovani GC, Fucio SB, Ambrosano GM, Correr-Sobrinho L, Puppin-Rontani RM. In situ bacterial accumulation on dental restorative materials. CLSM/COMSTAT analysis. *Am J Dent* 2015;**28**(1):3-8.
63. Auschill TM, Arweiler NB, Brecx M, Reich E, Sculean A, Netuschil L. The effect of dental restorative materials on dental biofilm. *Eur J Oral Sci* 2002;**110**(1):48-53.
64. Buergers R, Schneider-Brachert W, Hahnel S, Rosentritt M, Handel G. Streptococcal adhesion to novel low-shrink silorane-based restorative. *Dent Mater* 2009;**25**(2):269-75.
65. Montanaro L, Campoccia D, Rizzi S, Donati ME, Breschi L, Prati C, et al. Evaluation of bacterial adhesion of Streptococcus mutans on dental restorative materials. *Biomaterials* 2004;**25**(18):4457-63.
66. Poggio C, Arciola CR, Rosti F, Scribante A, Saino E, Visai L. Adhesion of Streptococcus mutans to different restorative materials. *Int J Artif Organs* 2009;**32**(9):671-7.
67. Mei L, Busscher HJ, van der Mei HC, Ren Y. Influence of surface roughness on streptococcal adhesion forces to composite resins. *Dent Mater* 2011;**27**(8):770-8.

68. Park JW, Song CW, Jung JH, Ahn SJ, Ferracane JL. The effects of surface roughness of composite resin on biofilm formation of Streptococcus mutans in the presence of saliva. *Oper Dent* 2012;**37**(5):532-9.
69. Teughels W, Van Assche N, Sliepen I, Quirynen M. Effect of material characteristics and/or surface topography on biofilm development. *Clin Oral Implants Res* 2006;**17 Suppl 2**:68-81.
70. Aykent F, Yondem I, Ozyesil AG, Gunal SK, Avunduk MC, Ozkan S. Effect of different finishing techniques for restorative materials on surface roughness and bacterial adhesion. *J Prosthet Dent* 2010;**103**(4):221-7.
71. Ionescu A, Wutscher E, Brambilla E, Schneider-Feyrer S, Giessibl FJ, Hahnel S. Influence of surface properties of resin-based composites on in vitro Streptococcus mutans biofilm development. *Eur J Oral Sci* 2012;**120**(5):458-65.
72. Ono M, Nikaido T, Ikeda M, Imai S, Hanada N, Tagami J, et al. Surface properties of resin composite materials relative to biofilm formation. *Dent Mater J* 2007;**26**(5):613-22.
73. Renner LD, Weibel DB. Physicochemical regulation of biofilm formation. *MRS Bull* 2011;**36**(5):347-55.
74. Pereira CA, Eskelson E, Cavalli V, Liporoni PC, Jorge AO, do Rego MA. Streptococcus mutans biofilm adhesion on composite resin surfaces after different finishing and polishing techniques. *Oper Dent* 2011;**36**(3):311-7.
75. Bowen WH, Koo H. Biology of Streptococcus mutans-derived glucosyltransferases: role in extracellular matrix formation of cariogenic biofilms. *Caries Res* 2011;**45**(1):69-86.
76. Koo H, Falsetta ML, Klein MI. The exopolysaccharide matrix: a virulence determinant of cariogenic biofilm. *J Dent Res* 2013;**92**(12):1065-73.
77. Xiao J, Klein MI, Falsetta ML, Lu B, Delahunty CM, Yates JR, 3rd, et al. The exopolysaccharide matrix modulates the interaction between 3D architecture and virulence of a mixed-species oral biofilm. *PLoS Pathog* 2012;**8**(4):e1002623.
78. Beyth N, Domb AJ, Weiss EI. An in vitro quantitative antibacterial analysis of amalgam and composite resins. *J Dent* 2007;**35**(3):201-6.
79. Karanika-Kouma A, Dionysopoulos P, Koliniotou-Koubia E, Kolokotronis A. Antibacterial properties of dentin bonding systems, polyacid-modified composite resins and composite resins. *J Oral Rehabil* 2001;**28**(2):157-60.
80. Matalon S, Slutzky H, Weiss EI. Surface antibacterial properties of packable resin composites: part I. *Quintessence Int* 2004;**35**(3):189-93.
81. Vermeersch G, Leloup G, Delmee M, Vreven J. Antibacterial activity of glass-ionomer cements, compomers and resin composites: relationship between acidity and material setting phase. *J Oral Rehabil* 2005;**32**(5):368-74.
82. Morrier JJ, Suchett-Kaye G, Nguyen D, Rocca JP, Blanc-Benon J, Barsotti O. Antimicrobial activity of amalgams, alloys and their elements and phases. *Dent Mater* 1998;**14**(2):150-7.
83. Netuschil L, Vohrer KG, Riethe P, Kasloff Z, Brecx M. Antibacterial effects of amalgams on mutans streptococci in an in vitro biofilm test procedure. *Acta Stomatol Belg* 1996;**93**(2):73-8.

84. Spencer P, Ye Q, Park J, Topp EM, Misra A, Marangos O, et al. Adhesive/Dentin interface: the weak link in the composite restoration. *Ann Biomed Eng* 2010;**38**(6):1989-2003.
85. De Munck J, Van Landuyt K, Peumans M, Poitevin A, Lambrechts P, Braem M, et al. A critical review of the durability of adhesion to tooth tissue: methods and results. *J Dent Res* 2005;**84**(2):118-32.
86. Hashimoto M, Ohno H, Kaga M, Endo K, Sano H, Oguchi H. In vivo degradation of resin-dentin bonds in humans over 1 to 3 years. *J Dent Res* 2000;**79**(6):1385-91.
87. Pashley DH, Tay FR, Breschi L, Tjaderhane L, Carvalho RM, Carrilho M, et al. State of the art etch-and-rinse adhesives. *Dent Mater* 2011;**27**(1):1-16.
88. Van Meerbeek B, De Munck J, Yoshida Y, Inoue S, Vargas M, Vijay P, et al. Buonocore memorial lecture. Adhesion to enamel and dentin: current status and future challenges. *Oper Dent* 2003;**28**(3):215-35.
89. Pashley DH, Tao L, Boyd L, King GE, Horner JA. Scanning electron microscopy of the substructure of smear layers in human dentine. *Arch Oral Biol* 1988;**33**(4):265-70.
90. Van Meerbeek B, Inokoshi S, Braem M, Lambrechts P, Vanherle G. Morphological aspects of the resin-dentin interdiffusion zone with different dentin adhesive systems. *J Dent Res* 1992;**71**(8):1530-40.
91. Nakabayashi N, Kojima K, Masuhara E. The promotion of adhesion by the infiltration of monomers into tooth substrates. *J Biomed Mater Res* 1982;**16**(3):265-73.
92. Tay FR, Gwinnett JA, Wei SH. Micromorphological spectrum from overdrying to overwetting acid-conditioned dentin in water-free acetone-based, single-bottle primer/adhesives. *Dent Mater* 1996;**12**(4):236-44.
93. Kanca J, 3rd. Resin bonding to wet substrate. 1. Bonding to dentin. *Quintessence Int* 1992;**23**(1):39-41.
94. Sano H, Takatsu T, Ciucchi B, Horner JA, Matthews WG, Pashley DH. Nanoleakage: leakage within the hybrid layer. *Oper Dent* 1995;**20**(1):18-25.
95. Hybrid Layer. [cited; Available from: http://pocketdentistry.com/7-biocompatibility/
96. Manuja N, Nagpal R, Pandit IK. Dental adhesion: mechanism, techniques and durability. *J Clin Pediatr Dent* 2012;**36**(3):223-34.
97. Perdigao J, Geraldeli S. Bonding characteristics of self-etching adhesives to intact versus prepared enamel. *J Esthet Restor Dent* 2003;**15**(1):32-41; discussion 42.
98. Pashley DH, Tay FR. Aggressiveness of contemporary self-etching adhesives. Part II: etching effects on unground enamel. *Dent Mater* 2001;**17**(5):430-44.
99. Hannig M, Bock H, Bott B, Hoth-Hannig W. Inter-crystallite nanoretention of self-etching adhesives at enamel imaged by transmission electron microscopy. *Eur J Oral Sci* 2002;**110**(6):464-70.
100. Yoshida Y, Nagakane K, Fukuda R, Nakayama Y, Okazaki M, Shintani H, et al. Comparative study on adhesive performance of functional monomers. *J Dent Res* 2004;**83**(6):454-8.

101. Ito S, Hashimoto M, Wadgaonkar B, Svizero N, Carvalho RM, Yiu C, et al. Effects of resin hydrophilicity on water sorption and changes in modulus of elasticity. *Biomaterials* 2005;**26**(33):6449-59.
102. Reis AF, Giannini M, Pereira PN. Influence of water-storage time on the sorption and solubility behavior of current adhesives and primer/adhesive mixtures. *Oper Dent* 2007;**32**(1):53-9.
103. Venz S, Dickens B. NIR-spectroscopic investigation of water sorption characteristics of dental resins and composites. *J Biomed Mater Res* 1991;**25**(10):1231-48.
104. Ito S, Hoshino T, Iijima M, Tsukamoto N, Pashley DH, Saito T. Water sorption/solubility of self-etching dentin bonding agents. *Dent Mater* 2010;**26**(7):617-26.
105. Malacarne J, Carvalho RM, de Goes MF, Svizero N, Pashley DH, Tay FR, et al. Water sorption/solubility of dental adhesive resins. *Dent Mater* 2006;**22**(10):973-80.
106. Spencer P, Wang Y, Walker MP, Wieliczka DM, Swafford JR. Interfacial chemistry of the dentin/adhesive bond. *J Dent Res* 2000;**79**(7):1458-63.
107. Tay FR, Frankenberger R, Krejci I, Bouillaguet S, Pashley DH, Carvalho RM, et al. Single-bottle adhesives behave as permeable membranes after polymerization. I. In vivo evidence. *J Dent* 2004;**32**(8):611-21.
108. Tay FR, Pashley DH. Water treeing--a potential mechanism for degradation of dentin adhesives. *Am J Dent* 2003;**16**(1):6-12.
109. Tay FR, Pashley DH, Suh BI, Carvalho RM, Itthagarun A. Single-step adhesives are permeable membranes. *J Dent* 2002;**30**(7-8):371-82.
110. Tay FR, Pashley DH, Yoshiyama M. Two modes of nanoleakage expression in single-step adhesives. *J Dent Res* 2002;**81**(7):472-6.
111. Tay FR, King NM, Chan KM, Pashley DH. How can nanoleakage occur in self-etching adhesive systems that demineralize and infiltrate simultaneously? *J Adhes Dent* 2002;**4**(4):255-69.
112. Pashley EL, Zhang Y, Lockwood PE, Rueggeberg FA, Pashley DH. Effects of HEMA on water evaporation from water-HEMA mixtures. *Dent Mater* 1998;**14**(1):6-10.
113. Spencer P, Wang Y. Adhesive phase separation at the dentin interface under wet bonding conditions. *J Biomed Mater Res* 2002;**62**(3):447-56.
114. Wang Y, Spencer P. Hybridization efficiency of the adhesive/dentin interface with wet bonding. *J Dent Res* 2003;**82**(2):141-5.
115. Jacobsen T, Soderholm KJ. Some effects of water on dentin bonding. *Dent Mater* 1995;**11**(2):132-6.
116. Cadenaro M, Antoniolli F, Sauro S, Tay FR, Di Lenarda R, Prati C, et al. Degree of conversion and permeability of dental adhesives. *Eur J Oral Sci* 2005;**113**(6):525-30.
117. Donmez N, Belli S, Pashley DH, Tay FR. Ultrastructural correlates of in vivo/in vitro bond degradation in self-etch adhesives. *J Dent Res* 2005;**84**(4):355-9.
118. Larsen IB, Freund M, Munksgaard EC. Change in surface hardness of BisGMA/TEGDMA polymer due to enzymatic action. *J Dent Res* 1992;**71**(11):1851-3.

119. Larsen IB, Munksgaard EC. Effect of human saliva on surface degradation of composite resins. *Scand J Dent Res* 1991;**99**(3):254-61.
120. Finer Y, Santerre JP. Biodegradation of a dental composite by esterases: dependence on enzyme concentration and specificity. *J Biomater Sci Polym Ed* 2003;**14**(8):837-49.
121. Jaffer F, Finer Y, Santerre JP. Interactions between resin monomers and commercial composite resins with human saliva derived esterases. *Biomaterials* 2002;**23**(7):1707-19.
122. Santerre JP, Shajii L, Tsang H. Biodegradation of commercial dental composites by cholesterol esterase. *J Dent Res* 1999;**78**(8):1459-68.
123. Lin BA, Jaffer F, Duff MD, Tang YW, Santerre JP. Identifying enzyme activities within human saliva which are relevant to dental resin composite biodegradation. *Biomaterials* 2005;**26**(20):4259-64.
124. Shokati B, Tam LE, Santerre JP, Finer Y. Effect of salivary esterase on the integrity and fracture toughness of the dentin-resin interface. *J Biomed Mater Res B Appl Biomater* 2010;**94**(1):230-7.
125. Kermanshahi S, Santerre JP, Cvitkovitch DG, Finer Y. Biodegradation of resin-dentin interfaces increases bacterial microleakage. *J Dent Res* 2010;**89**(9):996-1001.
126. Delaviz Y, Finer Y, Santerre JP. Biodegradation of resin composites and adhesives by oral bacteria and saliva: a rationale for new material designs that consider the clinical environment and treatment challenges. *Dent Mater* 2014;**30**(1):16-32.
127. Bourbia M, Ma D, Cvitkovitch DG, Santerre JP, Finer Y. Cariogenic bacteria degrade dental resin composites and adhesives. *J Dent Res* 2013;**92**(11):989-94.
128. Breschi L, Prati C, Gobbi P, Pashley D, Mazzotti G, Teti G, et al. Immunohistochemical analysis of collagen fibrils within the hybrid layer: a FEISEM study. *Oper Dent* 2004;**29**(5):538-46.
129. Hashimoto M, Ohno H, Sano H, Kaga M, Oguchi H. In vitro degradation of resin-dentin bonds analyzed by microtensile bond test, scanning and transmission electron microscopy. *Biomaterials* 2003;**24**(21):3795-803.
130. Pashley DH, Tay FR, Yiu C, Hashimoto M, Breschi L, Carvalho RM, et al. Collagen degradation by host-derived enzymes during aging. *J Dent Res* 2004;**83**(3):216-21.
131. Mazzoni A, Pashley DH, Nishitani Y, Breschi L, Mannello F, Tjaderhane L, et al. Reactivation of inactivated endogenous proteolytic activities in phosphoric acid-etched dentine by etch-and-rinse adhesives. *Biomaterials* 2006;**27**(25):4470-6.
132. Nishitani Y, Yoshiyama M, Wadgaonkar B, Breschi L, Mannello F, Mazzoni A, et al. Activation of gelatinolytic/collagenolytic activity in dentin by self-etching adhesives. *Eur J Oral Sci* 2006;**114**(2):160-6.
133. Tay FR, Pashley DH, Loushine RJ, Weller RN, Monticelli F, Osorio R. Self-etching adhesives increase collagenolytic activity in radicular dentin. *J Endod* 2006;**32**(9):862-8.
134. Martin-De Las Heras S, Valenzuela A, Overall CM. The matrix metalloproteinase gelatinase A in human dentine. *Arch Oral Biol* 2000;**45**(9):757-65.

135. Tjaderhane L, Larjava H, Sorsa T, Uitto VJ, Larmas M, Salo T. The activation and function of host matrix metalloproteinases in dentin matrix breakdown in caries lesions. *J Dent Res* 1998;**77**(8):1622-9.
136. Mazzoni A, Scaffa P, Carrilho M, Tjaderhane L, Di Lenarda R, Polimeni A, et al. Effects of etch-and-rinse and self-etch adhesives on dentin MMP-2 and MMP-9. *J Dent Res* 2013;**92**(1):82-6.
137. Hebling J, Pashley DH, Tjaderhane L, Tay FR. Chlorhexidine arrests subclinical degradation of dentin hybrid layers in vivo. *J Dent Res* 2005;**84**(8):741-6.
138. Baran G, Boberick K, McCool J. Fatigue of restorative materials. *Crit Rev Oral Biol Med* 2001;**12**(4):350-60.
139. Drummond JL. Degradation, fatigue, and failure of resin dental composite materials. *J Dent Res* 2008;**87**(8):710-9.
140. Hu X, Marquis PM, Shortall AC. Two-body in vitro wear study of some current dental composites and amalgams. *J Prosthet Dent* 1999;**82**(2):214-20.
141. Mazer RB, Leinfelder KF, Russell CM. Degradation of microfilled posterior composite. *Dent Mater* 1992;**8**(3):185-9.
142. Xu HH, Quinn JB, Giuseppetti AA. Wear and mechanical properties of nano-silica-fused whisker composites. *J Dent Res* 2004;**83**(12):930-5.
143. Belli R, Baratieri LN, Braem M, Petschelt A, Lohbauer U. Tensile and bending fatigue of the adhesive interface to dentin. *Dent Mater* 2010;**26**(12):1157-65.
144. Frankenberger R, Pashley DH, Reich SM, Lohbauer U, Petschelt A, Tay FR. Characterisation of resin-dentine interfaces by compressive cyclic loading. *Biomaterials* 2005;**26**(14):2043-52.
145. Staninec M, Kim P, Marshall GW, Ritchie RO, Marshall SJ. Fatigue of dentin-composite interfaces with four-point bend. *Dent Mater* 2008;**24**(6):799-803.
146. Frankenberger R, Kramer N, Petschelt A. Fatigue behaviour of different dentin adhesives. *Clin Oral Investig* 1999;**3**(1):11-7.
147. Dentistry — Testing of adhesion to tooth structure. [cited; Available from: https://http://www.iso.org/obp/ui/ - iso:std:iso:ts:11405:ed-3:v1:en
148. Braga RR, Meira JB, Boaro LC, Xavier TA. Adhesion to tooth structure: a critical review of "macro" test methods. *Dent Mater* 2010;**26**(2):e38-49.
149. McDonough WG, Antonucci JM, He J, Shimada Y, Chiang MY, Schumacher GE, et al. A microshear test to measure bond strengths of dentin-polymer interfaces. *Biomaterials* 2002;**23**(17):3603-8.
150. Sano H, Shono T, Sonoda H, Takatsu T, Ciucchi B, Carvalho R, et al. Relationship between surface area for adhesion and tensile bond strength--evaluation of a micro-tensile bond test. *Dent Mater* 1994;**10**(4):236-40.
151. Shono Y, Terashita M, Pashley EL, Brewer PD, Pashley DH. Effects of cross-sectional area on resin-enamel tensile bond strength. *Dent Mater* 1997;**13**(5):290-6.
152. Pashley DH, Sano H, Ciucchi B, Yoshiyama M, Carvalho RM. Adhesion testing of dentin bonding agents: a review. *Dent Mater* 1995;**11**(2):117-25.
153. Perinka L, Sano H, Hosoda H. Dentin thickness, hardness, and Ca-concentration vs bond strength of dentin adhesives. *Dent Mater* 1992;**8**(4):229-33.
154. Van Noort R, Noroozi S, Howard IC, Cardew G. A critique of bond strength measurements. *J Dent* 1989;**17**(2):61-7.

155. Van Noort R, Cardew GE, Howard IC, Noroozi S. The effect of local interfacial geometry on the measurement of the tensile bond strength to dentin. *J Dent Res* 1991;**70**(5):889-93.
156. Cantekin K, Avci S. Evaluation of shear bond strength of two resin-based composites and glass ionomer cement to pure tricalcium silicate-based cement (Biodentine(R)). *J Appl Oral Sci* 2014;**22**(4):302-6.
157. Chang JC, Hart DA, Estey AW, Chan JT. Tensile bond strengths of five luting agents to two CAD-CAM restorative materials and enamel. *J Prosthet Dent* 2003;**90**(1):18-23.
158. Griffith A.A. The phenomena of Rupture and Flow in Solids. *Phil Trans Roy Soc Lond* 1920:163-98.
159. Armstrong S, Geraldeli S, Maia R, Raposo LH, Soares CJ, Yamagawa J. Adhesion to tooth structure: a critical review of "micro" bond strength test methods. *Dent Mater* 2010;**26**(2):e50-62.
160. Sadek FT, Monticelli F, Muench A, Ferrari M, Cardoso PE. A novel method to obtain microtensile specimens minimizing cut flaws. *J Biomed Mater Res B Appl Biomater* 2006;**78**(1):7-14.
161. Bouillaguet S, Ciucchi B, Jacoby T, Wataha JC, Pashley D. Bonding characteristics to dentin walls of class II cavities, in vitro. *Dent Mater* 2001;**17**(4):316-21.
162. Al-Saleh M, El-Mowafy O. Microtensile Bond Strength of Restorative Composite Bonded wuth Self-adhesive Resin Cements to Enamel and Dentin. *Journal of research in Dentistry* 2013;**1**(1):3-16.
163. Soares CJ, Soares PV, Santos-Filho PC, Armstrong SR. Microtensile specimen attachment and shape--finite element analysis. *J Dent Res* 2008;**87**(1):89-93.
164. Ghassemieh E. Evaluation of sources of uncertainties in microtensile bond strength of dental adhesive system for different specimen geometries. *Dent Mater* 2008;**24**(4):536-47.
165. Perdigao J, Geraldeli S, Carmo AR, Dutra HR. In vivo influence of residual moisture on microtensile bond strengths of one-bottle adhesives. *J Esthet Restor Dent* 2002;**14**(1):31-8.
166. Armstrong SR, Vargas MA, Fang Q, Laffoon JE. Microtensile bond strength of a total-etch 3-step, total-etch 2-step, self-etch 2-step, and a self-etch 1-step dentin bonding system through 15-month water storage. *J Adhes Dent* 2003;**5**(1):47-56.
167. El Zohairy AA, de Gee AJ, de Jager N, van Ruijven LJ, Feilzer AJ. The influence of specimen attachment and dimension on microtensile strength. *J Dent Res* 2004;**83**(5):420-4.
168. Raposo LH, Armstrong SR, Maia RR, Qian F, Geraldeli S, Soares CJ. Effect of specimen gripping device, geometry and fixation method on microtensile bond strength, failure mode and stress distribution: laboratory and finite element analyses. *Dent Mater* 2012;**28**(5):e50-62.
169. Ki-Yeon Kim, In-Sung Yeo, Sung-Hun Kim, Jung-Suk Han, Jai-Bong Lee, Jae-Ho Yang. Effect of specimen preparation method on the microtensile bond strength of veneering ceramic to zirconia. *The Journal of the Korean Academy of Prosthodontics* 2011;**49**(2):114-19.

170. Placido E, Meira JB, Lima RG, Muench A, de Souza RM, Ballester RY. Shear versus micro-shear bond strength test: a finite element stress analysis. *Dent Mater* 2007;**23**(9):1086-92.
171. Browne RM, Tobias RS. Microbial microleakage and pulpal inflammation: a review. *Endod Dent Traumatol* 1986;**2**(5):177-83.
172. Bayne SC. Correlation of clinical performance with 'in vitro tests' of restorative dental materials that use polymer-based matrices. *Dent Mater* 2012;**28**(1):52-71.
173. Dennison JB, Sarrett DC. Prediction and diagnosis of clinical outcomes affecting restoration margins. *J Oral Rehabil* 2012;**39**(4):301-18.
174. Heintze SD. Clinical relevance of tests on bond strength, microleakage and marginal adaptation. *Dent Mater* 2013;**29**(1):59-84.
175. Dietschi D, Argente A, Krejci I, Mandikos M. In vitro performance of Class I and II composite restorations: a literature review on nondestructive laboratory trials--part I. *Oper Dent* 2013;**38**(5):E166-81.
176. Dietschi D, Argente A, Krejci I, Mandikos M. In vitro performance of Class I and II composite restorations: a literature review on nondestructive laboratory trials--part II. *Oper Dent* 2013;**38**(5):E182-200.
177. Scotti N, Comba A, Gambino A, Paolino DS, Alovisi M, Pasqualini D, et al. Microleakage at enamel and dentin margins with a bulk fills flowable resin. *Eur J Dent* 2014;**8**(1):1-8.
178. Sadek FT, Moura SK, Ballester RY, Muench A, Cardoso PE. The effect of long-term storage on the microleakage of composite resin restorations: qualitative and quantitative evaluation. *Pesqui Odontol Bras* 2003;**17**(3):261-6.
179. Carrera CA, Lan C, Escobar-Sanabria D, Li Y, Rudney J, Aparicio C, et al. The use of micro-CT with image segmentation to quantify leakage in dental restorations. *Dent Mater* 2015.
180. Sun J, Lin-Gibson S. X-ray microcomputed tomography for measuring polymerization shrinkage of polymeric dental composites. *Dent Mater* 2008;**24**(2):228-34.
181. Chen X, Cuijpers V, Fan M, Frencken JE. Marginal leakage of two newer glass-ionomer-based sealant materials assessed using micro-CT. *J Dent* 2010;**38**(9):731-5.
182. Eden E, Topaloglu-Ak A, Cuijpers V, Frencken JE. Micro-CT for measuring marginal leakage of Class II resin composite restorations in primary molars prepared in vivo. *Am J Dent* 2008;**21**(6):393-7.
183. Sun J, Eidelman N, Lin-Gibson S. 3D mapping of polymerization shrinkage using X-ray micro-computed tomography to predict microleakage. *Dent Mater* 2009;**25**(3):314-20.
184. Zeiger DN, Sun J, Schumacher GE, Lin-Gibson S. Evaluation of dental composite shrinkage and leakage in extracted teeth using X-ray microcomputed tomography. *Dent Mater* 2009;**25**(10):1213-20.
185. Li H, Li J, Yun X, Liu X, Fok AS. Non-destructive examination of interfacial debonding using acoustic emission. *Dent Mater* 2011;**27**(10):964-71.
186. L S, G S. Computer vision: Prentice Hall; 2001.

187. Geurtsen W, Leyhausen G. Chemical-Biological Interactions of the resin monomer triethyleneglycol-dimethacrylate (TEGDMA). *J Dent Res* 2001;**80**(12):2046-50.
188. Demarco FF, Correa MB, Cenci MS, Moraes RR, Opdam NJ. Longevity of posterior composite restorations: not only a matter of materials. *Dent Mater* 2012;**28**(1):87-101.
189. Krifka S, Federlin M, Hiller KA, Schmalz G. Microleakage of silorane- and methacrylate-based class V composite restorations. *Clin Oral Investig* 2012;**16**(4):1117-24.
190. Bagis YH, Baltacioglu IH, Kahyaogullari S. Comparing microleakage and the layering methods of silorane-based resin composite in wide Class II MOD cavities. *Oper Dent* 2009;**34**(5):578-85.
191. Poureslami HR, Sajadi F, Sharifi M, Farzin Ebrahimi S. Marginal Microleakage of Low-shrinkage Composite Silorane in Primary Teeth: An In Vitro Study. *J Dent Res Dent Clin Dent Prospects* 2012;**6**(3):94-7.
192. Reis AF, Giannini M, Pereira PN. Long-term TEM analysis of the nanoleakage patterns in resin-dentin interfaces produced by different bonding strategies. *Dent Mater* 2007;**23**(9):1164-72.
193. Yuan Y, Shimada Y, Ichinose S, Tagami J. Qualitative analysis of adhesive interface nanoleakage using FE-SEM/EDS. *Dent Mater* 2007;**23**(5):561-9.
194. Kim RJ, Kim YJ, Choi NS, Lee IB. Polymerization shrinkage, modulus, and shrinkage stress related to tooth-restoration interfacial debonding in bulk-fill composites. *J Dent* 2015;**43**(4):430-9.
195. Schreiner RF, Chappell RP, Glaros AG, Eick JD. Microtensile testing of dentin adhesives. *Dent Mater* 1998;**14**(3):194-201.
196. Li J, Li H, Yun X, Fok AS. A comparison of bond strengths measured using cantilever bending and micro-tensile methods. *Dent Mater* 2011;**27**(12):1246-51.
197. Campillo-Funollet M, Dargush GF, VanSlooten RA, Mollendorf JC, Kim H, Makowka SR. Size-dependent strength of dental adhesive systems. *Dent Mater* 2014;**30**(8):e216-28.
198. Rasmussen ST. Analysis of dental shear bond strength tests, sheer or tensile? *International Journal of Adhesion and Adhesives* 1996;**16**(3):147-54.
199. Soderholm KJ, Geraldeli S, Shen C. What do microtensile bond strength values of adhesives mean? *J Adhes Dent* 2012;**14**(4):307-14.
200. Huang SH, Lin LS, Rudney J, Jones R, Aparicio C, Lin CP, et al. A novel dentin bond strength measurement technique using a composite disk in diametral compression. *Acta Biomater* 2012;**8**(4):1597-602.
201. Tong J., Wong K.Y., Lupton C. Determination of interfcial fracture toughness of bone-cement interface using sandwich Brazilian disks. *Engineering Fracture Mechanics* 2007;**74**(12):1904-16.
202. Wang JS. Experimental determination of interfcail toughness curves using Brazil-Nut-Sandwiches. *Acta Metall Mater* 1989;**38**(7):1279-90.
203. Procopio AT, Zavalangios A, Cunningham J. Analysis of the diametrical compression test and the applicability to plastically deforming materials. *JOURNAL OF MATERIALS SCIENCE* 2003;**36**(17):3629-39.

204. ABAQUS 6.11 documentation. Providence, RI, USA. . In: Corp. DSS, editor.; 2011.
205. Sideridou I, Tserki V, Papanastasiou G. Study of water sorption, solubility and modulus of elasticity of light-cured dimethacrylate-based dental resins. *Biomaterials* 2003;**24**(4):655-65.
206. Chung SM, Yap AU, Tsai KT, Yap FL. Elastic modulus of resin-based dental restorative materials: a microindentation approach. *J Biomed Mater Res B Appl Biomater* 2005;**72**(2):246-53.
207. Emami N, Soderholm KJ, Berglund LA. Effect of light power density variations on bulk curing properties of dental composites. *J Dent* 2003;**31**(3):189-96.
208. Peyton FA, Mahler DB, Hershenov B. Physical properties of dentin. *J Dent Res* 1952;**31**(3):366-70.
209. Scherrer SS, Cesar PF, Swain MV. Direct comparison of the bond strength results of the different test methods: a critical literature review. *Dent Mater* 2010;**26**(2):e78-93.
210. Soares JB. Bimaterial Brazilian Specimen for determining interfacial fracture toughness. *Engineering Fracture Mechanics* 1998;**59**(1):57-71.
211. Atkinson C. Combined mode fracture via the cracked Brazilian disk test. *International Journal of Fracture* 1982;**18**(4):279-91.
212. da Silva JM, Rodrigues JR, Camargo CH, Fernandes VV, Jr., Hiller KA, Schweikl H, et al. Effectiveness and biological compatibility of different generations of dentin adhesives. *Clin Oral Investig* 2014;**18**(2):607-13.
213. Salvio LA, Hipolito VD, Martins AL, de Goes MF. Hybridization quality and bond strength of adhesive systems according to interaction with dentin. *Eur J Dent* 2013;**7**(3):315-26.
214. Dantas DC, Ribeiro AI, Lima LH, de Lima MG, Guenes GM, Braz AK, et al. Influence of water storage time on the bond strength of etch-and-rinse and self-etching adhesive systems. *Braz Dent J* 2008;**19**(3):219-23.
215. McLeod ME, Price RB, Felix CM. Effect of configuration factor on shear bond strengths of self-etch adhesive systems to ground enamel and dentin. *Oper Dent* 2010;**35**(1):84-93.
216. Perdigao J, Sezinando A, Monteiro PC. Effect of substrate age and adhesive composition on dentin bonding. *Oper Dent* 2013;**38**(3):267-74.
217. A.O C, M.RO. C, Rueggeberg FA, Ambrosaho GMB, Giannini M. Bond strength, biaxial flexural strength and flexural modulus of dentin bonding systems exposed to water. *International Journal of Adhesion and Adhesives* 2014;**49**:109-14.
218. Belli R, Sartori N, Peruchi LD, Guimaraes JC, Araujo E, Monteiro S, Jr., et al. Slow progression of dentin bond degradation during one-year water storage under simulated pulpal pressure. *J Dent* 2010;**38**(10):802-10.
219. Bouillaguet S, Gysi P, Wataha JC, Ciucchi B, Cattani M, Godin C, et al. Bond strength of composite to dentin using conventional, one-step, and self-etching adhesive systems. *J Dent* 2001;**29**(1):55-61.
220. Beazoglou T, Eklund S, Heffley D, Meiers J, Brown LJ, Bailit H. Economic impact of regulating the use of amalgam restorations. *Public Health Reports* 2007;**122**(5):657-63.

221. Bowen RL, Marjenhoff WA. Dental composites/glass ionomers: the materials. *Advances in dental research* 1992;**6**:44-9.
222. Bernardo M, Luis H, Martin MD, Leroux BG, Rue T, Leitao J, et al. Survival and reasons for failure of amalgam versus composite posterior restorations placed in a randomized clinical trial. *Journal of the American Dental Association* 2007;**138**(6):775-83.
223. Hickel R, Manhart J, Garcia-Godoy F. Clinical results and new developments of direct posterior restorations. *American Journal of Dentistry* 2000;**13**(Spec No):41D-54D.
224. Manhart J, Neuerer P, Scheibenbogen-Fuchsbrunner A, Hickel R. Three-year clinical evaluation of direct and indirect composite restorations in posterior teeth. *The Journal of prosthetic dentistry* 2000;**84**(3):289-96.
225. Mjor IA. Clinical diagnosis of recurrent caries. *Journal of the American Dental Association* 2005;**136**(10):1426-33.
226. Mjor IA. The location of clinically diagnosed secondary caries. *Quintessence international* 1998;**29**(5):313-7.
227. Sbordone L, Bortolaia C. Oral microbial biofilms and plaque-related diseases: microbial communities and their role in the shift from oral health to disease. *Clinical Oral Investigations* 2003;**7**(4):181-8.
228. Kreth J, Zhang Y, Herzberg MC. Streptococcal antagonism in oral biofilms: Streptococcus sanguinis and Streptococcus gordonii interference with Streptococcus mutans. *Journal of bacteriology* 2008;**190**(13):4632-40.
229. Sansone C, Vanhoute J, Joshipura K, Kent R, Margolis HC. The Association of Mutans Streptococci and Non-Mutans Streptococci Capable of Acidogenesis at a Low Ph with Dental-Caries on Enamel and Root Surfaces. *Journal of Dental Research* 1993;**72**(2):508-16.
230. Ono M, Nikaido T, Ikeda M, Imai S, Hanada N, Tagami J, et al. Surface properties of resin composite materials relative to biofilm formation. *Dental Materials Journal* 2007;**26**(5):613-22.
231. Gyo M, Nikaido T, Okada K, Yamauchi J, Tagami J, Matin K. Surface response of fluorine polymer-incorporated resin composites to cariogenic biofilm adherence. *Applied and Environmental Microbiology* 2008;**74**(5):1428-35.
232. Hayati F, Okada A, Kitasako Y, Tagami J, Matin K. An artificial biofilm induced secondary caries model for in vitro studies. *Australian Dental Journal* 2011;**56**(1):40-47.
233. Cenci MS, Pereira-Cenci T, Cury JA, Ten Cate JM. Relationship between gap size and dentine secondary caries formation assessed in a microcosm biofilm model. *Caries Research* 2009;**43**(2):97-102.
234. Rudney JD, Chen R, Lenton P, Li J, Li Y, Jones RS, et al. A reproducible oral microcosm biofilm model for testing dental materials. *Journal of applied microbiology* 2012;**113**(6):1540-53.
235. Goracci C, Grandini S, Bossu M, Bertelli E, Ferrari M. Laboratory assessment of the retentive potential of adhesive posts: A review. *Journal of Dentistry* 2007;**35**(11):827-35.

236. Huang SH, Lin LS, Rudney J, Jones R, Aparicio C, Lin CP, et al. A novel dentin bond strength measurement technique using a composite disk in diametral compression. *Acta Biomaterialia* 2012;**8**(4):1597-602.
237. Pascon FM, Kantovitz KR, Caldo-Teixeira AS, Borges AF, Silva TN, Puppin-Rontani RM, et al. Clinical evaluation of composite and compomer restorations in primary teeth: 24-month results. *Journal of Dentistry* 2006;**34**(6):381-8.
238. Goeres DM, Loetterle LR, Hamilton MA, Murga R, Kirby DW, Donlan RM. Statistical assessment of a laboratory method for growing biofilms. *Microbiology* 2005;**151**(Pt 3):757-62.
239. Sissons CH, Anderson SA, Wong L, Coleman MJ, White DC. Microbiota of plaque microcosm biofilms: effect of three times daily sucrose pulses in different simulated oral environments. *Caries Research* 2007;**41**(5):413-22.
240. Mjor IA, Dahl JE, Moorhead JE. Age of restorations at replacement in permanent teeth in general dental practice. *Acta Odontologica Scandinavica* 2000;**58**(3):97-101.
241. Burke FJT, Wilson NHF, Cheung SW, Mjor IA. Influence of patient factors on age of restorations at failure and reasons for their placement and replacement. *Journal of Dentistry* 2001;**29**(5):317-24.
242. Reinke SMG, Lawder JAD, Divardin S, Raggio D, Reis A, Loguercio AD. Degradation of the resin-dentin bonds after simulated and inhibited cariogenic challenge in an in situ model. *Journal of Biomedical Materials Research Part B-Applied Biomaterials* 2012;**100B**(6):1466-71.
243. Goracci C, Fabianelli A, Sadek FT, Papacchini F, Tay FR, Ferrari M. The contribution of friction to the dislocation resistance of bonded fiber posts. *Journal of Endodontics* 2005;**31**(8):608-12.
244. Hood JA. Experimental studies on tooth deformation: stress distribution in class V restorations. *The New Zealand dental journal* 1972;**68**(312):116-31.
245. Rees JS, Jacobsen PH. The effect of interfacial failure around a class V composite restoration analysed by the finite element method. *Journal of oral rehabilitation* 2000;**27**(2):111-6.
246. Heymann HO, Sturdevant JR, Bayne S, Wilder AD, Sluder TB, Brunson WD. Examining tooth flexure effects on cervical restorations: a two-year clinical study. *Journal of the American Dental Association* 1991;**122**(5):41-7.
247. Cury JA, Rebelo MAB, Cury AAD, Derbyshire MTVC, Tabchoury CPM. Biochemical composition and cariogenicity of dental plaque formed in the presence of sucrose or glucose and fructose. *Caries Research* 2000;**34**(6):491-97.
248. Tenuta LMA, Ricomini AP, Cury AAD, Cury JA. Effect of sucrose on the selection of mutans streptococci and lactobacilli in dental biofilm formed in situ. *Caries Research* 2006;**40**(6):546-49.
249. AamdalScheie A, Luan WM, Dahlen G, Fejerskov O. Plaque pH and microflora of dental plaque on sound and carious root surfaces. *Journal of Dental Research* 1996;**75**(11):1901-08.
250. Deng DM, ten Cate JM. Demineralization of dentin by Streptococcus mutans biofilms grown in the constant depth film fermentor. *Caries Research* 2004;**38**(1):54-61.

251. Rosan B, Lamont RJ. Dental plaque formation. *Microbes and Infection* 2000;**2**(13):1599-607.
252. Ilie O, van Loosdrecht MCM, Picioreanu C. Mathematical modelling of tooth demineralisation and pH profiles in dental plaque. *Journal of Theoretical Biology* 2012;**309**:159-75.
253. Banting DW. The diagnosis of root caries. *Journal of dental education* 2001;**65**(10):991-6.
254. Spencer P, Ye Q, Park J, Topp EM, Misra A, Marangos O, et al. Adhesive/Dentin Interface: The Weak Link in the Composite Restoration. *Annals of Biomedical Engineering* 2010;**38**(6):1989-2003.
255. Koshiro K, Inoue S, Sano H, De Munck J, Van Meerbeek B. In vivo degradation of resin-dentin bonds produced by a self-etch and an etch-and-rinse adhesive. *European Journal of Oral Sciences* 2005;**113**(4):341-48.
256. Ferracane JL. Hygroscopic and hydrolytic effects in dental polymer networks. *Dental Materials* 2006;**22**(3):211-22.
257. Reis A, Ferreira SQ, Costa TRF, Klein-Junior CA, Meier MM, Loguercio AD. Effects of increased exposure times of simplified etch-and-rinse adhesives on the degradation of resin-dentin bonds and quality of the polymer network. *European Journal of Oral Sciences* 2010;**118**(5):502-09.
258. Tay FR, Pashley DH. Have dentin adhesives become too hydrophilic? *Journal* 2003;**69**(11):726-31.
259. Tay FR, Pashley DH. Water treeing--a potential mechanism for degradation of dentin adhesives. *American Journal of Dentistry* 2003;**16**(1):6-12.
260. Finer Y, Santerre JP. The influence of resin chemistry on a dental composite's biodegradation. *Journal of biomedical materials research Part A* 2004;**69**(2):233-46.
261. Donmez N, Belli S, Pashley DH, Tay FR. Ultrastructural correlates of in vivo/in vitro bond degradation in self-etch adhesives. *Journal of Dental Research* 2005;**84**(4):355-9.
262. Xiao DW, Huang XC, Zheng YJ, Huang JX, Li KKH, Fok TF, et al. Circulating megakaryocytes during cardiopulmonary bypass and influence on neurological complications post-operation. *Blood* 2003;**102**(11):79b-79b.
263. Wadgaonkar B, Ito S, Svizero N, Elrod D, Foulger S, Rodgers R, et al. Evaluation of the effect of water-uptake on the impedance of dental resins. *Biomaterials* 2006;**27**(17):3287-94.
264. Tay FR, Pashley DH, Suh BI, Hiraishi N, Yiu CKY. Water treeing in simplified dentin adhesives - Deja Vu? *Operative Dentistry* 2005;**30**(5):561-79.
265. Ferrari M, Vichi A, Grandini S. Efficacy of different adhesive techniques on bonding to root canal walls: an SEM investigation. *Dental Materials* 2001;**17**(5):422-29.
266. Yassen GH, Platt JA, Hara AT. Bovine teeth as substitute for human teeth in dental research: a review of literature. *Journal of oral science* 2011;**53**(3):273-82.
267. Hara AT, Queiroz CS, Paes Leme AF, Serra MC, Cury JA. Caries progression and inhibition in human and bovine root dentine in situ. *Caries Research* 2003;**37**(5):339-44.

268. Indrani DJ, Cook WD, Televantos F, Tyas MJ, Harcourt JK. Fracture toughness of water-aged resin composite restorative materials. *Dent Mater* 1995;**11**(3):201-7.
269. Lohbauer U, von der Horst T, Frankenberger R, Kramer N, Petschelt A. Flexural fatigue behavior of resin composite dental restoratives. *Dent Mater* 2003;**19**(5):435-40.
270. Willems G, Lambrechts P, Braem M, Celis JP, Vanherle G. A classification of dental composites according to their morphological and mechanical characteristics. *Dent Mater* 1992;**8**(5):310-9.
271. Santerre JP, Shajii L, Leung BW. Relation of dental composite formulations to their degradation and the release of hydrolyzed polymeric-resin-derived products. *Crit Rev Oral Biol Med* 2001;**12**(2):136-51.
272. Shajii L, Santerre JP. Effect of filler content on the profile of released biodegradation products in micro-filled bis-GMA/TEGDMA dental composite resins. *Biomaterials* 1999;**20**(20):1897-908.
273. Li Y, Carrera C, Chen R, Li J, Lenton P, Rudney JD, et al. Degradation in the dentin-composite interface subjected to multi-species biofilm challenges. *Acta Biomater* 2013.
274. DeLong R, Douglas WH. An artificial oral environment for testing dental materials. *IEEE Trans Biomed Eng* 1991;**38**(4):339-45.
275. Frankenberger R, Strobel WO, Kramer N, Lohbauer U, Winterscheidt J, Winterscheidt B, et al. Evaluation of the fatigue behavior of the resin-dentin bond with the use of different methods. *J Biomed Mater Res B Appl Biomater* 2003;**67**(2):712-21.
276. Rudney JD, Chen R, Lenton P, Li J, Li Y, Jones RS, et al. A reproducible oral microcosm biofilm model for testing dental materials. *J Appl Microbiol* 2012;**113**(6):1540-53.
277. Dewhirst FE, Chen T, Izard J, Paster BJ, Tanner AC, Yu WH, et al. The human oral microbiome. *J Bacteriol* 2010;**192**(19):5002-17.
278. Larson TD, Douglas WH, Geistfeld RE. Effect of prepared cavities on the strength of teeth. *Oper Dent* 1981;**6**(1):2-5.
279. Mondelli J, Sene F, Ramos RP, Benetti AR. Tooth structure and fracture strength of cavities. *Braz Dent J* 2007;**18**(2):134-8.
280. Dejak B, Mlotkowski A. A comparison of stresses in molar teeth restored with inlays and direct restorations, including polymerization shrinkage of composite resin and tooth loading during mastication. *Dent Mater* 2015;**31**(3):e77-87.
281. da cunha Mello FS, Feilzer AJ, de Gee AJ, Davidson CL. Sealing ability of eight resin bonding systems in a Class II restoration after mechanical fatiguing. *Dent Mater* 1997;**13**(6):372-6.
282. Dewji HR, Drummond JL, Fadavi S, Punwani I. Bond strength of Bis-GMA and glass ionomer pit and fissure sealants using cyclic fatigue. *Eur J Oral Sci* 1998;**106**(1):594-9.
283. Margolis HC, Zhang YP, Lee CY, Kent RL, Jr., Moreno EC. Kinetics of enamel demineralization in vitro. *J Dent Res* 1999;**78**(7):1326-35.
284. Hoppenbrouwers PM, Driessens FC, Borggreven JM. The mineral solubility of human tooth roots. *Arch Oral Biol* 1987;**32**(5):319-22.

285. DeLong R, Pintado MR, Douglas WH, Fok AS, Wilder AD, Jr., Swift EJ, Jr., et al. Wear of a dental composite in an artificial oral environment: A clinical correlation. *J Biomed Mater Res B Appl Biomater* 2012;**100**(8):2297-306.
286. Jiang W, Zhang J, Chen H. Pyrosequencing analysis of oral microbiota in children with severe early childhood dental caries. *Curr Microbiol* 2013;**67**(5):537-42.
287. Kanasi E, Dewhirst FE, Chalmers NI, Kent R, Jr., Moore A, Hughes CV, et al. Clonal analysis of the microbiota of severe early childhood caries. *Caries Res* 2010;**44**(5):485-97.
288. Zhang M, Chen Y, Xie L, Li Y, Jiang H, Du M. Pyrosequencing of Plaque Microflora In Twin Children with Discordant Caries Phenotypes. *PLoS One* 2015;**10**(11):e0141310.
289. Jorth P, Turner KH, Gumus P, Nizam N, Buduneli N, Whiteley M. Metatranscriptomics of the human oral microbiome during health and disease. *MBio* 2014;**5**(2):e01012-14.
290. Kidd E, Fejerskov O, Nyvad B. Infected Dentine Revisited. *Dent Update* 2015;**42**(9):802-6, 08-9.
291. Schwendicke F, Diederich C, Paris S. Restoration gaps needed to exceed a threshold size to impede sealed lesion arrest in vitro. *J Dent* 2016.
292. Botelho MG. Inhibitory effects on selected oral bacteria of antibacterial agents incorporated in a glass ionomer cement. *Caries Res* 2003;**37**(2):108-14.
293. Jedrychowski JR, Caputo AA, Kerper S. Antibacterial and mechanical properties of restorative materials combined with chlorhexidines. *J Oral Rehabil* 1983;**10**(5):373-81.
294. Ribeiro J, Ericson D. In vitro antibacterial effect of chlorhexidine added to glass-ionomer cements. *Scand J Dent Res* 1991;**99**(6):533-40.
295. Chen ZX, Lei Q, He RL, Zhang ZF, Chowdhury AJ. Review on antibacterial biocomposites of structural laminated veneer lumber. *Saudi J Biol Sci* 2016;**23**(1):S142-7.
296. Imazato S. Antibacterial properties of resin composites and dentin bonding systems. *Dent Mater* 2003;**19**(6):449-57.
297. Xu C, Wang Y. Collagen cross linking increases its biodegradation resistance in wet dentin bonding. *J Adhes Dent* 2012;**14**(1):11-8.
298. Emilson CG, Bergenholtz G. Antibacterial activity of dentinal bonding agents. *Quintessence Int* 1993;**24**(7):511-5.
299. Fraga RC, Siqueira JF, Jr., de Uzeda M. In vitro evaluation of antibacterial effects of photo-cured glass ionomer liners and dentin bonding agents during setting. *J Prosthet Dent* 1996;**76**(5):483-6.
300. Scherer W, Cooper H, Antonelli J. Antimicrobial properties of dental dentin-enamel adhesives. *J Esthet Dent* 1990;**2**(5):140-1.
301. Koulaouzidou EA, Helvatjoglu-Antoniades M, Palaghias G, Karanika-Kouma A, Antoniades D. Cytotoxicity of dental adhesives in vitro. *Eur J Dent* 2009;**3**(1):3-9.
302. Saito K, Hayakawa T, Kawabata R, Meguro D, Kasai K. In vitro antibacterial and cytotoxicity assessments of an orthodontic bonding agent containing benzalkonium chloride. *Angle Orthod* 2009;**79**(2):331-7.

303. Jones CG. Chlorhexidine: is it still the gold standard? *Periodontol 2000* 1997;**15**:55-62.
304. Andre CB, Gomes BP, Duque TM, Stipp RN, Chan DC, Ambrosano GM, et al. Dentine bond strength and antimicrobial activity evaluation of adhesive systems. *J Dent* 2015;**43**(4):466-75.
305. Hiraishi N, Yiu CK, King NM, Tay FR. Effect of chlorhexidine incorporation into a self-etching primer on dentine bond strength of a luting cement. *J Dent* 2010;**38**(6):496-502.
306. Rosin-Grget K, Peros K, Sutej I, Basic K. The cariostatic mechanisms of fluoride. *Acta Med Acad* 2013;**42**(2):179-88.
307. Marquis RE, Clock SA, Mota-Meira M. Fluoride and organic weak acids as modulators of microbial physiology. *FEMS Microbiol Rev* 2003;**26**(5):493-510.
308. Bapna MS, Murphy R, Mukherjee S. Inhibition of bacterial colonization by antimicrobial agents incorporated into dental resins. *J Oral Rehabil* 1988;**15**(5):405-11.
309. Itota T, Nakabo S, Iwai Y, Konishi N, Nagamine M, Torii Y. Inhibition of artificial secondary caries by fluoride-releasing adhesives on root dentin. *J Oral Rehabil* 2002;**29**(6):523-7.
310. Kerber LJ, Donly KJ. Caries inhibition by fluoride-releasing primers. *Am J Dent* 1993;**6**(5):216-8.
311. Van Loveren C. Antimicrobial activity of fluoride and its in vivo importance: identification of research questions. *Caries Res* 2001;**35 Suppl 1**:65-70.
312. Agnihotri SA, Mallikarjuna NN, Aminabhavi TM. Recent advances on chitosan-based micro- and nanoparticles in drug delivery. *J Control Release* 2004;**100**(1):5-28.
313. Liu H, Du Y, Wang X, Sun L. Chitosan kills bacteria through cell membrane damage. *Int J Food Microbiol* 2004;**95**(2):147-55.
314. Elsaka SE. Antibacterial activity and adhesive properties of a chitosan-containing dental adhesive. *Quintessence Int* 2012;**43**(7):603-13.
315. Kudou Y, Obara K, Kawashima T, Kubota M, Abe S, Endo T, et al. Addition of antibacterial agents to MMA-TBB dentin bonding systems--influence on tensile bond strength and antibacterial effect. *Dent Mater J* 2000;**19**(1):65-74.
316. Imazato S, Torii M, Tsuchitani Y, McCabe JF, Russell RR. Incorporation of bacterial inhibitor into resin composite. *J Dent Res* 1994;**73**(8):1437-43.
317. Imazato S, Kinomoto Y, Tarumi H, Torii M, Russell RR, McCabe JF. Incorporation of antibacterial monomer MDPB into dentin primer. *J Dent Res* 1997;**76**(3):768-72.
318. Imazato S, Kinomoto Y, Tarumi H, Ebisu S, Tay FR. Antibacterial activity and bonding characteristics of an adhesive resin containing antibacterial monomer MDPB. *Dent Mater* 2003;**19**(4):313-9.
319. Imazato S, Tay FR, Kaneshiro AV, Takahashi Y, Ebisu S. An in vivo evaluation of bonding ability of comprehensive antibacterial adhesive system incorporating MDPB. *Dent Mater* 2007;**23**(2):170-6.
320. Imazato S, Tarumi H, Kato S, Ebisu S. Water sorption and colour stability of composites containing the antibacterial monomer MDPB. *J Dent* 1999;**27**(4):279-83.

321. Imazato S, Ebi N, Tarumi H, Russell RR, Kaneko T, Ebisu S. Bactericidal activity and cytotoxicity of antibacterial monomer MDPB. *Biomaterials* 1999;**20**(9):899-903.
322. Imazato S, Russell RR, McCabe JF. Antibacterial activity of MDPB polymer incorporated in dental resin. *J Dent* 1995;**23**(3):177-81.
323. Imazato S, Torii Y, Takatsuka T, Inoue K, Ebi N, Ebisu S. Bactericidal effect of dentin primer containing antibacterial monomer methacryloyloxydodecylpyridinium bromide (MDPB) against bacteria in human carious dentin. *J Oral Rehabil* 2001;**28**(4):314-9.
324. Imazato S, Kuramoto A, Takahashi Y, Ebisu S, Peters MC. In vitro antibacterial effects of the dentin primer of Clearfil Protect Bond. *Dent Mater* 2006;**22**(6):527-32.
325. Inacio AS, Domingues NS, Nunes A, Martins PT, Moreno MJ, Estronca LM, et al. Quaternary ammonium surfactant structure determines selective toxicity towards bacteria: mechanisms of action and clinical implications in antibacterial prophylaxis. *J Antimicrob Chemother* 2016;**71**(3):641-54.
326. Wessels S, Ingmer H. Modes of action of three disinfectant active substances: a review. *Regul Toxicol Pharmacol* 2013;**67**(3):456-67.
327. Caillier L, de Givenchy ET, Levy R, Vandenberghe Y, Geribaldi S, Guittard F. Synthesis and antimicrobial properties of polymerizable quaternary ammoniums. *Eur J Med Chem* 2009;**44**(8):3201-8.
328. Demirci M, Hiller KA, Bosl C, Galler K, Schmalz G, Schweikl H. The induction of oxidative stress, cytotoxicity, and genotoxicity by dental adhesives. *Dent Mater* 2008;**24**(3):362-71.
329. He J, Soderling E, Vallittu PK, Lassila LV. Preparation and evaluation of dental resin with antibacterial and radio-opaque functions. *Int J Mol Sci* 2013;**14**(3):5445-60.
330. Antonucci JM, Zeiger DN, Tang K, Lin-Gibson S, Fowler BO, Lin NJ. Synthesis and characterization of dimethacrylates containing quaternary ammonium functionalities for dental applications. *Dent Mater* 2012;**28**(2):219-28.
331. Cheng L, Weir MD, Zhang K, Arola DD, Zhou X, Xu HH. Dental primer and adhesive containing a new antibacterial quaternary ammonium monomer dimethylaminododecyl methacrylate. *J Dent* 2013;**41**(4):345-55.
332. Zhou C, Weir MD, Zhang K, Deng D, Cheng L, Xu HH. Synthesis of new antibacterial quaternary ammonium monomer for incorporation into CaP nanocomposite. *Dent Mater* 2013;**29**(8):859-70.
333. Xiao YH, Ma S, Chen JH, Chai ZG, Li F, Wang YJ. Antibacterial activity and bonding ability of an adhesive incorporating an antibacterial monomer DMAE-CB. *J Biomed Mater Res B Appl Biomater* 2009;**90**(2):813-7.
334. Cocco AR, Rosa WL, Silva AF, Lund RG, Piva E. A systematic review about antibacterial monomers used in dental adhesive systems: Current status and further prospects. *Dent Mater* 2015;**31**(11):1345-62.
335. Imazato S, Ehara A, Torii M, Ebisu S. Antibacterial activity of dentine primer containing MDPB after curing. *J Dent* 1998;**26**(3):267-71.

336. Imazato S, Imai T, Russell RR, Torii M, Ebisu S. Antibacterial activity of cured dental resin incorporating the antibacterial monomer MDPB and an adhesion-promoting monomer. *J Biomed Mater Res* 1998;**39**(4):511-5.
337. Zhang K, Cheng L, Imazato S, Antonucci JM, Lin NJ, Lin-Gibson S, et al. Effects of dual antibacterial agents MDPB and nano-silver in primer on microcosm biofilm, cytotoxicity and dentine bond properties. *J Dent* 2013;**41**(5):464-74.
338. Aires CP, Tabchoury CP, Del Bel Cury AA, Koo H, Cury JA. Effect of sucrose concentration on dental biofilm formed in situ and on enamel demineralization. *Caries Res* 2006;**40**(1):28-32.
339. Paes Leme AF, Koo H, Bellato CM, Bedi G, Cury JA. The role of sucrose in cariogenic dental biofilm formation--new insight. *J Dent Res* 2006;**85**(10):878-87.
340. Herrera M, Carrion P, Bravo M, Castillo A. Antibacterial activity of four dentin bonding systems. *Int J Antimicrob Agents* 2000;**15**(4):305-9.
341. Imazato S, Kuramoto A, Kaneko T, Ebisu S, Russell RR. Comparison of antibacterial activity of simplified adhesive systems. *Am J Dent* 2002;**15**(6):356-60.
342. Esteves CM, Ota-Tsuzuki C, Reis AF, Rodrigues JA. Antibacterial activity of various self-etching adhesive systems against oral streptococci. *Oper Dent* 2010;**35**(4):448-53.
343. Imazato S, Imai T, Ebisu S. Antibacterial activity of proprietary self-etching primers. *Am J Dent* 1998;**11**(3):106-8.
344. Kugler R, Bouloussa O, Rondelez F. Evidence of a charge-density threshold for optimum efficiency of biocidal cationic surfaces. *Microbiology* 2005;**151**(Pt 5):1341-8.
345. Muller R, Eidt A, Hiller KA, Katzur V, Subat M, Schweikl H, et al. Influences of protein films on antibacterial or bacteria-repellent surface coatings in a model system using silicon wafers. *Biomaterials* 2009;**30**(28):4921-9.
346. Lobo MM, Goncalves RB, Pimenta LA, Bedran-Russo AK, Pereira PN. In vitro evaluation of caries inhibition promoted by self-etching adhesive systems containing antibacterial agents. *J Biomed Mater Res B Appl Biomater* 2005;**75**(1):122-7.
347. de Carvalho FG, Puppin-Rontani RM, Soares LE, Santo AM, Martin AA, Nociti-Junior FH. Mineral distribution and CLSM analysis of secondary caries inhibition by fluoride/MDPB-containing adhesive system after cariogenic challenges. *J Dent* 2009;**37**(4):307-14.
348. Purevdorj B, Costerton JW, Stoodley P. Influence of hydrodynamics and cell signaling on the structure and behavior of Pseudomonas aeruginosa biofilms. *Appl Environ Microbiol* 2002;**68**(9):4457-64.
349. Paramonova E, Kalmykowa OJ, van der Mei HC, Busscher HJ, Sharma PK. Impact of hydrodynamics on oral biofilm strength. *J Dent Res* 2009;**88**(10):922-6.
350. Goeres DM, Hamilton MA, Beck NA, Buckingham-Meyer K, Hilyard JD, Loetterle LR, et al. A method for growing a biofilm under low shear at the air-liquid interface using the drip flow biofilm reactor. *Nat Protoc* 2009;**4**(5):783-8.
351. Rasmussen K, Reilly C, Li Y, Jones RS. Real-time imaging of anti-biofilm effects using CP-OCT. *Biotechnol Bioeng* 2016;**113**(1):198-205.

352. Park KH, Yu SH, Kim HS, Park HD. Inhibition of biofouling by modification of forward osmosis membrane using quaternary ammonium cation. *Water Sci Technol* 2015;**72**(5):738-45.